

The copyright of this thesis vests in the author. No quotation from it or information derived from it is to be published without full acknowledgement of the source. The thesis is to be used for private study or non-commercial research purposes only.

Published by the University of Cape Town (UCT) in terms of the non-exclusive license granted to UCT by the author.

5

*An Examination of the Spatially Extensive Heavy
Precipitation Events over South Africa and the Associated
Moisture Trajectories*

Ruwani Priyanthika Walawege

*Thesis Submitted for the Degree of
Master of Science
in the Department of Environmental and Geographical Science,
University of Cape Town*

February 2002

ABSTRACT

Precipitation is possibly the most important climatic variable in southern Africa. The absence of a good rainy season is often marked with low productivity and in some cases starvation. However, excessive rainfall can also bring with it disaster and destruction. Investigating the causes of such events has been the aim of a number of studies in the past.

The interest shown in extreme events, including that of precipitation has been growing in the last couple of years. This comes as a result of understanding that the change in the mean of variables can have a large influence on the extremes of these same variables. In fact, changes in the extremes can be disproportionate and often have more impact on both society and the environment. This raises concerns especially in poorer nations who often lack the financial resources to deal with such impacts.

The primary aim of the present study is to investigate spatially extensive heavy precipitation events in South Africa. It explores the possible spatial patterns that exists within these events and also investigates the non-local sources of moisture for them. In order to do this, the study firstly utilises a categorisation technique called Self Organising Maps (SOMs). A number of groups were identified through this process and sample events from this were then further analysed with the use of a kinematic trajectory model. The results indicated that moisture for these events were most likely to be transported from the south Indian Ocean. Although this finding has been shown previously in other similar studies, the present investigation shows that the possible source of moisture to be further south that previously thought. Further investigation was done by examining a case event more closely. The results also show that an area in the south Indian Ocean, east of Madagascar to be the possible source of moisture for this particular event.

ACKNOWLEDGEMENTS

During the course of this research there have been a number of people whose help, support and advice has helped me enormously. It is therefore not only appropriate but necessary to acknowledge them and thank them here. Firstly, to my parents, who have always encouraged and supported me through all of my studies, and have seen very little of me as a result in the last couple of years-thank you for loving me and caring about me.

To all my colleagues and friends at the **CSAG**, who have helped me with their advice and also humour, without which I am sure this would have been a much duller experience. Special thanks to Chris Jack for helping me with all the computer problems along the way and getting me to program! To Kerry, Amanda, Sharon, Christina and Liz to name a few, thank you for listening and sharing your experience with me. To Manny, thanks for all the encouragement and love even when I was unbearably stressed!

I would also like to thank the **Water Research Commission** for the financial support that they have provided for this research.

Finally, I would like to thank Bruce Hewitson, my supervisor, for all of his support and advice during this time and also for all the opportunities that he has provided me along the way.

TABLE OF CONTENTS

	Page
Abstract	i
Acknowledgements	ii
Table of Contents	iii
List of Figures	v
List of Tables	vi
Chapter 1 Introduction	1
1.1 The Atmospheric Circulation and Weather Patterns over South Africa	2
1.2 The Classification of Rainfall over South Africa	4
1.3 Aims and Objectives of the Study	7
1.4 Data and Methodology	7
<i>1.4.1 Data specifications</i>	8
<i>1.4.2 Methodologies practiced</i>	9
1.5 Thesis Structure	12
Chapter 2 Long term variability of precipitation	13
2.1 Introduction	13
2.2 Interannual Variability in Precipitation	13
2.3 Wet spells over South Africa	15
2.4 Causes of Interannual Rainfall Variability	19
<i>2.4.1 The Walker circulation, ENSO and South African rainfall</i>	19
<i>2.4.2 Sea surface temperature variability</i>	22
2.5 Precipitation Variability and Extreme Events	23
<i>2.5.1 Variability of extreme precipitation events</i>	24
<i>2.5.2 Future predictions for extreme precipitation events</i>	26
2.6 Conclusion	30
Chapter 3 Categorization of extreme precipitation events	32
3.1 Artificial Neural Networks	32
3.2 Self Organizing Maps	36
3.3 Data Preparation	38
3.4 The SOM Procedure	39

3.5 Classification Results and Discussion	41
Chapter 4 Trajectory modeling	51
4.1 Introduction	51
4.2 Trajectory Modelling	51
4.3 Methodology	52
<i>4.3.1 The kinematic model</i>	53
<i>4.3.2 Source data</i>	55
<i>4.3.3 Sample selection</i>	56
4.4 Results and discussion	59
<i>4.4.1 Trajectory results</i>	59
<i>4.4.2 Sample trajectory results</i>	60
<i>4.4.3 Vertical changes of the trajectories</i>	68
<i>4.4.4 Discussion of findings</i>	73
4.5 Conclusion	82
Chapter 5 Case study of an extreme event	86
5.1 Introduction	86
5.2 Synoptic Analysis of the Event	86
5.3 Results of Trajectory Analysis and Discussion	89
<i>5.3.1 Trajectory results</i>	89
<i>5.3.2 Discussion of results</i>	93
5.4 Conclusion	100
Chapter 6 Summary and Conclusions	102
6.1 Findings of the Study	102
6.2 Caveats of the Study	104
6.3 Future Research Directions	105
<i>6.3.1 Importance of extreme studies</i>	105
<i>6.3.2 Directions for future research</i>	106
6.4 Conclusion	107
REFERENCES	109
APPENDICES	

LIST OF FIGURES

- FIGURE 1.1: Circulation features around southern Africa.
- FIGURE 1.2: Classification of synoptic types for southern Africa based on surface and 500hPa circulation.
- FIGURE 1.3: Classification of rain-bearing synoptic systems of southern Africa based on low-level circulation and upper-level features and cloud cover.
- FIGURE 2.1: Percentage variance associated with 10-12 years, quasi 18-year, 2.3 years and 3.5 years rainfall oscillations over South Africa
- FIGURE 2.2: Areal averaged seasonal rainfall over the north-eastern region of South Africa for the period 1910 to 1990.
- FIGURE 2.3: Schematic representation of circulation types responsible for rainfall.
- FIGURE 2.4: The seven rainfall regions for South Africa identified through correlation with circulation types.
- FIGURE 2.5: Model of the meridional circulation over South Africa during the wet and dry spells.
- FIGURE 2.6: ENSO episodes and the Walker Circulation.
- FIGURE 2.7: The correlation between the SOI and rainfall over South Africa in summer.
- FIGURE 2.8: Summer rainfall trends from 1900-01 to 1995-96 as anomalies from the 1961-1990 average.
- FIGURE 2.9: Trends in heavy precipitation and total precipitation during the rainy seasons in different countries.
- FIGURE 2.10: Percentage changes in intensity of 10-year high rainfall events between 1931-1960 and 1961-1990.
- FIGURE 2.11: Graph showing changes in extremes with a change in mean, variance and both.
- FIGURE 2.12: Simulated percentage changes of extreme daily rainfall totals for 10 year and 30 year return periods.
- FIGURE 3.1: A simple neuron.
- FIGURE 3.2: A simple neural network.
- FIGURE 3.3: A competitive layer.
- FIGURE 3.4: The two topologies available in SOM- a) hexagonal and b) rectangular.
- FIGURE 3.5: Initial summer season SOM results.

FIGURE 3.6: Modified summer season SOM results.

FIGURE 3.7: Frequencies of each node in the summer SOM.

FIGURE 3.8: Frequency of extreme precipitation days during the summer seasons.

FIGURE 3.9: Frequency of events in Nodes [0 0], [2 0] and [2 3] for the period 1950-1998.

FIGURE 4.1: Sigma Levels showing the terrain following surfaces.

FIGURE 4.2: Trajectories for event days mapped to the three selected nodes.

FIGURE 4.3: Starting locations for the sample trajectories from each selected node.

FIGURE 4.4: Trajectories for sample days from node [0 0].

FIGURE 4.5: Trajectories for sample days from node [2 0].

FIGURE 4.6: Trajectories for sample days from node [2 3].

FIGURE 4.7: Sigma level changes for sample days in node [0 0] for trajectories starting at a) 00h00 and b) 12h00 SAST.

FIGURE 4.8: Sigma level changes for sample days in node [2 0] for trajectories starting at a) 00h00 and b) 12h00 SAST.

FIGURE 4.9: Sigma level changes for sample days in node [2 3] for trajectories starting at a) 00h00 and b) 12h00 SAST.

FIGURE 4.10: Comparison of sigma level changes for trajectories originating from different directions.

FIGURE 4.11: Horizontal divergence fields for the sample days investigated.

FIGURE 5.1: The SOM nodes [0 0], [1 2] and [2 2] to which the case event mapped.

FIGURE 5.2: Locations of the starting points of the trajectories for the case event.

FIGURE 5.3: Trajectories calculated for the case event.

FIGURE 5.4: Changes in the moisture content (a) of the trajectories shown in (b).

FIGURE 5.5: Sigma level changes of the trajectories during the event days.

LIST OF TABLES

Table 1.1: NCEP variables used.

Table 3.1: The post-1979 dates for each SOM node.

Table 4.1: Synoptic conditions prevailing during the days being investigated.

University of Cape Town

Albert Einstein
Imagination is more important than knowledge

CHAPTER ONE: INTRODUCTION

Southern Africa is an arid to semi-arid region and therefore water plays an important role, in both the personal lives of its people and in the economic growth and development of its countries. Precipitation is therefore possibly the most important climatic factor to both the human population as well as the ecosystems of this region. Changes in the precipitation, be it natural or man-made, can cause considerable damage. Droughts caused by prolonged dry spells are often experienced in many of the countries in the region. Equally however, heavy rains can cause devastating floods. The damage caused by the floods of 2000 and 2001 in parts of Mozambique, Zambia and South Africa for example, is still being repaired in 2002. The cost of reconstruction for the Mozambique government alone has been estimated to be around US\$449.6 million (Christie and Hanlon, 2001). Changes in such extreme events affect the ecosystem and society much more than changes that may occur in the mean of a variable. Understanding these extreme climatic events is therefore essential.

The definition given by the Intergovernmental Panel on Climate Change (IPCC) on extreme weather event states that it is “... *an event that is rare within its statistical reference distribution at a particular place...as rare as or rarer than the 10th or 90th percentile*” (IPCC, 2001, pg 88). The identification of extreme events practically is however rather more difficult than stated here. This thesis attempts to expand on the upper end of the scale by looking more closely at the spatially extensive high precipitation events occurring over South Africa. The size of the selected domain itself leads to a number of difficulties in trying to choose a method that will best select the necessary days for the study. The variation that exists both spatially and seasonally for precipitation over the country, must also be kept in mind. For this reason it is not possible to simply set a precipitation limit above which the event day will be selected. Rather a percentile value is best selected, as this will preserve the spatial variation in precipitation over the country. The spatially extensive nature of the event must also be incorporated into the method. Therefore not only must the percentile for the precipitation amount be set but also the total area that falls above this set value must be selected. Through this the necessary extreme event days for the study may be selected.

In order to understand these events more comprehensively however, it is necessary to understand the atmospheric circulation patterns that govern the area and the dynamics that control these events. Tyson and Preston-Whyte (2000) give a thorough conceptual review of the processes involved as well as the general atmospheric patterns seen over Southern Africa.

In addition there are numerous publications made in the various climatological and atmospheric journals on the dynamics of the atmospheric circulation of the region. A summary of the atmospheric circulation and weather patterns observed over South Africa is presented here.

1.1: The Atmospheric Circulation and Weather Patterns over South Africa

The climate of South Africa is affected by a number of factors of which orography is an important one. The interior plateau with an average elevation of 1600 meters is separated from the narrow, lower coastal regions by a relatively steep escarpment (over 3000 meters in places). The topography is seen to influence the airflow pattern in these areas as well as enhancing convection near the escarpment (Garstang *et al.*, 1987). Rainfall is observed to be highest along the eastern side of the escarpment, decreasing on the leeward slopes, and towards the western interior (Lindesay, 1998; Tyson, 1986).

The climate is also greatly affected by the oceans and the currents that surround the region. The sea surface temperatures of the Agulhas current that flows along the eastern margins of the country can vary between 22° and 28°C in summer, whilst that of the Benguela Current along the west coast remains much colder at around 16°C. The warmer waters are thought to contribute to the moisture for precipitation over the region, especially over the coastal areas (Walker & Lindesay, 1989).

The position of the country in relation to the pressure regimes also influences the climate that is experienced (Tyson, 1986). Both the Hadley and Ferrel cells descend in the subtropics and this results in the existence of a quasi-stationary high pressure belt. The South Atlantic (SAA) and South Indian Anticyclones (SIA) are positioned within this belt or zone, to the west and east of the subcontinent respectively. The positions of these anticyclones are known to shift both latitudinally and longitudinally during the year (Tyson & Preston-Whyte, 2000). The proximity of the SIA to the coast influences the transport of maritime air into the subcontinent and thereby affecting the weather of the region. In the same manner the ridging of the SAA to the south of the country in summer has an influence over the rainfall over the region (Tyson & Preston-Whyte, 2000). The northwards shifting of the SAA during the winter months also allow passing mid-latitude depressions (lows) to move across the southwestern parts of the country, bringing precipitation to this region.

The weather over the region is thus controlled through such features of the general circulation, which are temperate, tropical or subtropical in nature (Tyson & Preston-Whyte, 2000). The influence of the anticyclones described above and the continental high are subtropical features. The tropical control is effected through tropical easterly flows and the occurrence of easterly waves and lows. The temperate control over the region's weather on the other hand is effected through disturbances in the westerlies, which can take the form of westerly waves or lows travelling from the west to the east (Tyson & Preston-Whyte, 2000). Other features that are of a smaller scale but fall in the same category are west coast troughs and coastal lows. These synoptic features (Figure 1.1) thus control the rainfall over the country as well as the region.

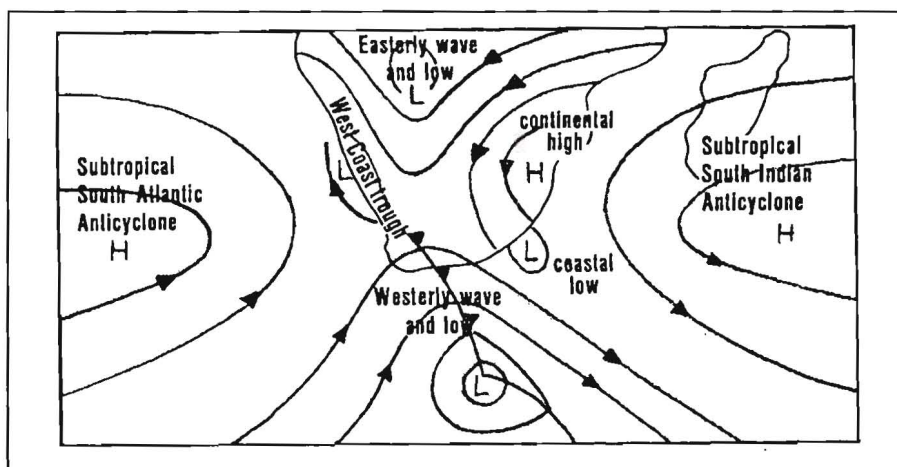


Figure 1.1: Circulation features around Southern Africa (from Tyson and Preston-Whyte, 2000)

Besides the southwestern parts of the country that receives most of its rainfall in the winter, the majority of the country is a summer rainfall region. During this time southwesterly air from the south Atlantic, northeasterly monsoon air from the equator and tropical easterlies from the south Indian Ocean are all seen to converge at around 20°S in the Inter-Tropical Convergence Zone (ITCZ) (Lindesay, 1998; Tyson, 1986). The ITCZ is a zone of high convection and latent heat release and migrates seasonally between north of the equator during the austral winter and south during the summer (Tyson, 1986). Another zone of convergence is found over southern Angola and northern Namibia and Botswana. This is known as the Zaire Air Boundary (Crimp *et al.*, 1997). Tropical easterlies from the south Indian Ocean and the recurved southwesterlies from the south Atlantic are seen to converge in this zone. Low pressure systems are also found to develop here (Taljaard, 1972) with easterly waves and troughs extending southwards from these (Lindesay, 1998; Tyson, 1986), often resulting in heavy precipitation over the summer rainfall region. Classification of these

summer rainfall-producing systems has been of major interest in the past and has been attempted in South Africa.

1.2 The Classification of Rainfall over South Africa

Early attempts to produce a synoptic classification of the rainfall producing systems was based on the surface data alone and therefore failed to include any upper air forcing (Crimp *et al.*, 1997). Upper air observations and satellite imagery was incorporated into the later schemes and the development of a more generalised classification of the summer rain-bearing synoptic systems across the country was achieved (Tyson, 1986; Harrison, 1984a; 1984b). Two of the best known classification schemes for the region are those of Tyson (1986) and Harrison (1984a).

The classification of Tyson (1986) identifies surface circulation types and their accompanying mid-tropospheric circulations (Fig 1.2).

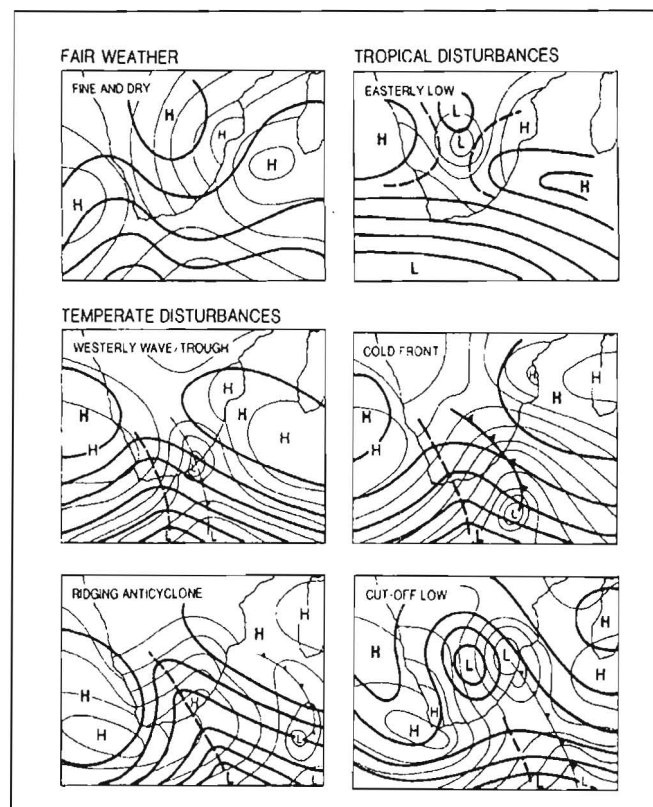


Figure 1.2: Classification of synoptic types for southern Africa based on surface (light lines) and 500hPa (heavy lines) circulation (from Tyson, 1986).

In Harrison (1984a) the characteristic cloud patterns are incorporated into the classification to identify five resultant synoptic types (Fig 1.3).

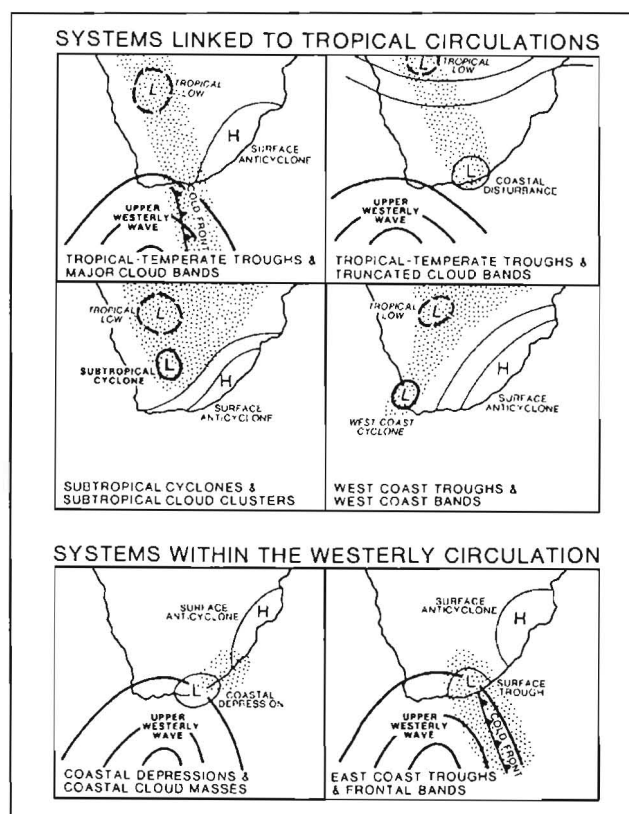


Figure 1.3: Classification of rain-bearing synoptic systems of southern Africa based on low-level circulation (light lines), upper-level features (heavy lines) and cloud cover (shaded) (from Harrison, 1984a).

In both classifications the synoptic types can be linked to either disturbances in the tropical circulation or to the westerly circulation. From Harrison (1984a) examination of the cloud bands, it has been found that major cloud bands are associated with those systems linked to the tropical circulation. Systems linked with the westerly circulation on the other hand are seen to produce a more local effect (Tyson & Preston-Whyte, 2000; Harrison, 1984a).

The contribution of each of these identified systems to the annual rainfall differs from region to region. Examination of these patterns have however shown that the cloud bands linking the tropical low over the interior to the westerly waves in the south, to be the most important for the summer rainfall region of the country (Harrison, 1984a; 1984b). These systems are commonly referred to as tropical-temperate troughs. The location of these bands also plays an important role in determining the amount of rainfall received over the country (Crimp *et al.*, 1997; Harrison, 1984a). During predominantly wet summer months, the bands are seen to concentrate over the interior of the country along a northwest-southeast axis. During the

dry summer months however, an eastward shift of the cloud bands to the Malagasy region is evident (Harrison, 1984a).

In addition to the study and classification of the rain-bearing synoptic systems, investigations into the sources and transport of moisture for these rain events have also increased (D'Abreton, 1996; D'Abreton & Tyson, 1996; 1995; D'Abreton & Lindesay, 1993). Part of the increase in interest in this field can be attributed to the region's vulnerability to water resources. The increasing population and development throughout the region is constantly placing enormous pressure on the limited water supply. An understanding of the conditions that are favourable for rain over the region is therefore essential in improving the potential to predict or forecast rainfall in future. Moisture transport studies in the past have shown that the most important source of moisture for rain events over South Africa lies in the tropical equatorial Indian Ocean, north of Madagascar (D'Abreton & Tyson, 1996; 1995; D'Abreton & Lindesay, 1993). These studies now use trajectory modelling as a tool to understand the pathways of moisture in the atmosphere. With the use of such a trajectory model, Joubert *et al.*, (1999) have shown a different source of moisture - one that lies further south in the Indian Ocean. A similar technique of trajectory modelling is also being implemented in this study of spatially extensive heavy precipitation events.

Examination of such extreme events has been growing in the climate research field (Gordon *et al.*, 1992; Yonetani & Gordon, 2001; Liebman *et al.*, 2001; Mason *et al.*, 1999; Mason & Joubert, 1997). There is a growing understanding that due to changes caused by global warming, the frequency of extreme events such as floods may increase in future (Houghton *et al.*, 2001; Mearns *et al.*, 1984). Extreme precipitation in South Africa has been examined in the past through reviews of case studies (Joubert *et al.*, 1999; D'Abreton & Tyson, 1996; Lindesay & Jury, 1991; Walker & Lindesay, 1989; Triegaardt *et al.*, 1988). The variability and the occurrence of these events in the future for the region have also recently been studied (Joubert *et al.*, 1999). In the present study these findings are kept in mind and the aims and objectives have been set out accordingly to hopefully improve on existing findings of extreme precipitation events.

1.3: Aims and Objectives of the Study

The primary objectives of this study are to better understand the spatially extensive extreme precipitation events over South Africa and to ascertain the possible sources of moisture for the events. The recent publication of the findings of Working Group I of the IPCC (IPCC, 2001) has also stated the importance of understanding extreme climatic events. There is also a need for more studies especially in Africa in order to better understand the processes involved and to make appropriate policies in the future.

With this in mind the aims of the study are set out to best achieve these objectives. They are summarised as follows:

- To categorize the extreme events over South Africa into clusters or groups.
- To evaluate the atmospheric circulation driving these events.
- To understand the moisture flux patterns associated with the events.
- To study the variability of these events and their relationship with other climate phenomenon such as ENSO.
- To model the moisture trajectories of the events.
- To investigate the non-local sources of moisture for these precipitation events.

Achieving these aims and objectives require suitable data for the domain of interest and an appropriate methodology to extract the necessary information from the data. Although it sounds simple these choices ultimately influence the investigation, hence it is important to understand the implications of the choices made.

1.4: Data and Methodology

In trying to understand extreme precipitation events, this study is confined to looking at events over South Africa alone based on the availability of data for the research and the time frame available. The availability of an extensive body of literature on the atmospheric circulation and dynamics for the same domain also facilitates the analysis of the results of this study. As the rainfall cycle in South Africa is strongly seasonal (Lindesay, 1998; Tyson, 1986), the study data was divided into two sets to look at both the summer (December to February) and winter (June to August) months, for extreme events.

1.4.1: Data Specifications

In view of the spatial variability of rainfall, a comprehensive station network of data is required to adequately capture the spatial characteristics of an event. The Computing Centre for Water Research (CCWR) provides a comprehensive collation of separate sources of station daily accumulated precipitation data, and was used in this project. The data was available for the period 1950 to 1998, at the time of this study. This data set, which is made up of approximately 7000 stations from around South Africa, was regridded at a 0.25 degree resolution, for the domain extending from 20.75°S to 34.75°S and 14.25°E to 33.25°E. The regridding process involves estimating an approximate area average for the precipitation values by simply averaging stations within a 0.25° grid box, using at least three ground station observations per grid cell.

Due to some errors being present in the original station data set, the regridded data set does contain some inevitable inaccuracies. These arise as a result of missing data for some stations and also due to incorrect values being captured for certain stations (e.g rainfall recorded as 0 when surrounding stations record large values). The area average computed in these cases will have errors as a result. However, as the occurrence of these errors is not large, the use of the data set was deemed suitable for this study.

In addition to precipitation, a number of other atmospheric variables are needed for the analysis and trajectory modelling aspects of the study. The NCEP¹/NCAR² Reanalysis data set, provided by the NOAA³-CIRES⁴ Climate Diagnostic Center, was used for these tasks. This global data set, is a model assimilation of observational data from a number of sources including, land station, ship, rawinsonde, pibal, aircraft, and satellite, from 1957 to 1998 (see Kalnay *et al.*, 1996). However, the data quality prior to 1979 for the Southern African region has recently been found to be problematic (Tennant, 2002; Kistler *et al.*, 2001). As a result, only data from 1979 to 1998 for the South African domain (20° S to 37.5° S; 12.5°E to 37.5°E) has been selected from this data set to be used in this study.

¹ National Center for Environmental Prediction

² National Center for Atmospheric Research

³ National Oceanic and Atmospheric Administration

⁴ Cooperative Institute for Research in Environmental Sciences

The NCEP/NCAR data set provides a comprehensive suite of atmospheric variables at the surface and different pressure levels. Only a selected number of these are used in the present study. These are listed below (Table 1.1) along with the resolutions at which they were available. As can be noted, all pressure level data is available on a 2.5° latitude-longitude grid, whilst the surface flux data is available on a T62 Gaussian grid. This gives the latter a $1.88^\circ \times 1.88^\circ$ resolution. All the variables were available at a six-hourly temporal resolution.

Table 1.1: NCEP variables used

Variable	Grid Resolution	Levels
Geopotential height	$2.5^\circ \times 2.5^\circ$	500 hPa
Specific Humidity	$2.5^\circ \times 2.5^\circ$	500 hPa and 700 hPa
Sea Level Pressure	$2.5^\circ \times 2.5^\circ$	Sea Level
V wind	$2.5^\circ \times 2.5^\circ$	10 hPa, 500hPa, 700hPa
U wind	$2.5^\circ \times 2.5^\circ$	10 hPa, 500hPa, 700hPa
Specific humidity at 2m	$1.88^\circ \times 1.88^\circ$	2m above the surface
Sensible heat net flux	$1.88^\circ \times 1.88^\circ$	At the surface
Latent heat net flux	$1.88^\circ \times 1.88^\circ$	At the surface

1.4.2: Methodologies practiced

The growth of the computer technology field has brought with it a number of advantages to the scientific research community. It is now possible to analyse volumes of data that in previous decades would have taken far too much time. Climatology and atmospheric science in general has benefited greatly from these advances. The use of these technologies has enabled research methodologies to progress from labour and time intensive manual methods to more automated ones. Even within this category however, there are a number of choices available. The methods discussed here will focus on those that are used in the field of climatology for the purpose of categorization. One of the requirements of the present study is

to categorize extreme precipitation events so as to highlight the patterns that exist within them. Categorization or classification is often used for this purpose. The methodologies available for this involve clustering or grouping. Yarnal (1993) gives a good overall description of those that are commonly implemented for this purpose. Amongst the automated methods is correlation and eigenvector based classifications.

Correlation-based methods are used mainly for map pattern classification, which is usually based on the patterns formed by one variable such as surface pressure. The eigenvector-based methods are used for this and in addition may also be used for synoptic types classification and regionalizations. These classify similar weather properties so that they represent a mixture of variables such as temperature, humidity, pressure and wind speeds.

The correlation-based map pattern classification was first introduced by Lund (1963). It is a simple method by which similar map patterns are placed into discrete categories. The simplicity and the fact that the input and output data are real pressure pattern maps, may contribute to its popularity (Yarnal, 1993). The eigenvector outputs on the other hand, may be more complex and not readily interpretable. Even so, its use in synoptic climatology is extensive.

Even within the eigenvector-based classification there are a number of different possible methods based on the mode of decomposition and type of dispersion matrix chosen. Yarnal (1993) describes these choices in detail. Further distinction is also made through the type of analysis chosen. The three that climatology is familiar with are common factor analysis (CFA), principal component analysis (PCA) and empirical orthogonal function (EOF). The CFA model is more complex than the latter two and is often discouraged, unless the user is familiar with the theory behind the model (Yarnal, 1993). This has made the PCA and the EOF methods more popular and more widely used. Although Lorenz introduced EOF to the meteorology community in 1956 (Yarnal, 1993), the climatology research field has preferred to use PCA as it provides more information. Precipitation studies often use this method for both regionalization (Ehrendorfer, 1987; Andres *et al.*, 2000) and classification (Harrison, 1984a).

The main objective in all of these methods however, is to form groups or clusters into which the input data may be categorised. The algorithms used in this process attempt to ideally

minimize the within group differences and maximise the between group differences. The formation of these discrete groups results in artificial boundaries being imposed on the data set, which is in essence a continuum. As a consequence, there is generalisation of synoptic types or patterns. This is a major disadvantage, especially when trying to study extreme events, which often get grouped into more general categories.

As an alternative to these classical methods Hewitson and Crane (1992) proposed a method of empirical downscaling. Many methodologies for this, such as linear regression and Artificial Neural Nets (ANNs), have since been developed. Self Organising Maps (SOMs) were introduced by the same authors, to the geography community, through a broader discussion on ANN (Hewitson & Crane, 1994). Although its popularity in climatology is still weak, it is one of the methods that is best suited for the purposes of categorising and visualization of data. The disadvantages of data linearity and orthogonality that are faced with the previous methods are not experienced with SOMs. It has been used successfully in the categorization of synoptic data by Tennant (2002), Gutowski (2001), Cavazos (2000), Hudson (1998) and Main (1997). It is the proposed method of categorization within this study. A background on ANN and SOM and specific details on its use in this study is given in the Chapter Three.

The second major objective of the thesis is to understand the possible non-local moisture sources for extreme events experienced in South Africa. This requires comprehensive three-dimensional data with appropriate spatial and temporal resolution, from which trajectories and transport can be analysed. The growing availability of global reanalysis data makes this now a possibility.

Environmental issues such as increases of certain atmospheric pollutants, has encouraged the use of trajectory modelling to establish the transport patterns as well as the source and sinks of these particles. In Southern Africa a number of studies have been carried out in this field (D'Abreton & Tyson, 1998; D'Abreton, 1996; Swap *et al.*, 1996; Garstang *et al.*, 1996). More recently however focus has been placed on understanding moisture transport within the atmosphere. Such water vapour transport over Southern Africa has been discussed previously by D'Aberton and Tyson (1996; 1995), Tyson *et al.*, (1996a) and D'Abreton and Lindesay (1993). The focus in these papers was on the general circulation and not specifically on extreme precipitation events. The present study uses a trajectory model that

calculates the seven-day back-trajectories from any given coordinate point. Such back-trajectories were carried out for specific events identified through the categorization process. Through these an investigation of the source and path of moisture was undertaken in this study. A description of the model used is given in Chapter Four as well as a discussion on the results obtained through this process.

1.5: Thesis Structure

The thesis is structured such that the two main tasks or processes of the study, that of the synoptic categorization and moisture trajectory modelling, are presented in separate chapters. Chapter Three will thus concentrate on the categorization process of the extreme events more closely. A background or literature review on ANNs and SOMs is given here. A discussion of the findings of the categorization process is presented within this chapter.

Chapter Four, as mentioned before, focuses on the trajectory modelling of the moisture transport that is carried out upon completion of the categorization process. A literature review on the method and background on trajectory modelling is also provided. As in the previous chapter the results and a discussion is also in this chapter. The case study of a single extreme event is the focus of Chapter Five. The results are once again discussed and comparisons with other similar work done in the past are also presented.

As variability of precipitation is an important aspect in the southern African region, it is important to examine this issue before we attempt to discuss the findings of the present study. The next chapter, Chapter Two, examines this topic by providing a literature review here as well as a discussion on the variability of extreme events and the relationship that they might have with other climate phenomenon such as ENSO. The importance of the study of extreme events will hopefully be established here.

In the final chapter, a summary of the findings of this study is presented. This chapter will thus bring together both the findings from previous studies carried out in the region on relevant topics as well as those that have been found in this study of spatially extensive heavy precipitation. Recommendations for future work will be presented here.

CHAPTER TWO: LONG TERM VARIABILITY OF PRECIPITATION

2.1: Introduction

Spatial and temporal variability in precipitation is experienced throughout the continent of Africa (Nicholson, 1989). These changes have a profound impact on the ecosystems and populations alike. Prolonged droughts or major floods are known to cause damage to both human lives and economies. Understanding the patterns of change and the possible causes of the variability is important in order to be able to understand the possible changes that may occur in future. However, studying variability is often difficult especially in Africa, due to a lack of consistent and reliable data (Easterling *et al.*, 1999; Mason *et al.*, 1999; Houghton *et al.*, 1996). Nevertheless, in recent years attempts have been made to understand the temporal changes in precipitation over different parts of Africa. Southern African climate variability has been of great interest and a number of publications now exist in this field (Lindesay, 1998; Mason & Jury, 1997; Rocha & Simmons, 1997a; Hulme, 1992; Nicholson, 1989; Tyson, 1986; Vines, 1980; 1982;). The temporal variability in rainfall over the region is known to occur both inter- and intra-annually. This chapter will examine the interannual variability in southern African rainfall, the possible causes for this and the implication it has for extreme precipitation events.

2.2: Interannual variability in precipitation

The interannual variability in rainfall over the southern African region is known to be very high (Tyson, 1986). It has also been found that the variability exhibits a statistically significant cycle (Tyson, 1986). Analysis of the rainfall series using spectral analysis has been attempted to reveal the existence of a number of distinct oscillations at preferred wavelengths (Tyson, 1986; Lindesay, 1984; Vines, 1980). Separate investigations on the different data series of several countries in the region have indicated the existence of quasi-periodicities on times scales of around 2.3, 3.5 and 5.0 to 6.0 years (Lindesay, 1998; Jury & Levy, 1993). These are thought to be possibly associated with the stratospheric Quasi-Biennial Oscillation (QBO) of equatorial zonal winds (Mason & Lindesay, 1993; Mason &

Tyson, 1992), sea surface temperature fluctuations in the tropics and subtropics (Jury & Levy, 1993; Nicholson, 1986), as well as influences of the El Niño-Southern Oscillation events, discussed further below.

In addition to these there are also lower frequency quasi-periodicities in the southern parts of the region (see Figure 2.1). Along the southern coast of South Africa, a 10 to 12- year spectral peak is evident (Tyson, 1986). In addition a quasi-18-year periodicity is also present in the annual rainfall totals of Zimbabwe, Lesotho, Swaziland, parts of Namibia and over the summer rainfall areas of South Africa (Tyson, 1986). This 18-year oscillation is believed to be responsible for much of the temporal variability experienced in the summer rainfall region of South Africa (Tyson, 1986).

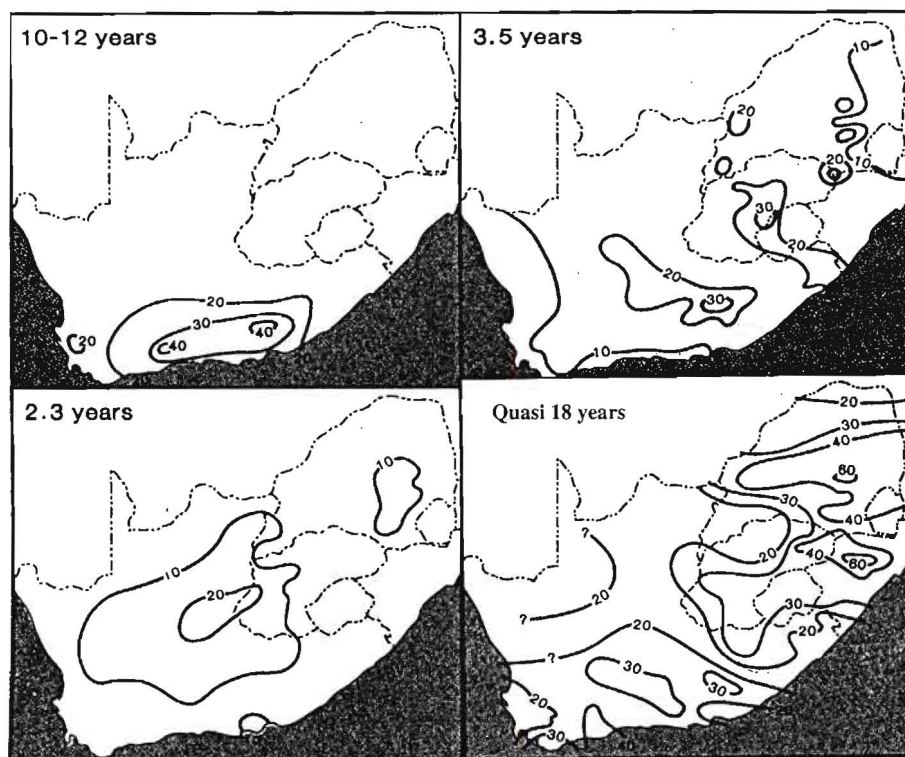


Figure 2.1: Percentage variance associated with 10-12 years, quasi 18-year, 2.3 years and 3.5 years rainfall oscillations over South Africa (from Tyson, 1986)

However, examining the actual annual rainfall totals themselves (Figure 2.2) shows the interannual variability and how this may fall outside the observed trend by a large margin. The 18-year oscillation can therefore only be used to predict the future trend of precipitation and not for a year-to-year forecast (Lindesay, 1998). Observation of this rainfall series for the region has revealed alternating periods of wetter or drier than average conditions (see Fig

2.2). The duration of these spells may range from weeks to months and even years. Much research has been done to observe the conditions that prevail during such dry and wet spells. Extreme events usually fall into these periods and as the interest of this study is in high precipitation events, the next section will discuss the synoptic conditions prevalent during wet spells.

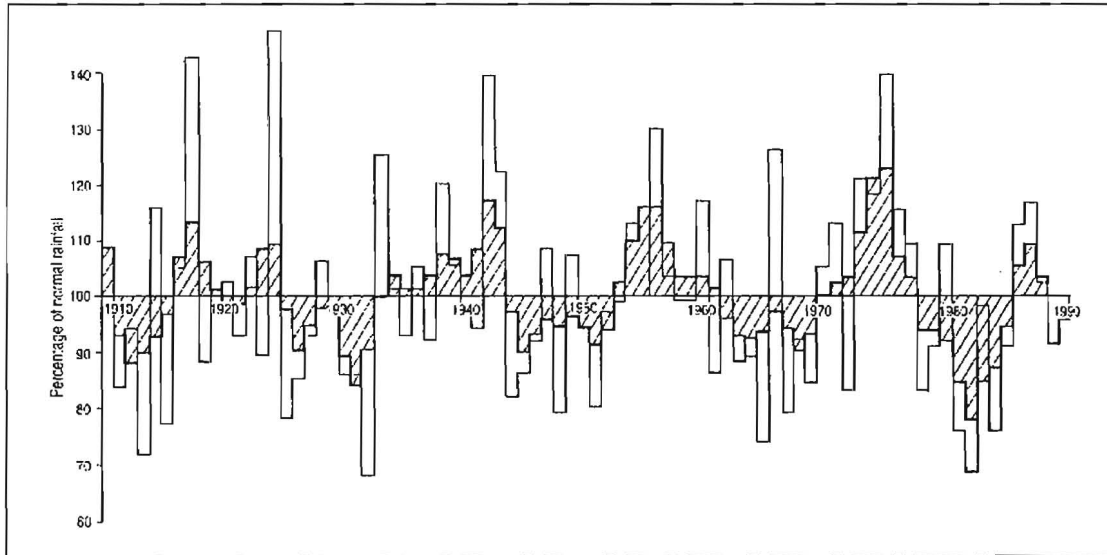


Figure 2.2: Areal averaged seasonal rainfall over the north-eastern region of South Africa for the period 1910 to 1990. The hatched area show the smoothed rainfall trend whilst the actual rainfall is represent with unshaded lines (from Tyson & Preston-Whyte, 2000).

2.3: *Wet spells over South Africa*

Rubin's (1956) observation of the short wet spell showed changes in the surface pressure field between the wet and dry periods (in Tyson, 1986). Below normal pressure was prevalent over the summer and winter rainfall regions during wet periods. The opposite was seen to occur during drier spells (Tyson, 1986). The surrounding oceans and the pressures prevailing over them were then also examined. Examination of the mean monthly conditions during the longer wet spells have shown that surface pressure anomalies exist over the Gough and Marion Island regions (Tyson & Preston-Whyte, 2000; Tyson, 1986). During a wet spell, positive anomalies appear over the Gough Island region with a negative anomaly over the Marion Island and over South Africa (Tyson & Preston-Whyte, 2000). The opposite situation is present during the dry spells. These observations are noted to occur for short spells as well as for longer spells (Tyson, 1986; Miron & Tyson, 1984; Tyson 1981). Tyson (1984) carried out principle component analysis using the pressures at various levels, to examine the

distinctive circulation types that exist on an annual scale. From this it is believed that most of the predominant controls lie at the 500hPa level for a large part of the country (Tyson & Preston-Whyte, 2000). The schematic representation of the circulation types responsible for the rainfall is given in the Figure 2.3. Correlations with rainfall to identify the specific regions affected by each of the circulation types were then done using the geopotential fields (Tyson, 1986). All together seven rainfall regions have been identified through this method and are represented in the Figure 2.4 along with the circulation type that correlates best to it.

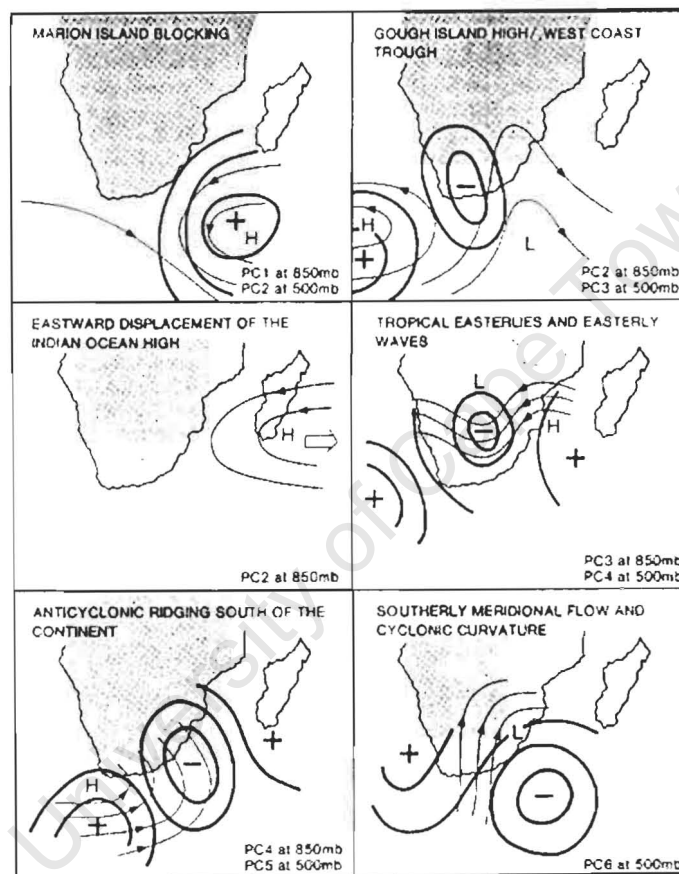


Figure 2.3: Schematic representation of circulation types responsible for rainfall (from Tyson, 1986).

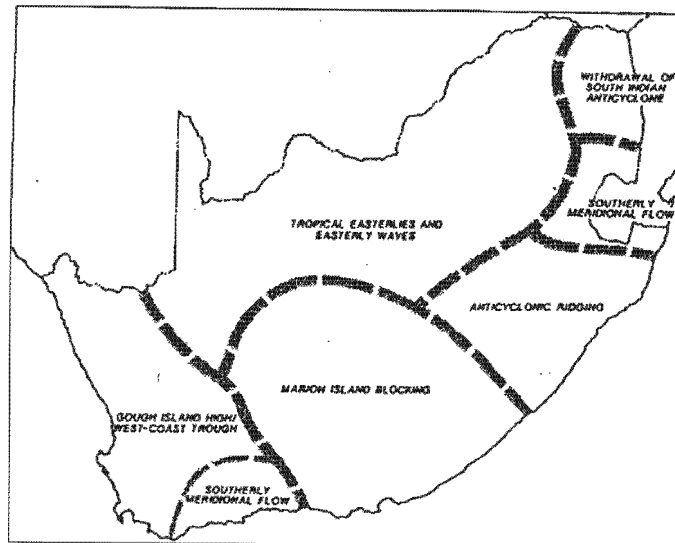


Figure 2.4: The seven rainfall regions for South Africa identified through correlation with circulation types (from Tyson & Preston-Whyte, 2000)

Figure 2.3 shows that when pressures over the Indian Ocean around Marion Island rise there is a distinct spatial rain pattern over the country (represented in Fig 2.4). This is termed as Marion Island blocking. Similarly a rise in pressure around Gough Island with a decrease around the west coast is categorized as the Gough Island High/West coast Trough. Passing cut off-lows are incorporated into this group (Tyson, 1984).

Tyson (1986) has also proposed a conceptual model of the atmospheric circulation that may be present during the wet and dry conditions. Analysis of the atmospheric condition associated with the wet spells reveal that the ascending limb of the Walker Cell is situated over tropical Africa over much of this time. A predominantly easterly flow is also observed in the upper zonal flow and more westerly flow is seen in the lower atmosphere (Tyson & Preston-Whyte, 2000; Tyson, 1986). A southerly subtropical jet is also observed. In Figure 2.5 (top) these conditions of the wet spells are summarised. In contrast the dry spells have very different conditions associated with them (Figure 2.5-lower).

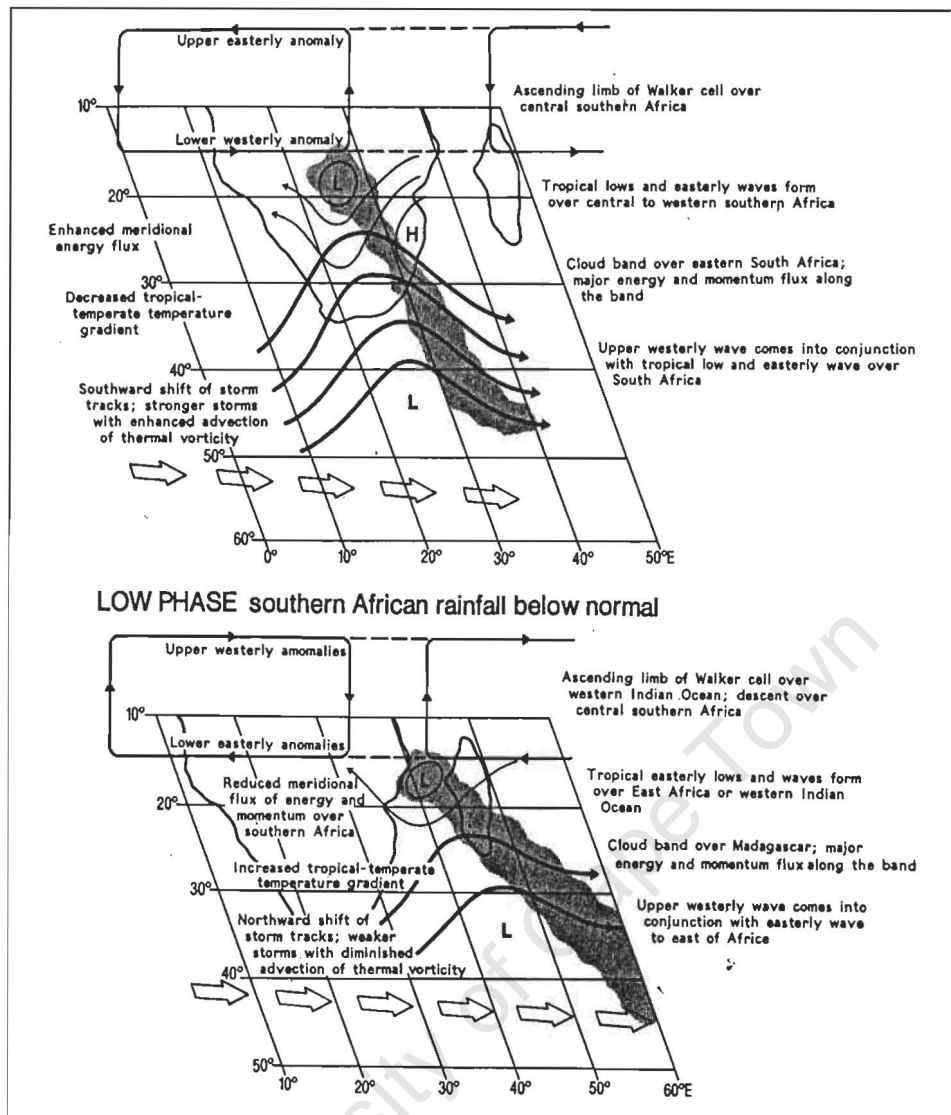


Figure 2.5: Model of the meridional circulation over South Africa during wet (above) and dry spells (below) (from Tyson & Preston-Whyte, 2000).

The studies carried out thus far indicate that despite the relatively high degree of interannual variability of rainfall in the region, there still exist clear statistically significant fluctuations that underlie the rainfall series. The relationship of these cycles has been compared to those of the rest of Africa (Nicholson, 1989), South America (Vine, 1982), Australia and New Zealand rainfall series (Vine, 1980). The existence of similar spectral peaks suggests the possibility of teleconnections between these regions, and that the variations may be hemispheric rather than just regional.

2.4: Causes of Interannual Rainfall Variability

Southern African rainfall variation is thought to be most affected by two principle components. One is the fluctuation caused by the El Niño-Southern Oscillation (ENSO) phenomenon and the other is by the variation in sea surface temperature (SST) in the oceans surrounding the subcontinent. Although these are not the only causes of variability in rainfall over the region, they are thought to be the most significant and will be discussed further.

2.4.1: The Walker Circulation, ENSO and South African rainfall

The ENSO phenomenon has in recent years been extensively documented. It involves the coupling of the atmospheric and oceanic anomalies across the tropical Pacific Ocean with the occurrence of extremes at irregular intervals. The pressure between the Pacific and Indian Oceans is seen to oscillate from time to time as a result of changes to the Walker cell caused by changes in sea surface temperatures in the Pacific Ocean. This pattern was given the name *Southern Oscillation* by Sir Gilbert Walker who first documented it (Diaz & Kiladis, 1992). The change can be measured using the pressure difference between Tahiti and Darwin, and is called the Southern Oscillation Index (SOI).

When the SOI is negative (low phase) the pressure over the Indonesian region is seen to be higher with low sea surface temperatures around the region. The pressure over the eastern Pacific Ocean falls with higher sea surface temperatures being present. Therefore the Walker circulation is such that the ascending limb is seen over the eastern Pacific Ocean and the descending limb over Indonesia. A descending limb is also present over eastern southern Africa and South America. This is what is termed as an El Niño event. During the high phase or positive SOI, the La Niña event, the eastern Pacific Ocean waters cool so that the pressure gradient is reversed. The Walker circulation is seen to reverse with the ascending limbs now over Indonesia, southern Africa and South America.

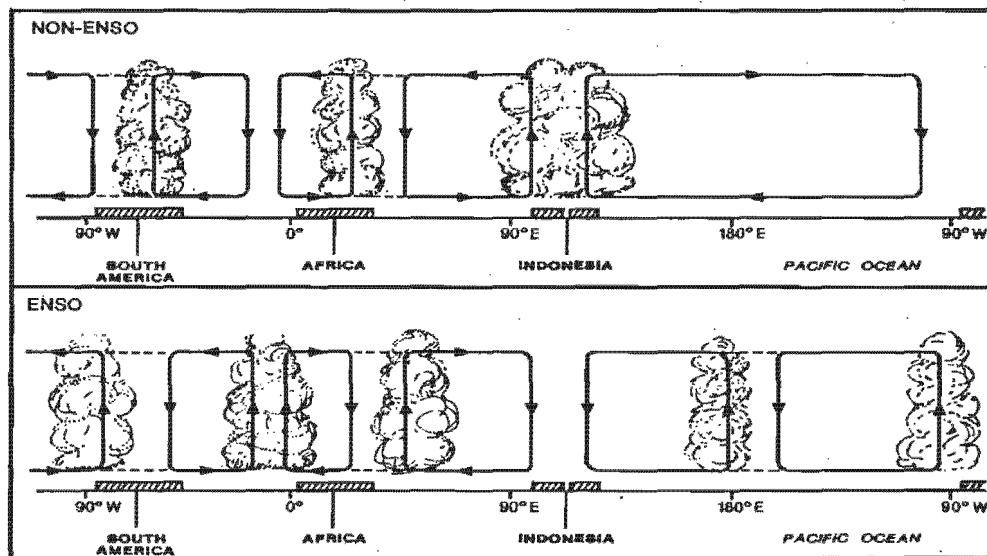


Figure 2.6: ENSO episodes and the Walker Circulation (from Tyson & Preston-Whyte, 2000).

ENSO is believed to be the largest single source of interannual variability on a global scale (Diaz & Markgraf, 1992). The relationship that ENSO has on southern African rainfall has been examined by Lindesay (1988). The frequent droughts experienced in the region are thought to be directly linked to the El Niño episodes in the Pacific Ocean. Work done by Rocha & Simmons (1997a) indicate that such a relationship may indeed exist. In their study, the SOI is used to find the correlation that might exist with rainfall over the eastern region of southern Africa. The findings show that there is a positive correlation between the SOI and the rainfall in this south eastern part of Africa. A region over the Northern province and Mpumalanga is seen to have a significant lag correlation with the SOI with up to a four months lead-time (Rocha & Simmons, 1997a).

It has been shown that during the high phase (La Niña) of the SOI, the central and eastern South Africa and Lesotho experiences good rainfall (Lindesay, 1988), with the correlation between seasonal rainfall and SOI values being significant over a large area (see Fig 2.7). During the low phase of SOI (El Niño) on the other hand there is often a decrease in rainfall in these same areas (Nicholson, 1993).

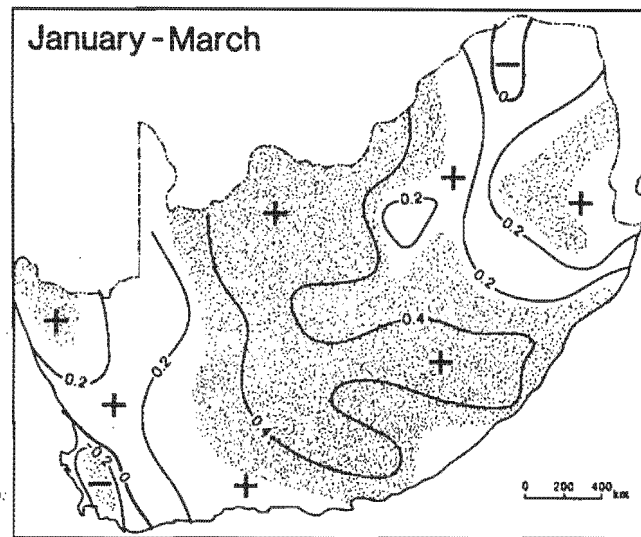


Figure 2.7: The correlation between the SOI and rainfall over South Africa during late summer. Shading shows 95% significance or better (from Lindesay, 1998).

Examining the circulation patterns during these two events (El Niño and La Niña) show marked differences over the southern African region. The circulation anomalies of these events are found to be identical to those of the dry and wet spells (Lindesay, 1998) discussed above. A physical mechanism by which the ENSO phase changes affect the rainfall over the region has thus been attempted (Lindesay, 1988; Lindesay *et al.*, 1986).

During La Niña events it is observed that the convective activity over the Indonesian region is enhanced (see Fig 2.6). Such a change has effects on the convective cell over southern Africa, which is the weakest of the three cells (Lindesay, 1998). La Niña conditions also sees easterly anomalies in the upper troposphere across the Indian Ocean and all over the subcontinent. Such anomalies are linked with the intensification of the tropical convection which also seems to be a precondition for the formation of tropical-temperate troughs and cloud bands over the region (Lindesay, 1998). Poleward transfer of angular momentum also occurs through these systems in late summer along the upper branch of the intensified Hadley Cell over the eastern subcontinent, whilst momentum is returned to the surface by midlatitude westerlies (Lindesay, 1998). All anomalies are reversed during El Niño events. Thus the preferred location of the principal rain-bearing systems is displaced eastwards (see Fig 2.5) and may form less frequently (Lindesay, 1998).

The relationship between ENSO and southern African rainfall with the Quasi-Biennial Oscillation (QBO) has also been examined. The QBO is a reversal of the stratospheric tropical zonal airflow from westerly to easterly. The SOI is found to be stronger when the QBO is in a westerly flow (Mason & Lindesay, 1993). During this westerly phase of the QBO, convection and upper-level divergence may be enhanced through the strengthening of the upper tropospheric westerlies off the east coast of southern Africa (Mason & Jury, 1997). Although there is much research that needs to be done on QBO, its influence over southern Africa does seem to be significant (Mason & Jury, 1997).

2.4.2: Sea surface temperature variability

In addition to ENSO phases causing variability of the rainfall in the region, changes in the sea surface temperatures of the South Indian and South Atlantic oceans also contribute to the variability experienced.

Recent studies have shown correlations between SSTs in certain parts of the surrounding oceans and the summer rainfall over the subcontinent (Mason & Jury, 1997; Rocha & Simmonds, 1997a). Walker (1990) has identified that the Benguela upwelling region along the west coast of South Africa and Namibia, the Mozambique and Agulhas currents along the east coast and the Agulhas Retroflection region in the south as the most important for rainfall over the subcontinent. Mason and Jury (1997) notes how the correlation between rainfall and SSTs in the Indian Ocean are linked to the monsoon and ENSO events. El Niño conditions in the Pacific has been associated with warmer SSTs over the northern Indian Ocean which leads to stronger convection over this region and decreased convergence over the subcontinent (Mason & Jury, 1997). However, the association between SSTs over equatorial Indian Ocean and rainfall appears to be nonlinear (Mason & Jury, 1997). Although dry conditions over the subcontinent do occur with warmer SSTs over western tropical Indian Ocean, the area is also thought to be a source of moisture for rain events (D'Abreton & Tyson, 1996; 1995; D'Abreton & Lindesay, 1993). Similar findings have also been presented in this study and therefore, increases in SSTs in this region could enhance rainfall over the subcontinent. It is therefore clear that the relationship is a more complex one. A broader discussion is presented in Mason and Jury (1997) and Lindesay (1998) where the changes of SSTs in the South Atlantic are also discussed. However, the findings indicated that a large-scale direct link between SSTs and rainfall is unlikely (Lindesay, 1998). Instead both signals

are likely to be a response to the atmospheric circulation changes caused by local or non-local events (e.g ENSO). The resultant SST anomalies and atmospheric circulation however can enhance or inhibit rainfall over the region (Lindesay, 1998).

2.5: Precipitation variability and extreme events

Although earlier studies of the precipitation records in the region indicated no definite overall increase or decrease (Lindesay, 1998), more recent findings show a decrease of about 10% over northern Botswana, Zimbabwe and eastern South Africa, for the standard periods between 1931-60 and 1961-90 (Gondwe & Jury, 1997; Hulme, 1992). Further evidence for a decrease in the mean annual rainfall is given by Mason (1996) for the eastern lowveld region of the country. This pattern is shown more clearly in Figure 2.8, in which the anomalies between the rainfall over the past century and the average calculated by Hulme *et al.*, (1996) for the 1961-90 period are plotted.

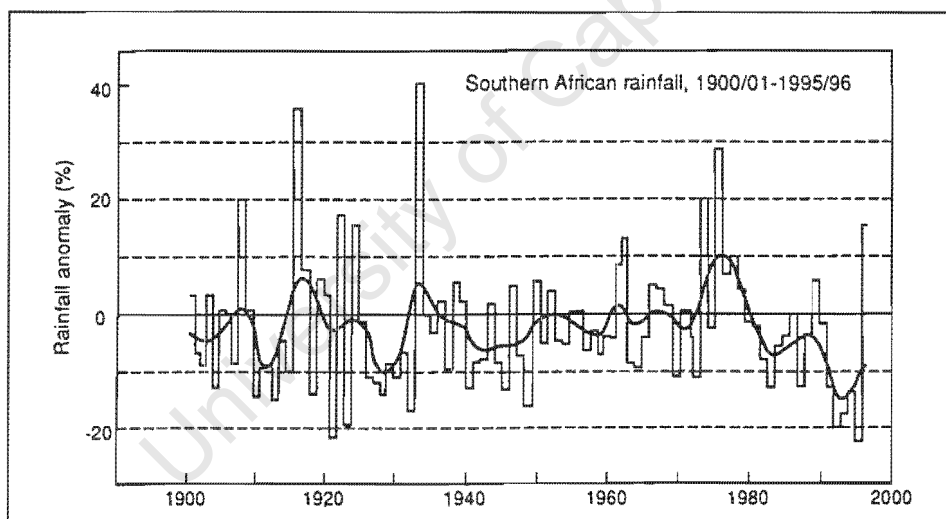


Figure 2.8: Annual rainfall trend for Southern Africa for the period 1900-01 to 1995-96 as anomalies from the 1961-90 average. Smooth curve shows the variation that is longer than 10 years (from Hulme *et al.*, 1996).

However, the annual zonally averaged precipitation for the regions between 0°S to 55°S increased by about 2% (Houghton *et al.*, 2001). The increase over the northern hemisphere is much greater at 7-12% for zones 30°N to 85°N (Houghton *et al.*, 2001). In addition to examining the accumulated total rainfall in different regions and their trends, the frequency of rain days and the intensity of the events are also important. These different aspects of studying precipitation make it a more difficult and complex task. Greater interest has been

placed more recently on understanding these issues and the impact climate change may have on them. Extreme events are thus the focus as the magnitude of change of these events may be far greater than previously thought.

2.5.1: Variability of extreme precipitation events

The Second Assessment Report of the IPCC mentioned the difficulty of studying these events due to the lack of homogeneous and high quality data (Houghton *et al.*, 1996). This issue is made further problematic with the fact that instruments used for climate data gathering have been inconsistent (Easterling *et al.*, 1999; Mason *et al.*, 1999). Therefore, comparisons over the years and between regions are made more difficult. Several recent publications have highlighted the existence of these problems when studying extreme events (Easterling *et al.*, 2000; Karl & Easterling, 1999; Joubert *et al.*, 1996). In many countries, especially in the developing ones, there still exists a lack of reliable climate data. This makes the examination of some extreme events impossible. The precipitation and temperature records for South Africa however, do date back to the end of the 19th century. There is also a reasonable consistency in the spatial coverage, which allows them to be used in observing the trends that may exist in them. Although globally there is still insufficient evidence to state a change in extreme events (Houghton *et al.*, 2001; Karl & Easterling, 1999), the region specific studies do show some important trends.

Easterling *et al.* (2000) summarises some of the findings from work done in various parts of the world regarding a number of extremes. The results on heavy precipitation show that the frequency has generally increased or decreased in the same manner as the overall precipitation of that region. In some cases, as for China for example, the area affected by extreme precipitation events has increased significantly (Houghton *et al.*, 2001). Karl and Knight (1998) found that over half of the annual precipitation increase over the US could be attributed to increases in the upper 10% of the daily precipitation amounts. This contribution that the heavy rainfall events make is pronounced during the summer (Karl & Knight, 1998). Comparisons of the total annual precipitation amounts and the contribution that heavy precipitation make to these have been done by Easterling *et al.* (2000) for a number of different countries, and indicates that the heavy precipitation events do indeed contribute to a large portion of the total amount (see Fig. 2.9 below).

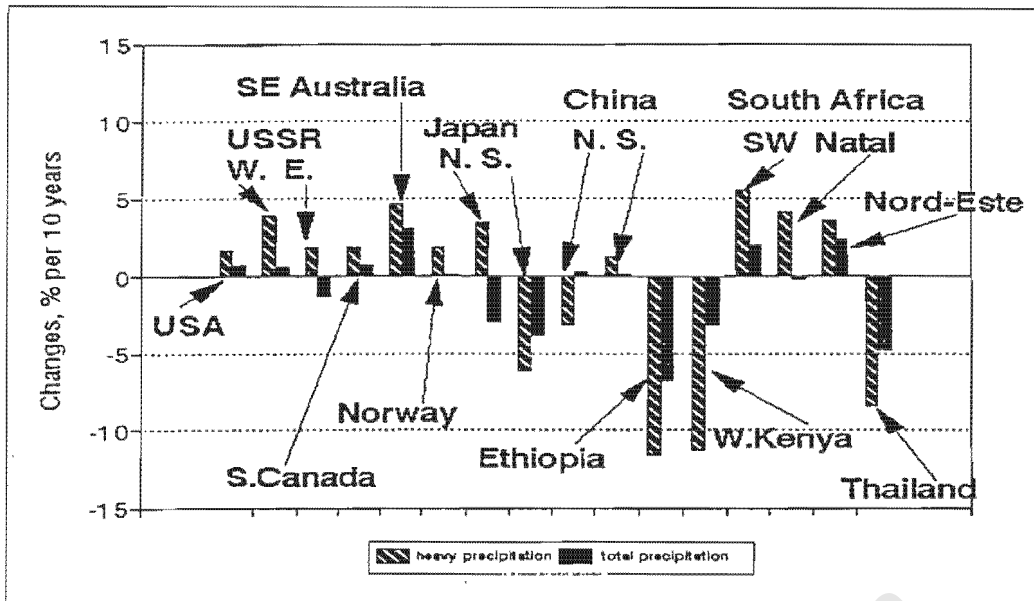


Figure 2.9: Trends in heavy precipitation and total precipitation during the rainy seasons in different countries (from Easterling *et al.*, 2000).

Similar studies have been attempted in South Africa to assess any possible change in heavy precipitation events. Mason *et al.*, (1999) examined the daily station rainfall data from 1931–1990 period. From the selected 316 stations, the annual maxima were used to test for changes in the intensity of extreme rainfall events. For the 10-year high rainfall events, increases in the intensities of the high annual maxima were noted in a large part of central South Africa (Mason *et al.*, 1999). Decreases were observed over the eastern part down to Lesotho, in the north-west and over the south-west (Fig 2.10).

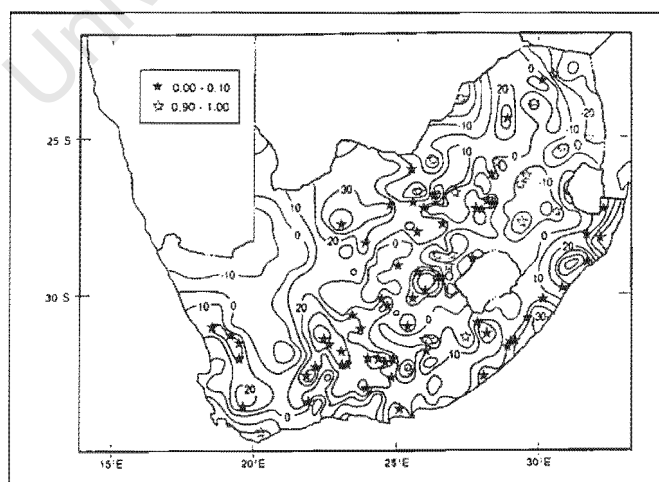


Figure 2.10: Percentage changes in intensity of 10-year high rainfall events between 1931-1960 and 1961-1990. Solid and hollow stars indicate stations where increase and decreases in intensity are significant at 90% level (from Mason *et al.*, 1999).

The increases in 65 of the stations in this case were significant at the 90% confidence level. This result means that the changes in intensity can be accepted to have occurred. Similarly the changes in the intensity of the low annual maxima were also obtained and seen to show a spatially less coherent picture. The magnitude of the changes in this case is also seen to be smaller. The areas affected by a decrease are over the west and south coasts and in the north-east (Mason *et al.*, 1999).

From Mason *et al.*, (1999) however, it was not possible to attribute the changes in intensity of the events to the changes in frequency or intensity of any one particular synoptic systems responsible for rainfall over South Africa. The cause for the increase in intensity over Durban in Fig 2.10 has been linked to the tropical cyclone Demoina of 1984 (Mason *et al.*, 1999). There is also evidence for a number of intense cut off lows that may have been important contributors to some of the heavy rainfall. Further studies are however needed in order to establish to what degree these features may have affected the intensity changes discussed here.

2.5.2: *Future predictions for extreme precipitation events*

With increased awareness of global warming and its impacts, scientists are now focusing on trying to assess the possible scenarios for specific regions so that mitigation measures where appropriate can be taken. The study of the possible changes in the means of various climate variables due to an increase in greenhouse gas concentration has been done extensively over the last decade, on both the global and the regional scales (Houghton *et al.*, 2001; 1996; Easterling *et al.*, 2000; Meehl *et al.*, 2000; Mason & Joubert, 1997; Gordan *et al.*, 1992). Understanding the effect on the extremes of these same atmospheric variables as a result of these changes in the mean has been one of the issues raised from these studies. There is sufficient evidence to suggest that such changes in these extremes will be disproportionate to those of the mean (Katz & Brown, 1992; Mearns *et al.*, 1984), and will therefore be more important in future studies. The relationship between the changes in the mean and extremes is more clearly understood through the use of an example.

If we consider the distribution of a climate variable, such as temperature, plotted on a graph, the result will show a normal distribution or a bell shaped curve. If at any point there is a shift in this distribution, it will be accompanied by an increase of the extremes on one end

and a decrease in the other (see Figure 2.11). This shift, which may occur due to a change in the mean or variance of the variable, is accompanied by a disproportionate change in the extremes (Mearns *et al.*, 1984). In the case of a change in the mean (Fig 2.11a), the frequency of the upper end of the extremes has increased nonlinearly with the change in the mean. The small change in the mean in this case has resulted in a large change in the frequency of the extremes (Meehl *et al.*, 2000).

The variance or standard deviation of the variable can also alter and cause a change in the distribution pattern (Fig 2.11b). Extreme events are thought to be more sensitive to such changes in the variance than to those of the mean (Katz & Brown, 1992). This change however must be greater than one standard deviation from the mean for this to hold (that is events that are highly extreme) (Meehl *et al.*, 2000). Lastly both the mean and the variance may change at the same time to also change the frequency of extremes. This is illustrated in Figure 2.11(c).

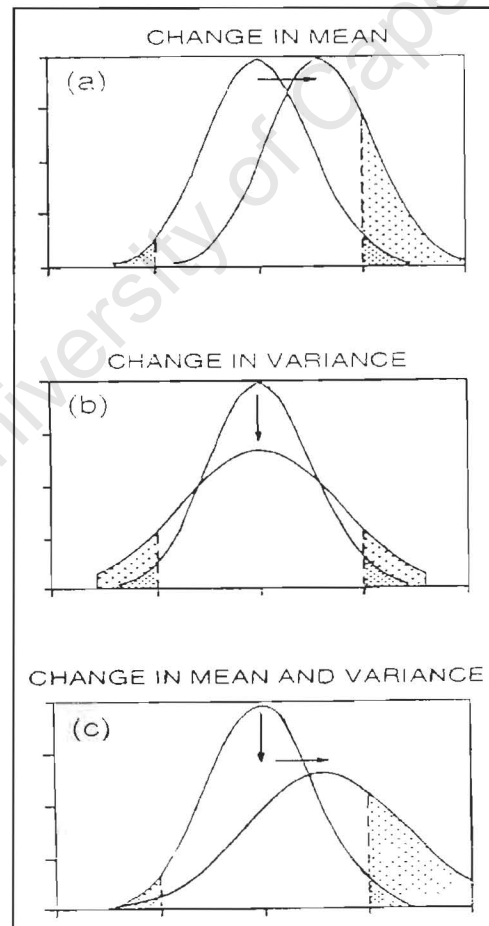


Figure 2.11: Graph showing change in extremes (shaded) with change in (a) mean, (b) variance and (c) mean and variance (from Meehl *et al.*, 2000).

However, the distribution pattern for precipitation is more complex than that of the normal curve shown above. It is often described as a gamma distribution (Groisman *et al.*, 1999). The mean and variance are connected through their dependence on the shape and scale parameter of this gamma distribution. This allows for the variance of the precipitation to change as well along with any change in the mean (Groisman *et al.*, 1999). Such complex relationships within a variable make the prediction of changes in future more difficult.

Observations of disproportional change in precipitation have been made in several countries and confirm the relationship explained above (Easterling *et al.*, 2000). Even though understanding precipitation events is a highly complex problem, with the use of specialised extreme statistics, it is possible to predict the extreme values without the detailed knowledge of the existing complete distribution (Meehl *et al.*, 2000). With these methods the change in the frequency of these events may be calculated for future climate scenarios. The simulations of future climate scenarios, which have been done for a number of regions around the world, now include the observation of the changes in extremes. These changes are expected to cause the most impact on both society and the ecosystems as a whole.

Simulations into the future using increased CO₂ scenarios have also been attempted in South Africa (Joubert & Hewitson, 1997; Mason & Joubert, 1997; Joubert *et al.*, 1996; Tyson, 1991). Under doubled CO₂ conditions, the simulation over Southern Africa using the Commonwealth Scientific and Industrial Research Organisation nine-level model (CSIRO9), showed an increase in the mean annual rainfall over much of the area (Mason & Joubert, 1997). However, only over the central part of the interior was there any significant change. This was accompanied with only small increases over the country of the actual number of rain days. The simulation also predicted a small increase in the intensity of the rainfall over most of Southern Africa. A larger increase of this is seen in the south western part of the country (Mason & Joubert, 1997). Joubert and Hewitson (1997) compared the results of both mixed-layer and coupled models to assess the possible changes due to CO₂ increases. Both sets predict a decrease in the summer rainfall in a range of 10-20%. An empirical downscaling technique was then used to see whether the predictions would differ. The results indicate a decrease in the eastern parts of South Africa of about 10-15% (Joubert & Hewitson, 1997). This is accompanied by a slightly extended late summer rain season (Joubert & Hewitson, 1997). These changes in the mean, although small can have a greater

impact on the frequency of extreme precipitation. The simulations of these are therefore also necessary and have been attempted in the study done by Mason and Joubert (1997).

When extreme events were examined, the simulation of flood events with a return period of 10-30 years (Fig 2.12) showed that the intensities of these events would increase, especially over the south eastern part of the country (Mason and Joubert, 1997). The changes of the 5-day accumulated rainfall extremes were also found to be similar.

The increase in heavy rain events over the north-east of the country, seen in Mason and Joubert (1997), may possibly be as a result of an increase in tropical cyclones frequency. This is conceivable, as an increase in SSTs (caused by the higher atmospheric temperatures) in the adjacent Indian Ocean may enhance the development of the cyclones. The changes in the temperature can have an effect on the hydrological cycle such that the intensities of these tropical storms may also increase. However at present, there is no clear evidence to indicate that the frequency or the intensities of these storm have been increasing. In fact in certain cases, such as for hurricanes in the Atlantic, the intensity of these storms have been found to have decreased (Easterling *et al.*, 2000). The observations over the Australian region have also shown a decrease in frequency of the total number of cyclones although the frequency of intense storms have increased, but it is not statistically significantly (Nicholls *et al.*, 1998). There also seems to be a correlation between the SOI and tropical cyclone numbers in this region. In the north Indian and south-west Indian Ocean there have been no long-term variation in the total number of tropical storms. The possible increases in the extreme events over South Africa in future must therefore be caused by other systems in addition to tropical cyclones. Further examinations and studies need to be carried out before a conclusive answer can be reached as to the exact manner in which rainfall will be affected in the region in future.

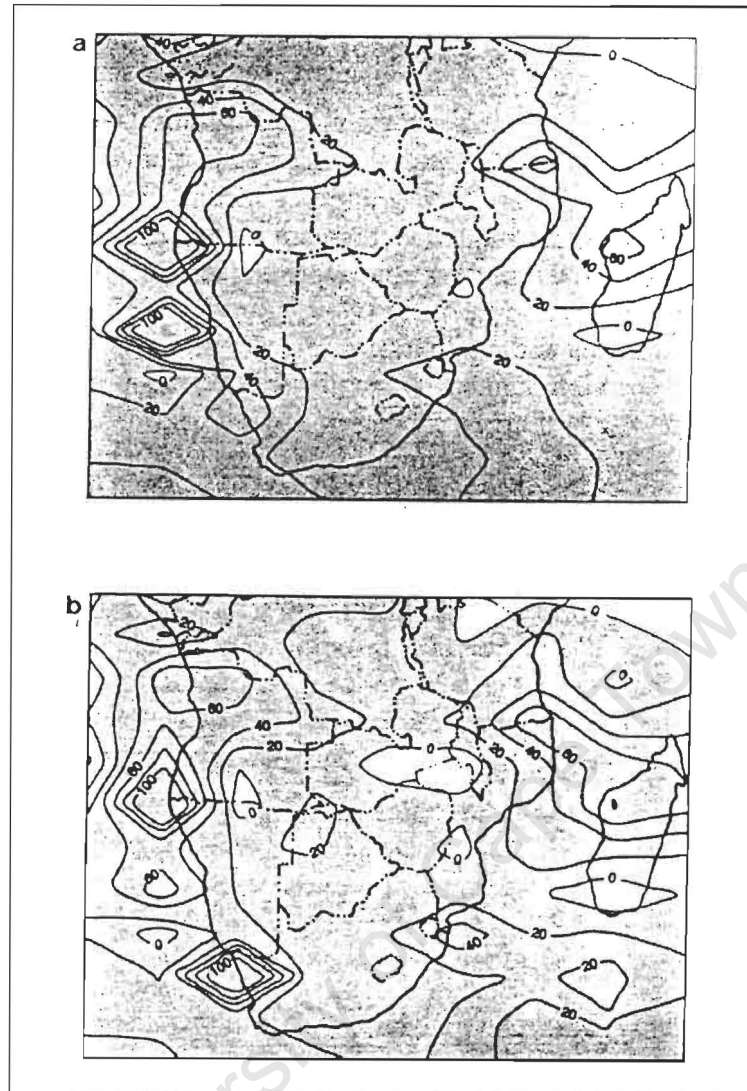


Figure 2.12: Simulated percentage changes in extreme daily rainfall totals for (a) 10 year (b) 30 – year return periods (from Mason & Joubert, 1997).

2.6: Conclusion

The aim of this chapter was to introduce the existing literature and findings with regards to the question of variability in precipitation over the region. It is clear that the topic has been much researched in the past and still remains a most important topic to climatologists in the region. Understanding the variability in the data record becomes important in order to find better ways to predict or forecast future trends. The complexity of understanding rainfall patterns and causes was hopefully also gained through this chapter

In recent years the understanding of extreme events has become more and more important as the impacts of these events are usually large and widespread. Although there has been no clear indication that extreme events have been increasing in the region, it is clear that changes caused by climate change are bound to affect the frequency and intensities of these events. If initial findings on the variability of rainfall in the region are taken into account, there is definitely a high possibility that the number of heavy precipitation events affecting South Africa will increase. The intensities of these events may also increase such that the damage that may be caused can be even higher than those experienced in the recent past. The costs of these events to both the communities that are vulnerable and the countries economies need to be also assessed. Through this mitigation measures such as better government policies, may be made in future. Modelling work that are being carried out now are therefore sensitive to these issues and are more likely to include observations of any change in these events along with changes in the means of variables.

In the following chapter, attempts will be made to categorise the heavy precipitation experienced in the country and to observe any spatial patterns that exists within them. The frequency distribution of these events will also be examined. The possible sources of moisture and their transport for the events will be investigated with the use of a kinematic model.

CHAPTER THREE: CATEGORIZATION OF EXTREME PRECIPITATION EVENTS

One of the questions that this study investigates is the spatial structure of extensive heavy precipitation over South Africa and whether there may exist cohesive patterns to these events. The categorization process tries to address this question. In the previous chapter, the various categorization methods were discussed. The Self Organizing Map (SOM) method was chosen for its advantages as stated previously. In this chapter, background information is given on this method as well as information on Artificial Neural Networks (ANNs). The SOM is a special form of an ANN, and an understanding of these neural networks will be useful in comprehending the final results from this method.

3.1: Artificial Neural Networks

Artificial Neural Networks can be described as “*networks of highly interconnected neural computing elements that have the ability to respond to input stimuli and to learn to adapt to the environment*” (Patterson, 1996, pg 1). They were initially based around the design of our own biological neural network, the central nervous system. However the present models have advanced to a degree that this resemblance may no longer exist.

A neural network is characterized by its *architecture* (pattern of connections), its *training or learning algorithm* (method determining the weights on each connection), and its *activation function* (Fausett, 1994). The neural network is comprised of a large number of neurons, units, cells or nodes, which are the simple processing elements. Each of these have corresponding *weights* and they are all connected to other neurons. The weights act to either increase or decrease the input signals to the next neuron (Patterson, 1996). The diagram below (Fig. 3.1), illustrates how such a simple neuron works.

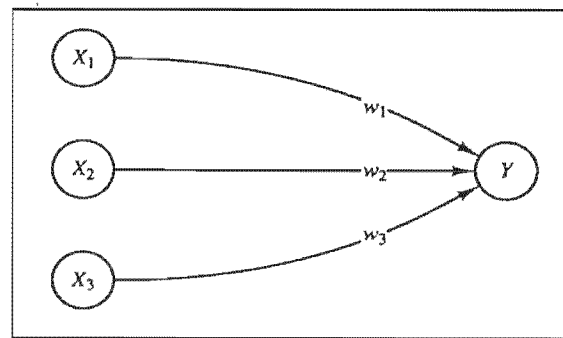


Figure 3.1: A simple neuron Y , which receives input from neurons X_1 , X_2 and X_3 whose associate weights are w_1 , w_2 and w_3 respectively (from Fausett, 1994).

Neuron Y above receives inputs from neurons X_1 , X_2 and X_3 and the weights associated with these three input neurons are w_1 , w_2 and w_3 respectively. The activations or output signals from the input neurons can be labelled x_1 , x_2 and x_3 . The net input to neuron Y , y_{in} , is therefore the sum of the weighted signals from these input neurons, i.e.,

$$y_{in} = w_1 x_1 + w_2 x_2 + w_3 x_3 \quad (\text{Fausett, 1994}) \quad (3.1)$$

In a simple neural network, the neuron Y may be further connected to other neurons (e.g. Z_1 and Z_2) with respective weights (v_1 and v_2) (Fig 3.2). In this case Z_1 and Z_2 will receive different input values from neuron Y due to the different weights associated with them.

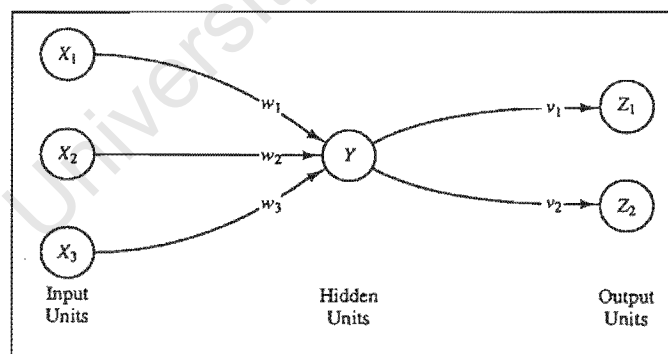


Figure 3.2: A simple neural network in which there is an input unit layer X_1 , X_2 and X_3 whose associate weights are w_1 , w_2 and w_3 , a hidden layer with neuron Y with weights v_1 and v_2 leading to the output unit layer Z_1 and Z_2 (from Fausett, 1994).

In the above illustration, we can consider the hidden units/neurons to be part of one *layer* and the output units to be part of another. All units within a layer behave in the same manner. The arrangement of the neurons into these layers and the connective patterns they form is part of the net architecture (Fausett, 1994).

Neural networks (or nets) can be divided into single layer or multilayer structures. The number of layers in a net can be defined as the number of weighted interconnected links between slabs of neurons (Fausett, 1994). Therefore the net illustrated in Figure 3.2 consists of two layers. The direction of the signal flow in either of these cases, (i.e. single layer or multilayer), maybe feedforward or recurrent. In the feedforward nets, the signals flow from the input units to the output units in a forward direction. However in the recurrent net, there are closed-loop signal paths from a unit back to itself. This is the case for a competitive net as illustrated below (Fig. 3.3). The weights of the competitive interconnections in this case are $-\epsilon$. Self Organizing Maps, discussed in the following section, are part of competitive nets.

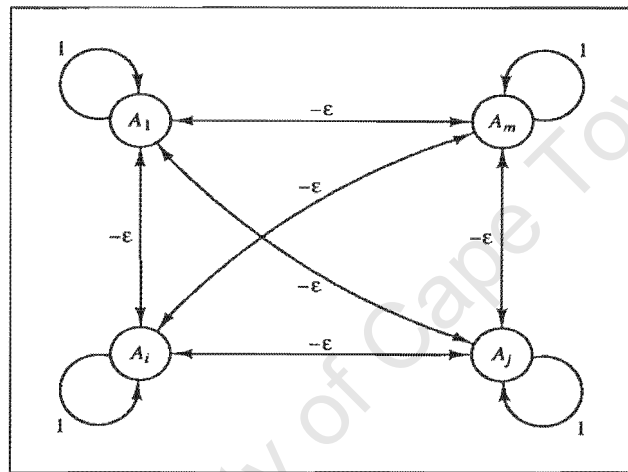


Figure 3.3: A competitive layer of A_1 , A_i , A_j and A_m neurons with $-\epsilon$ weights associated with them and some recurrent signal flows to the neurons shown with 1 (from Fausett, 1994)

In addition to the structure of the networks, the allocation of weights or the training process is an important one, and can differentiate neural networks. The two major types of training are supervised and unsupervised training. Supervised training involves presenting the net with a sequence of training vectors, or patterns, each with a target output vector. The weights are then adjusted according to a learning algorithm in an attempt to reduce the error between the predicted output pattern and the target output vector. Training is complete when the error can no longer be improved and has reached an acceptable level for the new set of patterns not initially available in the training data set. Once this is achieved any input data set, which is within the bounds of the training set, may be presented to the net (Hewitson & Crane, 2002).

In unsupervised training, there are no target output vectors specified. In this method, the net modifies the weights so that the most similar input vectors are assigned to the same output (or

cluster) unit (Fausett, 1994). Learning is accomplished by strengthening the weights on the neural units that respond the most to the input training signals or vectors. Those with weaker responses are either ignored or their weights are reduced. Competitive learning is based on this and is an important class of the unsupervised training method.

Neural nets are also distinguished by their different activation functions. For the input units, this function is known as the identity function and sometimes is associated with a step function to convert the net input, which is a continuously valued variable, to an output unit that is a binary or bipolar signal (Faucett, 1994). The activation function for all neurons within a layer is usually the same and it may be a nonlinear function such as a sigmoid function, with a threshold that is rounded (softer) compared to the step function (Dayhoff, 1990). Most multilayer nets however, utilize nonlinear functions such as logistic or hyperbolic tangent functions.

These different architectures and training methods have been developed over time, to enable ANNs to be used in a variety of fields. ANNs have a range of potential uses such as in signal processing (e.g. reducing noise on telephone lines), control (e.g. in manufacturing to improve efficiency and effectiveness), pattern recognition (e.g. handwriting recognition), medicine, speech production and recognition, business and many more (Faucett, 1994; Patterson, 1996; Tarassenko, 1998). In the research field ANNs also have major advantages that are now being seen and used. It was introduced into the field of geography (Hewitson and Crane, 1994) and since then there have been a number of papers published using ANNs (Gardner & Dorling, 1998; Marzban & Stumpf, 1996; Bankert, 1994; Navone & Ceccatto, 1994; Badran & Thiria, 1991). In climate research, ANNs can offer a number of benefits. The ability to detect patterns in noisy data is one of the most important benefits as this forms the basis of a range of research in the field. The ability to handle large volumes of data and process it extremely fast is also useful. Amongst the many methods that exist for use of this technology is that of Self Organizing Maps. Although its use in climate research is still small, a number of recent studies using SOMs exist. Hewitson and Crane (1992) used it in a study that considered the large scale atmospheric control on local precipitation. It was also successfully used by Main (1997) for categorizing observed sea level pressure data and those from a GCM run. Other studies using SOMs for categorization are those of Hewitson & Crane (2002), Tennant (2002), Gutowski (2001), Cavazos (2000) and Hudson (1998). In the present study the SOM method is used for the categorization purpose of extreme precipitation events that

are spatially extensive. A better explanation of the SOM method itself is given in the subsequent section. This will make it easier to understand its use in this study and the results obtained.

3.2: Self-Organizing Maps

The Self Organizing Map method was developed by Teuvo Kohonen in the early 1980's. It is essentially a tool for use in clustering, visualization and abstraction (Kohonen, 1997). The SOM architecture comprises of an output layer of nodes arranged in a single or multi-dimensional lattice. There are two topological structures that may be chosen, a hexagonal or a rectangular lattice (Fig. 3.4).

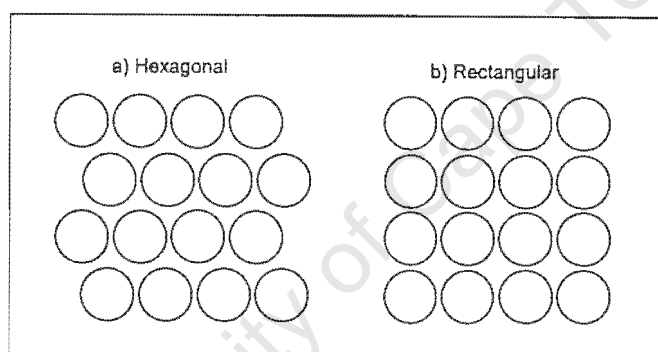


Figure 3.4: The two topologies available in SOM - a) hexagonal and b) rectangular (from Hudson, 1998).

The choice of the lattice has been shown to have little effect on the end product (Openshaw, 1994) but the rectangular lattice is better for visual display and analysis. The weights associated with each of the nodes are initialised with a starting value, before the training session. As is the case with other competitive networks, during the training process, the node whose weight vector matches the input pattern most closely is chosen as the 'winner'. The associated weight vector is then updated. However, unlike in other networks, the neighbouring units of the 'winner' also benefit from the learning process by adjusting their weights such that each vector converges to the input pattern. The area within which these nodes and their associated weights are updated is known as the *update neighbourhood*, with the 'winning' node at the centre. The weights are updated based on the following function;

$$m_i(t+1) = m_i(t) + h_{ci}(t)[x(t) - m_i(t)] \quad (3.2)$$

where m_i is the vector of weights associated with node i , $x(t)$ is the input vector at time t , and $h_{ci}(t)$ is the neighbourhood kernel (Kohonen *et al.*, 1995). The neighbourhood kernel determines which of the surrounding nodes are updated. It may be described using the following expression;

$$h_{ci} = \alpha(t) \cdot \exp[-d^2 / 2\sigma^2(t)] \quad (3.3)$$

where d is the distance from the winning node, $\sigma(t)$ is the radius of the neighbourhood at time t , and $\alpha(t)$ is the learning rate at time t (Kohonen *et al.*, 1995).

This function results in the update rate of nodes decreasing outwards from the ‘winning’ node. During the SOM training, the radius, σ , decreases to a small constant, whilst the learning rate, α , which determines how easily the weights can be altered, decreases to zero. The number of training iterations, t , is chosen such that convergence is achieved at the end of the training. This number can be anything from 100 to 100 000. As a “rule of thumb”, it is recommended that the iterations should be at least 500 times the number of nodes (Kohonen, 1997). If the sample of input data is smaller than the number of iterations, then the sample is used reiteratively in the training. This process results in more nodes being placed where there is a higher data density and few where data is sparse. The vectors adjust during the iterations such that they span the entire data space, and each of the nodes will represent a position that is approximately the mean of the nearby data samples (Hewitson & Crane, 2002). This produces the “arch-type” points in the data space.

After the training is complete, the vectors of the weights associated with the nodes or “arch-type” points, can be mapped to display the features present within each of them. The next step involves mapping each individual data sample to the node with which it has the lowest error. A record of this is kept and can provide frequency results of the mappings to each of the nodes.

In this study the SOM was applied with the use of the SOM_PAK version 3.1 software⁵. The requirements of the input data for use in this software meant that some data preparation had to be done before hand. This process is explained in the following section.

⁵ Available online at http://www.cis.hut.fi/research/som_lvq_pak.shtml.

3.3: Data Preparation

From the daily CCWR precipitation data, days classified as extreme events needed to be extracted. The criterion for such an event in this study is based on the magnitude of the accumulated daily precipitation amount. This meant that the duration of the event was considered to be only one day. Since the 'normal' precipitation in South Africa differs greatly depending on the area or region, the threshold upon which the specific days are collected had to be chosen carefully. Initially this was based on the 95th percentile for each of the cells in the domain. To select days with extreme rain over a widespread area, the days selected were then those that had 800 or more cells within the domain, equal to or above their respective 95th percentiles. This method yielded 816 days from a total of 4320 days for the summer season, and 118 days from a total of 4416 days for the winter season for the years 1950-1998. The SOM_PAK software is also capable of handling missing data within the set and therefore, this did not pose as a problem.

The results of the initial run prompted further changes to be applied to the input data. Firstly it was noted that the use of the absolute precipitation values in the SOM might not be ideal. These values if plotted represent an exponential curve. The use of absolute values in such a case may cause most of the SOM nodes to be located at one extreme and not show the entire range evenly. The use of the natural logarithmic (ln) values instead will eliminate this by creating a more linear data curve along which the nodes may be placed. The SOM is then able to bring out better results in the clustering process. The CCWR data set was also smoothed spatially using a 9 X 9 weighted kernel, before extracting the extreme event days. This was done to better represent the spatial pattern and avoid bias towards single grid cells experiencing a localized event.

Although both the winter and summer seasons were initially used for analysis, focus was later placed on just examining the summer seasonal data. The results of the initial SOM for the winter seasons showed few diverse clusters with the main focus being on the coastal and the Western Cape regions. This was as expected since these areas are the main winter rainfall regions of the country. For the possible application of the results at a later stage, it was also taken into consideration that the agricultural sector of the country is primarily based within the summer rainfall region and is thus most likely to be affected by extreme events such as those being investigated here. Therefore, they would benefit most from the results of this study if the focus was placed on the summer season alone.

The criteria that were used to select the extreme event days were also modified after the initial SOM runs. It was found that the initial criterion allowed for an unbiased selection based on the 95th percentile of each cell or pixel within the domain. This meant that a cell or pixel could be included even if the magnitude of rainfall was low, due to the range of rainfall for that cell being on the lower end of the scale. This is seen to occur in the more arid regions of the country. The selection process was therefore including days with very low overall rainfall amounts as extreme event days. Although it falls within the definition of extreme events as used in the study, it is not climatological significant. In order to eliminate these inclusions, a maximum precipitation threshold was set at 20mm instead of using the 95th percentile. This threshold value was selected after scanning the range of maximum precipitation observed within the domain for the set time period. The number of cells that needed to be above the threshold per day in order to be selected as an extreme event day remained at 800. This selection however, does not mean that all the selected cells are placed in the same area. There are days selected therefore, in which no coherent rain event is apparent but rather scattered high values throughout the domain is obvious. The satisfaction of the criterion that 800 pixels are above the threshold allows such days to be selected into the subgroup as an extreme event day. The number of such inclusion however was found to be low and since no alternative method was found for the selection criterion, the final selection using this process was kept. A new input data set for the SOM procedure with 439 days (from the summer season) was thereby selected for the classification. The exact settings that the SOM_PAK software used are discussed next.

3.4: The SOM Procedure

The detailed description of the program packages contained in SOM_PAK version 3.1 is given by Kohonen *et al.*, (1995). The SOM is implemented in four stages. Within each of these stages different options are available for use. The ones chosen in this study are explained here. The first stage is the **map initialisation** process. This step primary deals with initialising the reference vectors (or weights) of the node as well as establishing the type and size of lattice and the neighbourhood function type to be used. Either a random initialisation or a linear initialisation may be chosen. In the latter, the reference vectors are initialised orderly along a two-dimensional subspace between two principal eigenvectors of the input data (Kohonen *et al.*, 1995). The random initialisation, which is used in this study, allocates random numbers to the reference vectors evenly distributed in the data space. Two

choices also exist for the lattice type as was mentioned in the previous section. In this study a rectangular lattice was preferred. The size of the lattice was set to 3 by 4 for the final runs. The final step in this first stage is to then specify the neighbourhood function type, which determines which of the surrounding nodes will be updated. This may either be done with a Gaussian function, or with a step function (called 'bubble' in SOM_PAK) as was used here. This function is in essence a smoothing kernel defined over the lattice points and is a function of both time and space (i.e. the chosen radius). The results from this stage are then used in the next.

The second stage of the SOM is the **map training** process. The initialised node vectors are trained using the precipitation data with the self-organizing map algorithm (3.2) discussed in the previous section. This training is done in two phases. The first with an initial training radius of three and a learning rate parameter set at 0.1. The training in this phase is when the ordering of the map occurs and the length of the training need not be too long. This was set at 8000 iterations. The proper ordering of the map is also better achieved if the radius is set to begin with a higher value. This is then allowed to decrease linearly to one. If the radius is set too small at this initial stage, various kinds of errors of the map may occur (Kohonen, 1997; Clothiaux & Bachman, 1994). During the second training phase the number of iterations was increased to 80 000. Final convergence or the fine adjustment of the map occurs in this phase and requires a longer time period. The radius for this phase was also reduced to one so that only nearest-neighbour interactions remained. This allows for a better response to the local structure in the input vectors (Clothiaux & Bachman, 1994). The learning rate was decreased to 0.05 and during both training phases this rate will decrease to zero.

The **evaluation of the quantization error** and monitoring forms the basis of the third stage of the SOM. For each input vector, the winning node is selected through an assessment of the Euclidian distance to the node vectors. The shortest distance or quantization error is thus calculated and the input vector is allocated to that node. The best SOM map is attained when the smallest average quantization error is obtained. This is the average of all the minimum Euclidian distances of the input vectors (Cavazos, 2000). Monitoring the progress of the SOM is often useful in detecting any errors or problems, and can be done quickly with the use of the Sammon mapping technique (program available in SOM_PAK). This is a method of non-linear mapping that allows the mapping of high dimensional data space to a lower

dimensional space whilst maintaining the structure of the data (Sammon, 1969). It can be used here in conjunction with the SOM to create a two dimensional image of the reference vectors (nodes). The distances between the image vectors approximate the euclidean distance in data space. This method is therefore useful in trying to assess the spread of the SOM across data space. The Sammon map should not represent any folds in the image, as the interpretation of such an outcome becomes more complex (Tennant, 2002). However, if this has occurred the SOM process can be easily repeated to produce a better result. The SOM itself will not be identical, as it is not reproducible since the initialisations will be different in each case, but the results of all of them are valid (Tennant, 2002).

The final step in this process is the **map visualisation**. This is done so that each data sample can be allocated to the best matching node in the map. The individual quantization errors of these are saved into an output file along with the node or class label. This file is useful when calculating the frequency data for each node and other statistical information on the nodes. The information on the vector points or nodes in the map are saved in a similar manner to the original input data itself. It is therefore possible to view this output file using visualisation software such as GrADS (Grid Analysis and Display System)⁶. In the following sections the results obtained are examined and explained.

3.5: Classification Results and Discussion

The aim of the SOM procedure was to classify the days identified as spatially extensive extreme event days into several groups or clusters so that they could be further analysed. This is seen to have been achieved as will be shown here.

The results of the SOM are displayed as a series of maps with the aid of the GrADS software. One of the advantages of using the SOM method over the more traditional ones is that it enables the visualisation of the relationships between the nodes (Hewitson and Crane, 2002). This is achieved through the ability of the method to arrange the distribution of the nodes into a two-dimensional array with similar nodes located close together and the dissimilar ones further apart. The transitional states are placed between these nodes. Therefore, in the following diagrams (Figs 3.5, 3.6), the maps next to each other can be said to share some

⁶ Available free from <http://grads.iges.org/grads>

similarity, whilst those further away have much less similarity to each other or are dissimilar. This transition from one map to the next can be visually observed in the SOM diagrams. The results of the initial SOM are given in Figure 3.5 so that it can be compared with the one done after the modifications of the initial input data. The final SOM results are presented in Figure 3.6.

University of Cape Town

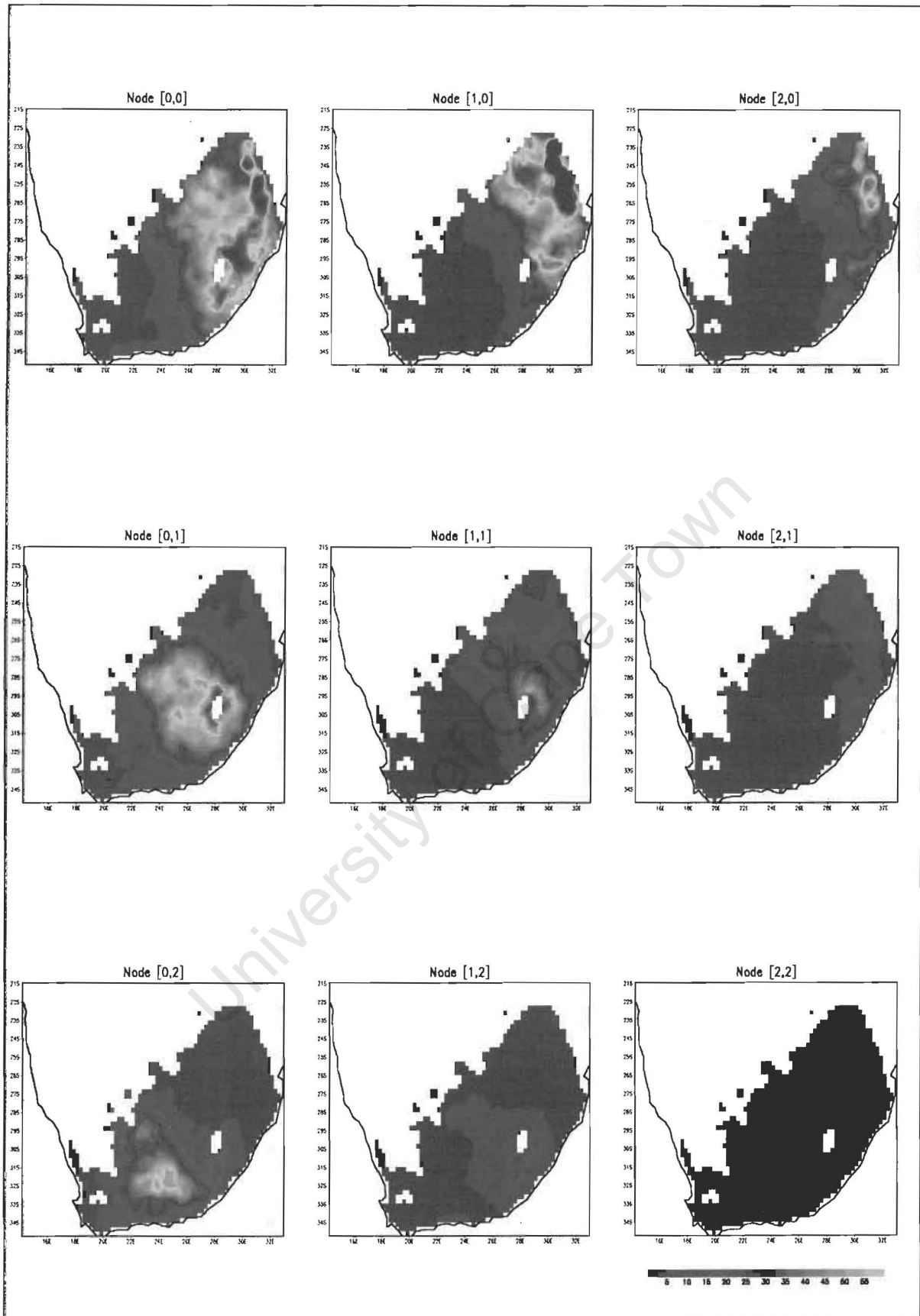


Figure 3.5: Initial 3X3 summer (DJF) SOM results. Colours represent actual precipitation amounts in millimetres.

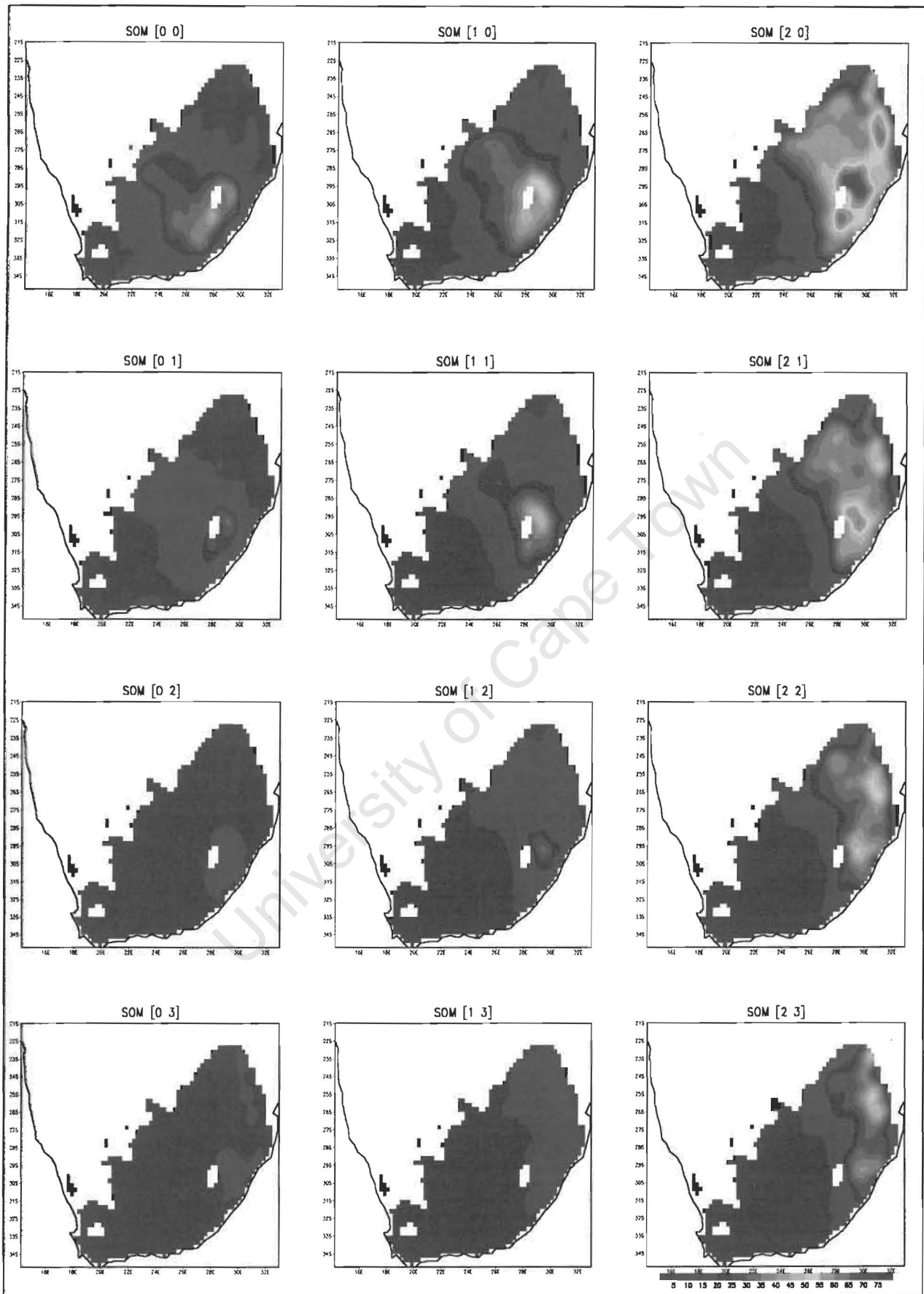


Figure 3.6: Modified 3X4 summer SOM results. The colours represent actual precipitation amounts in millimetres

Comparing the summer SOM results of the initial (Fig 3.5) and final maps (Fig 3.6) show that there are a number of similarities between the two classifications. The areas with the highest total precipitation are seen on both sets of results to be in the eastern and northeastern sectors of the country. The final SOM diagram does however show a more distinct pattern across the interior of the country with northwest-southeast axis (nodes [0 0], [1 0] and [1 1]). If we consider the possible synoptic condition that may have resulted in such a pattern, it is likely to be caused by tropical-temperate troughs. As was discussed in the previous chapter, these systems are responsible for a large portion of the summer rainfall over the region (Harrison, 1984a; Lindesay, 1998). It is therefore conceivable that such a pattern would be represented in the classification. The transition states from this pattern are also clearly seen in the maps of Figure 3.6.

The final summer SOM diagram also shows that there are nodes represented by very low precipitation values (e.g. node [0 2], [0 3] and [1 3]) present. The node maps themselves are however representations of the average of all the input samples (days) that are mapped to them. Therefore it does not necessarily mean that all the days associated with the node will have the exact same characteristics shown on the maps of the SOM diagram. If particular input days have low rainfall values scattered within the domain, the resultant node map representative of these days may be represented with a pattern similar to the ones seen in node [0 2], [0 3] and [1 3]. From the criteria used in the selection process, it was shown how this occurrence is possible. This led to the decision to eliminate these nodes from further analysis and to concentrate rather on ones that show higher precipitation values.

It is also possible to analyse the frequency of each of the resultant SOM nodes using the output results. This has been done for the final SOM results and the graph in Figure 3.7 represents these findings. Examining the frequency graph shows that the node [2 2] has the highest number of events mapped to it, whilst node [1 0] has the least. The distribution of the events in general however appears to be dispersed more evenly. The frequency also seems indicate that events occurring in the northern, northeastern and eastern parts of the country are heavily numbered (e.g nodes [2 0], [2 2] and [2 3]). Therefore not only does the classification show that the actual amount of rainfall in these regions to be the highest but the frequency of events in these same regions are found to also be highest.

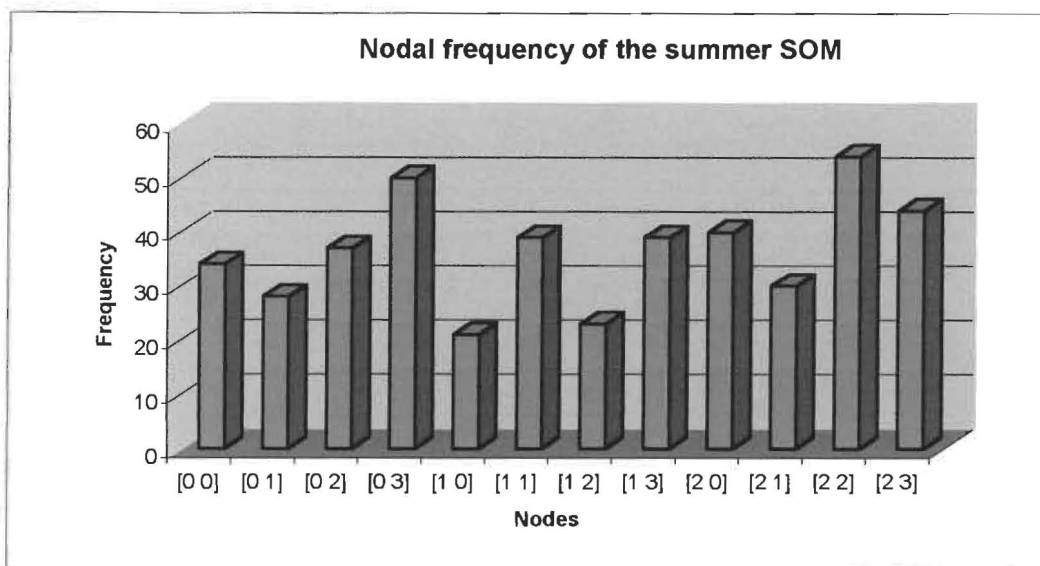


Figure 3.7: Frequencies of each node in the modified summer SOM shown in Figure 3.6.

It was also noted that node [0 3], which in fact showed a precipitation pattern with very low overall values, has the second highest frequency in the classification. This pattern, which as explained earlier is most likely due to the selection process, has incorporated a large percentage of the total number of days/events for classification.

The SOM process also retains a record of the actual event dates that are mapped to each of the nodes. This information can be used when analysing any particular node to a greater extent. The general atmospheric circulation pattern associated with these days can then be analysed with the use of the NCEP reanalysis data. This type of analysis was only attempted with the event days post-1979 as a precaution with the use of NCEP data (as was explained previously). The total number of days that were available for analysis for each node is given in the Table 3.1. Of the total 12 nodes in the SOM map, only three ([0 0], [2 0] and [2 3]) were used in the detailed examination. This was done for a practical reason and the nodes chosen for this purpose were those that are outliers in Figure 3.6. As was earlier explained, the SOM mapping is done in such a way that the nodes allocated in corners or the diagonals of the SOM, approximate the two dominant eigen modes. The places in between these are filled with the transitional nodes. As the study examines the heavy precipitation patterns, looking at these dominant patterns is most useful. Node [0 3] was also excluded in this examination as the pattern represented by this node was of low precipitation values with no coherent spatial pattern, so that it would be of relatively little additional value to this study.

Table 3.1: The 1979-1998 days used from each of the three SOM nodes (see fig. 3.6) for further examination.

<p style="text-align: center;">NODE [0 0]</p> <p>Total number of days after 1979 = 9</p> <p>18-Jan-81 13-Jan-83 30-Jan-84 10-Feb-88 15-Feb-88 22-Feb-88 24-Feb-88 07-Jan-89 23-Jan-91</p>	<p style="text-align: center;">NODE [1 0]</p> <p>Total number of days after 1979 = 8</p>	<p style="text-align: center;">NODE [2 0]</p> <p>Total number of days after 1979 = 14</p> <p>19-Feb-80 23-Jan-81 24-Jan-81 25-Jan-81 26-Jan-81 28-Jan-84 13-Jan-85 15-Jan-85 21-Feb-88 23-Dec-94 24-Dec-94 26-Dec-94 11-Feb-96 12-Feb-96</p>
<p style="text-align: center;">NODE [0 1]</p> <p>Total number of days after 1979 = 14</p>	<p style="text-align: center;">NODE [1 1]</p> <p>Total number of days after 1979 = 14</p>	<p style="text-align: center;">NODE [2 1]</p> <p>Total number of days after 1979 = 13</p>
<p style="text-align: center;">NODE [0 2]</p> <p>Total number of days after 1979 = 13</p>	<p style="text-align: center;">NODE [1 2]</p> <p>Total number of days after 1979 = 9</p>	<p style="text-align: center;">NODE [2 2]</p> <p>Total number of days after 1979 = 19</p>
<p style="text-align: center;">NODE [0 3]</p> <p>Total number of days after 1979 = 13</p>	<p style="text-align: center;">NODE [1 3]</p> <p>Total number of days after 1979 = 4</p>	<p style="text-align: center;">NODE [2 3]</p> <p>Total number of days after 1979 = 13</p> <p>16-Jan-85 09-Feb-85 10-Feb-85 19-Feb-88 03-Feb-89 11-Feb-89 13-Feb-89 16-Feb-89 05-Dec-90 15-Feb-91 23-Dec-92 28-Dec-93 14-Jan-95</p>

The total number of extreme events (i.e. from 1950-1998) can be analysed to observe any trends they may have. This was done with the above results and is displayed in the graph below.

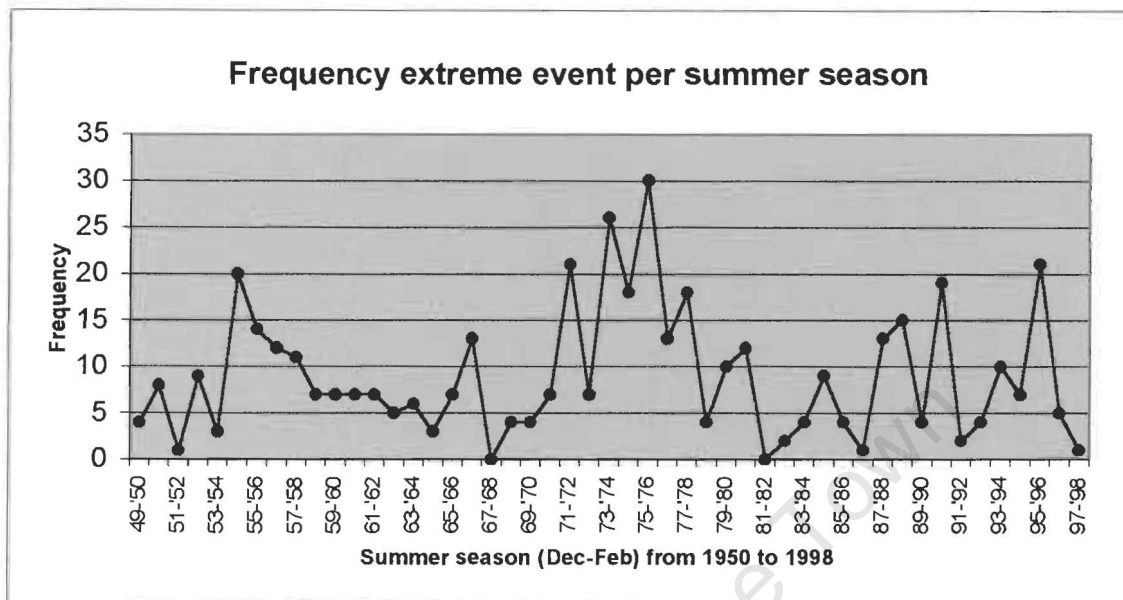


Figure 3.8: Frequency of extreme precipitation days during the summer season (Dec-Feb) from 1950 to 1998.

Since the classification of days in this study is based on accumulated precipitation over a 24-hour period, an event that may have had a longer duration would be counted as multiple events. For example, if an extreme event was experienced over an area over three consecutive days, the selection process would have classified this as three separate event days. This is an important point to remember when looking at the specific number of days in the graph. Although a cyclic trend does seem to exist in the data, further analysis would be necessary to confirm this. Comparison of the dates of the events in this study with the time series show in Chapter Two (Figure 2.2) indicates that these events may have occurred during predominantly wet spells (e.g. 1973/74 to 1978/79). Flood events in the past have also been associated with La Nina events (Lindesay *et al.*, 1986). These events may have thus contributed to a large extent to result in above normal seasonal rainfall. This would in essence be what Easterling *et al.*, (2000) have found in their studies as is shown in Figure 2.9.

In addition to this, the variability of the events mapped to each of the nodes against time was also examined. The three graphs below (Fig 3.9) show the results of this analysis done for nodes [0 0] [2 0] and [2 3], and shows the occurrences of these events over the past fifty years (1950-1998).

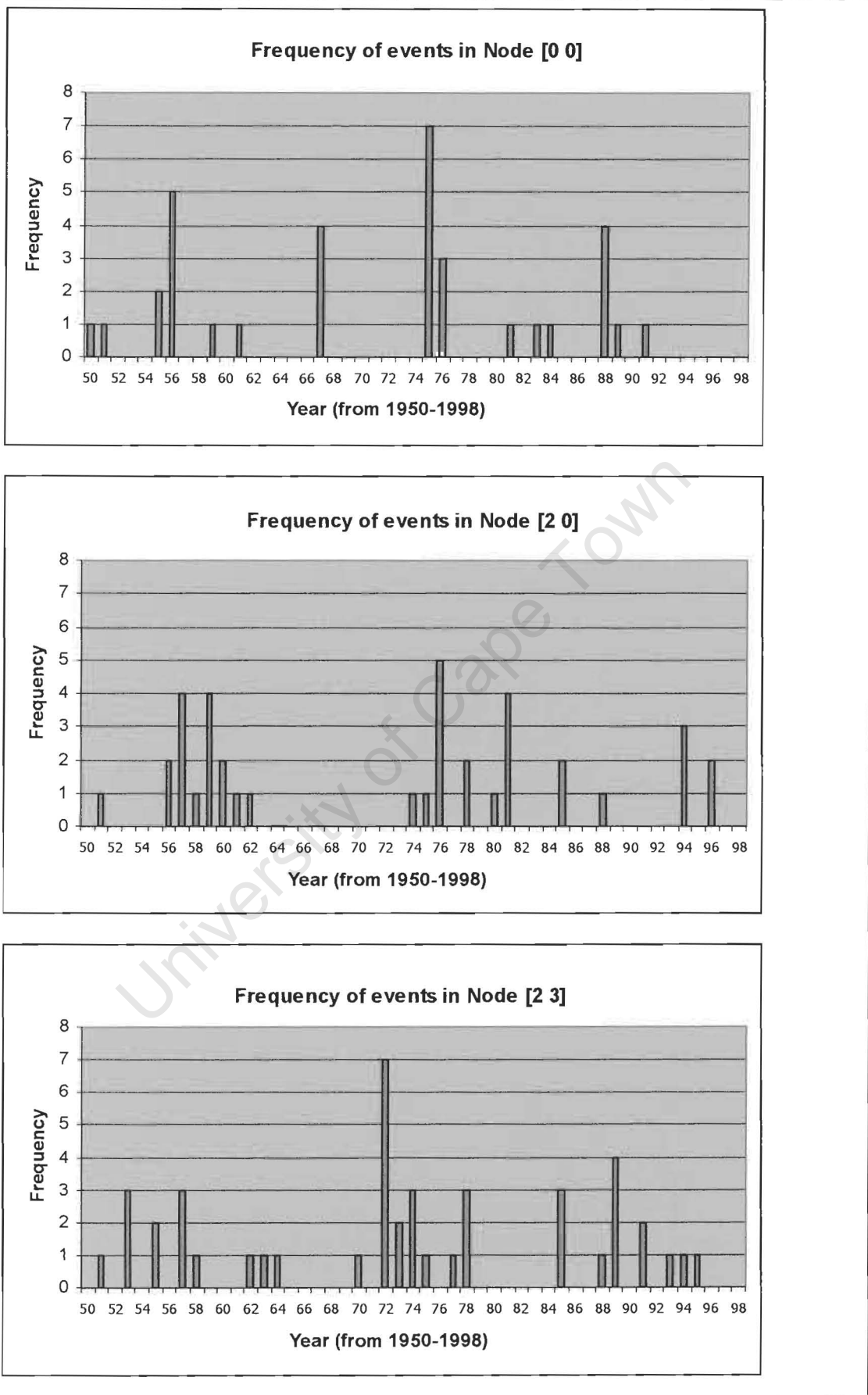


Figure 3.9: Frequency of events in Nodes [0 0], [2 0] and [2 3] for the period 1950-1998.

The intervals between the events however do in some cases form a pattern that is captured in the graphs. It is however unclear whether such a pattern exists for the events occurring in node [0 0]. This may be due to the fewer events available for analysis in this node, or it may be that the events are themselves occurring in a random manner.

Within the other two nodes however, a pattern does seem to exist. This is most clearly seen on the graph corresponding to node [2 3]. The events (days) shown on this graph seem to form clusters with breaks that range from 3 to 6 years. The groupings in the node [2 0] are not as obvious. The breaks in this case are however even longer, with the shortest being 3 years and the longest being 12 years. It is also noted that the onset of the events for the two nodes do not coincide. The graphs indicate that events in the node [2 3] may occur several seasons prior to those of node [2 0]. The large scale atmospheric circulation associated with these events may therefore be such that a spatial shift occurs to cause this pattern. It is also possible that these events are linked to hemispheric scale interaction such as those associated with ENSO. The evidence is however insufficient to confirm this. However, if this were to be the case the moisture sources for the events in both of the nodes may be related. Further investigation of these events is therefore necessary to confirm this. The trajectory modelling is thus useful in establishing this and will be attempted next.

The total number of events to be examined however still remained substantial and a further reduction was necessary through a sample selection. This is done in the next chapter where the atmospheric conditions associated with the sample days as well as the conditions prior to these days are examined and trajectory modelling undertaken. The chapter also describes the trajectory model used as well as providing a background on such modelling.

CHAPTER FOUR: TRAJECTORY MODELLING

4.1: Introduction

In the previous chapter, the spatial patterns that are present within the data set were analysed with the use of the SOM and this forms the first step in investigating possible non-local sources of moisture for spatially extensive heavy precipitation events. The use of a trajectory model at this stage enables further analysis of pathways and transport of moisture.

4.2: Trajectory Modelling

Trajectory models have been employed within the environmental sciences for a number of years. Their main use has been in the investigations of trace gas and aerosol particle movements in the atmosphere (Stohl & Trickl, 1999; Tyson & D'Abreton, 1998; D'Abreton, 1996; Garstang *et al.*, 1996; Tyson *et al.*, 1996(a); Krishnamurti *et al.*, 1993; and Eliassen, 1980). The principle benefit of using these models is that they enable the visualization of the path that a particle or air mass may have taken given a time series of atmospheric conditions, which is not always apparent from static maps of circulation fields.

The movement of air may be viewed as either *Eulerian* or *Lagrangian*. In the Eulerian perspective, the focus is on fixed points in space and the air that travels through them (Stohl, 1998). The Lagrangian method however considers the movement of the individual air parcel or pollutant particle as it moves through time and space (Stohl, 1998). These paths are what are known as trajectories. The study of moisture transport is often done using the Lagrangian perspective (Tyson & D'Abreton, 1998; D'Abreton, 1996) as has been done in this study. The discussion that follows will be constrained to this view only.

Two methods exist within the Lagrangian perspective that are widely employed in the construction of three-dimensional trajectories; the *isentropic* and *kinematic* methods. The advantage of using the isentropic model is that it does not require vertical motion data in order to calculate the trajectories. Vertical displacement is instead assumed to occur as parcels move along the sloping isentropic surfaces (Fuelberg *et al.*, 1996). A direct estimate of vertical motion is thus calculated. It is further assumed that in the adiabatic, frictionless flow, potential temperature is conserved during the motion (D'Abreton, 1996; Fuelberg *et al.*,

1996). This assumption may be valid for use for periods of several days when observing cloud-free regions away from the surface, but for longer periods and in regions of precipitation and in the boundary layer, it can no longer be held true. This makes the use of the model over land surfaces or for calculating trajectories for a large number of days inappropriate (Fuelberg *et al.*, 1996).

The kinematic approach however, utilizes observed horizontal and vertical wind velocity components in tracing the movement of air parcels, and makes no explicit assumptions about the flow (D'Abreton, 1996; Fuelberg *et al.*, 1996). If vertical velocity data is not available then it may be calculated using the principle of continuity (D'Abreton, 1996). This has however been shown to produce higher vertical displacements and greater diabatic rates than acceptable in theory (Fuelberg *et al.*, 1996). Provided with a good set of input data however, this can be avoided and reasonable trajectories have been produced using kinematic models (McGowan *et al.*, 2000; Sturman *et al.*, 1997; D'Abreton, 1996; Fuelberg *et al.*, 1996). This approach is especially appropriate to southern Africa during summer when the region experiences significant precipitation and cloudy conditions. In the present study trajectories are calculated using such a kinematic model.

The resolution of the data used in calculating the trajectories play an important role in the accuracy of the end result. In the absence of reliable observed data that cover the entire domain being investigated, reanalysis data such as NCEP is used for modelling purposes. The horizontal resolution of such data however, is often low. In these cases, certain small scale features are not resolved and incorporated into the data. Convective processes in the atmosphere are often not captured in the data if the vertical resolution is low. This can therefore create an inaccuracy in the data that is subsequently used for other studies such as the present one. This must be noted and the results analysed keeping this in mind.

4.3: Methodology

This thesis uses an established trajectory model (Hewitson *et al.*, 2000; 2001; Hewitson, 2002) and thus it is not the intent of this chapter to discuss in great detail the mathematics involved in trajectory modelling. Rather the focus is placed more on the results that have been obtained through the use of the model in this study. A brief explanation of the model

and the basic principles are however presented here in order to better understand the results presented in the following section.

4.3.1: The Kinematic model

The kinematic model used in this project was developed specifically for moisture transport investigations. It has some similarity to other models such as the HYSPLIT4⁷, FLEXTRA⁸ and FLEXPART⁹. However the present model is able to handle a large number of trajectories for much longer time periods than those mentioned above. The model also differs from the others in its use of a sigma coordinate system in the vertical. This coordinate system is based on a ratio between the pressure at a given point in the atmosphere and the surface. The dimensionless quantity σ , which defines the vertical levels, is calculated simply as

$$\sigma = (p - p_t) / (p_s - p_t) \dots \dots \dots (4.1)$$

where p is the atmospheric pressure at that level, p_t is a specific constant top pressure, and p_s is the surface pressure. This results in levels that are terrain following at the surface but flattens out as one rises in the atmosphere (Fig 4.1). The levels are parallel to the pressure surface at the top of the atmosphere (MMMD, 2000).

The constant top pressure in the model is set to be 100hPa and 12 sigma levels have been pre-defined. The advantage of using such a system is that the problem of pressure levels intersecting terrain is not encountered. This is a problem that is faced when using trajectory models and usually a pressure level is preset for the surface and the top of the atmosphere. Any trajectories outside of these levels are then deemed lost.

⁷ <http://www.arl.noaa.gov/ss/models/hysplit.html>

⁸ <http://www.forst.uni-muenchen.de/LST/METEOR/stohl/flextra.html>

⁹ <http://www.forst.uni-muenchen.de/LST/METEOR/stohl/flexpart.html>

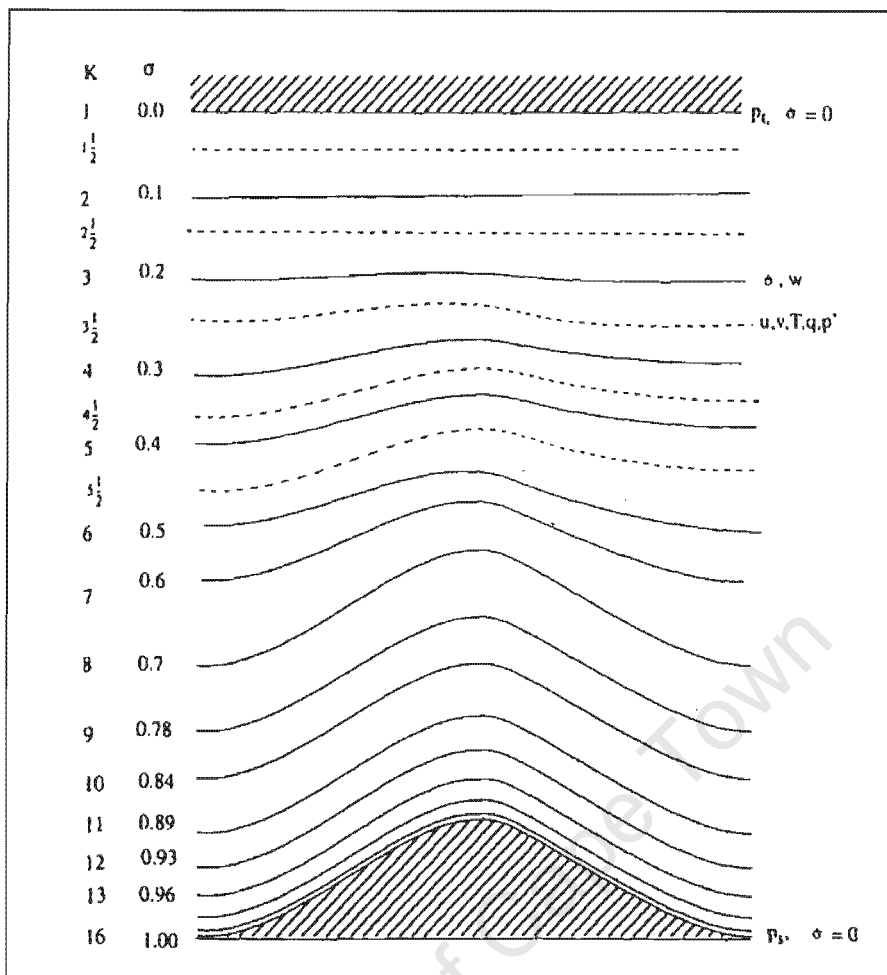


Figure 4.1: Example of sigma levels with σ being 1 at the surface, where the pressure is defined as p_s , and 0 at the top where the pressure is defined as p_t . The number of levels is defined by k (from MMMD, 2000).

The vertical interpolation used in this model, with the sigma levels, is a log-based interpolation. On the horizontal however a simpler, computationally efficient, linear interpolation is employed. Trajectories may be computed in a forward or backward direction with the model. The position of a parcel of air or particle is calculated by solving the trajectory equation;

$$x(t + \Delta t) = x(t) + V [x(t)] \Delta t \dots\dots\dots(4.2)$$

where $x(t + \Delta t)$ is the new three dimensional position at time $t + \Delta t$. The old position is $x(t)$ and $V(t)$ is the velocity vector (D’Abreton, 1996). The present model is set to calculate trajectories at a time step, Δt , of one hour. This was chosen after multiple tests with different time steps varying from 10 minutes to 6 hours. Choosing a smaller time step gave very little difference in the results. With a one hour time step the trajectories are not expected to travel more than half a grid cell spacing of the driving atmospheric data, and hence it was deemed suitable for this study.

The trajectories can be calculated for a total of seven days in either the forward or backward directions and the position is saved every four hours during this time. In this study only backward trajectories were calculated. The starting point for each trajectory calculation is chosen on a 1° grid in the horizontal over the continent and on a particular sigma level in the vertical. The model adopts a stochastic perturbation on the horizontal positioning of this starting location whereby instead of having a fixed point on a grid, the grid is composed of cells and each trajectory will start from a random location within each cell. This reduces the potential bias in the results and may be more sensitive to local variation due to topography. During the evolution of the trajectory, each position calculated at each time step may produce fractional positions between sigma levels and between grid cells. The forcing U, V and W triplet of velocity is interpolated from the source data to this fractional position to derive the motion for the next time step. A full description of the kinematic model may be found in Hewitson (2002).

The calculation of the moisture content within the air parcel during the trajectory can be done using different methods. D'Abreton and Tyson (1996) used a method of calculating the approximate water vapour content by using the water vapour tendency equation. This makes the assumption that water vapour is a passive tracer. In the present model however, this water vapour tendency equation was not used. Instead the water vapour content is simply spatially and temporally interpolated from the NCEP reanalysis data using specific humidity. The specific humidity values are saved along with the spatial position of the trajectory every four hours.

4.3.2: Source Data

The source data used in computing the trajectories is the NCEP reanalysis data discussed in Chapter One. This data set provides six-hourly surface pressure, surface U and V winds and vertical motion (at 10m), surface specific humidity (at 2m) and all these same variables at 12 different pressure levels (1000, 925, 850, 800, 700, 600, 500, 400, 300, 200, 150 and 100 hPa). These data are interpolated as mentioned, to the fractional horizontal and sigma coordinates of a given trajectory point to define the motion of the next time step. If a pressure surface intersects the lower boundary, the surface pressure is used along with the data from the next higher pressure level above the surface.

The surface boundary is defined by a topography data set obtained from a global 5' horizontal resolution data set. Since the resolution of NCEP reanalysis data set is 2.5° by 2.5°, the topography data had to be smoothed to match the atmospheric grid resolution. This smoothing is implemented so that the atmospheric data driving the model is consistent with the topography used in the model.

It has been noted that the quality of NCEP reanalysis data prior to 1979 is problematic for the southern African region (Tennant, 2002; Tennant & Hewitson, 2002; Kistler *et al.*, 2001). This arises due to several reasons. Firstly, the Southern Hemisphere has more data-sparse areas than the Northern Hemisphere. Therefore, more model generated data may be present in the reanalysis data set (Kistler *et al.*, 2001). Although improvements have been made in this regards, large parts of the Southern Hemisphere still remains unmonitored. The introduction of satellite data from the late seventies has led to improvements in the availability of observed data in both hemispheres. Changes such as this and changes in observational instruments have also had an impact on the reanalysis data (Kistler *et al.*, 2001; Tennant, 2002). For these reasons it is often recommended, especially for the Southern Hemisphere data, that the data be checked carefully for errors prior to use. As in this study such checks were not undertaken, instead the post 1979 data was used as there is greater confidence in this part of the data set. The spatial domain selected for the analysis stretches from 80° W to 120° E and 70° S to 20° N. Any calculated trajectory that leaves this domain is then deemed lost.

4.3.3: Sample Selection

Trajectory analysis for this study was done on days identified in the previous chapter as spatially extensive heavy precipitation events. Ideally all the spatial patterns identified through the SOM analysis process would be investigated to locate all possible moisture sources. However, as this task is too large, a subset of the identified SOM patterns is investigated. The nodal maps of interest that were thus chosen were those of nodes [0 0], [2 0] and [2 3]. These particular nodes were selected as mentioned in the previous chapter because they represent three of the dominant spatially extensive heavy precipitation modes. The remaining corner of the SOM array, node [0 3], represented a spatial pattern of relatively lower precipitation values compared to the other nodes. It was thus not included since this study focuses on high precipitation events.

The total number of days that were available for the trajectory analysis from these nodes ranged from nine to fourteen days for each node. Even though trajectory calculations were done for all of these days, it was found that the sample was still too large for an in-depth investigation. Therefore, through visual inspection of the samples a smaller number of days for each node were chosen. These days were those that shared the greatest similarity in terms of the spatial extensiveness of the precipitation when compared with generalized pattern of the SOM node. Through this selection a manageable sample was obtained. Once the days were selected, the starting locations for the backward trajectories were chosen from around the nominal central location of maximum precipitation for each particular event. CCWR precipitation data was used to locate these areas rather than NCEP reanalysis data.

In addition to the selection of the location, a sigma level for the starting point is also chosen. In this study it was set at 0.95 sigma level. Transport of water vapour is thought to occur almost exclusively below the 700hPa over South Africa (McGee (1970) in D'Abreton & Tyson, 1995). For this reason investigation from the 0.95 sigma level was thought to be sufficient for the purposes of this preliminary study. The set location and level will thus be the point at which the backward trajectory commences. The model, as explained, also tracks the moisture content of the air mass along the trajectory path. These values are represented along the trajectory path in a graphical format as presented below.

It is often recommended that multiple trajectories be calculated from the starting locations. This is to eliminate the possible error factor that may exist with the use of the trajectory model. Firm conclusions cannot be made on the movement of air particles based on a single trajectory (Stohl, 1998). For this reason models are often run to calculate hundreds and even thousands of trajectories. The analysis of such a vast number of trajectories as a result also becomes more complex and difficult. With this in mind, the event days examined in this chapter were done with multiple trajectories calculated from a number of starting points and at two different starting times. The initially examination of the nodes resulted in a total of 36 trajectories (shown in Fig 4.2). With the fewer events selected from each node to be further examined, a higher number of starting locations for the trajectories were picked. This therefore resulted in a total of 74 trajectories for the samples. These results and the discussion are presented in the next section.

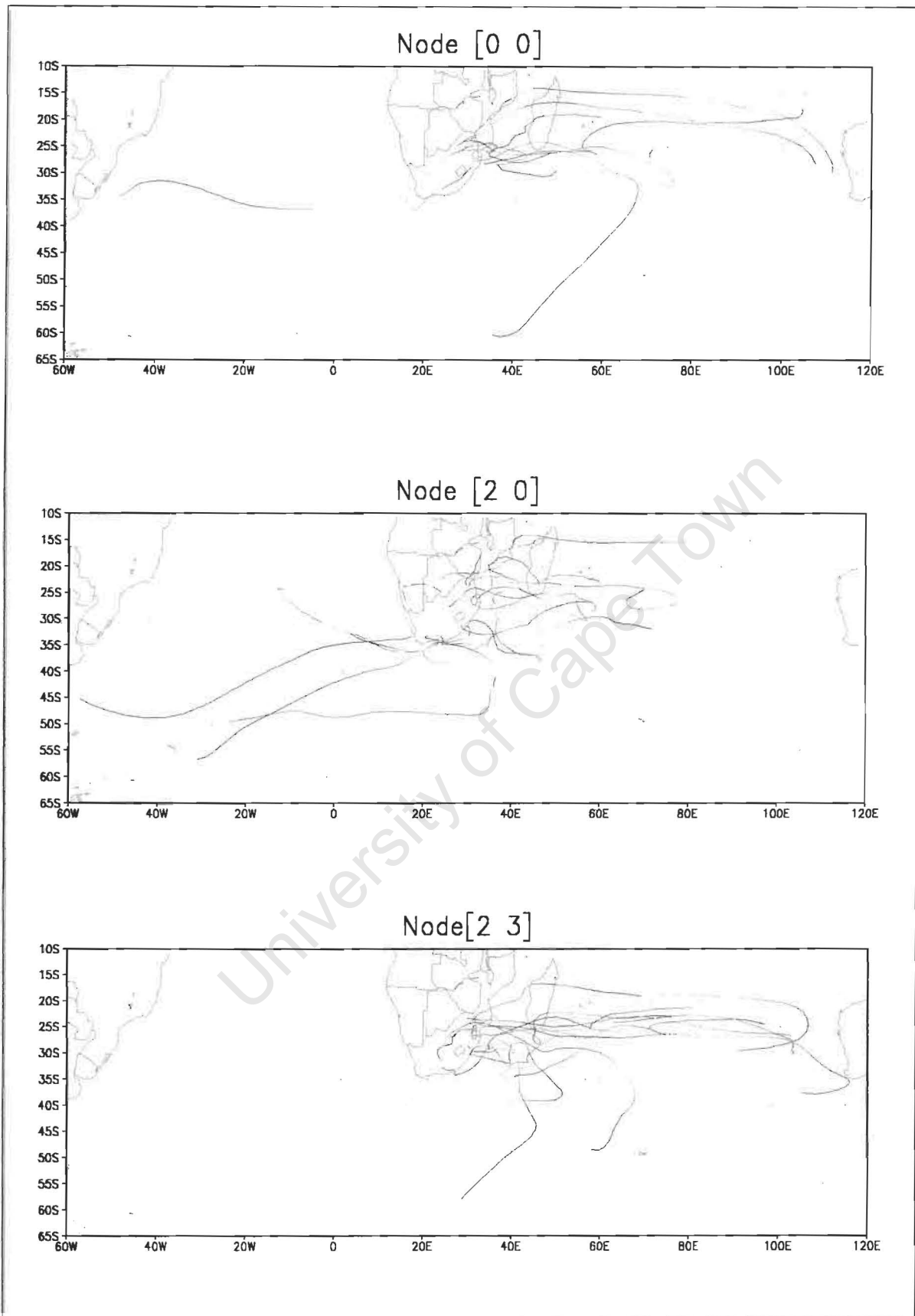


Figure 4.2: Trajectories for event days from the three selected nodes. The colours represent relative values of moisture with the more red colours corresponding to higher specific humidity values than the blues.

4.4: Results and Discussion

4.4.1: Trajectory Results

When examining the results of the calculated trajectories, it is important to keep in mind the assumptions, caveats and errors. Notably that the forcing data is relatively low resolution reanalysis data from a GCM. Initially, as discussed above, the days corresponding to SOM nodes [0 0], [2 0] and [2 3] were investigated and displayed in Figure 4.2. The moisture of the air mass (i.e. specific humidity) along the trajectories is also represented here with the use of colour. The trajectories for all three nodes show that they originate predominantly from an easterly direction. Some paths were seen to extend from the Atlantic and as far west as South America. Observations of the trajectories of node [0 0] show only one path having originated close to South America. Of the other trajectories one is seen to have originated in the southern seas. The easterly predominance is seen clearly in the trajectories of this particular node and node [2 3]. Trajectories from the days mapped to node [2 0] were rather more widespread in the direction of the paths. Several were seen to have origins in the south Atlantic while those that originate east of the continent stretch from northern Madagascar to the south Indian Ocean. More trajectories were however seen to be originating in the south Indian Ocean.

From Figure 4.2 it is apparent that most of the observed trajectories originating from the high latitude and the south Atlantic regions carry less moisture than the air masses originating in the South Indian Ocean. Of those that were seen to originate in the south Indian Ocean, increases in moisture were more often observed to occur in the areas just east of the Madagascan island and in the Mozambique channel. This is expected to be due to the higher sea surface temperatures and the surface moisture fluxes in these areas.

Increases in the moisture content were however also observed to occur in-land. Such increases were seen to occur in samples of all three nodes. The reason for such an increase is difficult to account for here but it is possibly influenced by the soil water content and vegetation in these areas. This however will need to be examined further in order to establish if it is indeed the case. Therefore, a sample of days from each of the three nodes was selected for further analyses. The findings are presented in the following section and a separate discussion of the results will follow.

4.4.2: *Sample trajectory results*

After the initial trajectory calculations for the events in all three selected nodes, a sample of three days from each of the nodes were selected to be analysed further. This smaller sample allows for a more comprehensive analysis to be carried out with the trajectory modelling. The starting locations for each of these trajectories for the sample days are given in Figure 4.3. These locations were chosen around the area of greatest precipitation as can be seen from the precipitation fields in Figure 4.3. Two sets of trajectories were calculated—one starting at 00h00 SAST whilst a second set started at 12h00 SAST for each of the sample days. This was done to examine how the trajectories may differ over the whole region under heavy precipitation, and whether the calculated trajectories are representative of the circulation at the time. An individual trajectory may represent a single random occurrence. Calculating multiple trajectories over different starting time was thought to reduce the chance of forming a conclusion for the event based on such random trajectories.

The results of these are presented in Figures 4.4, 4.5 and 4.6. The diagrams represent the path of the air parcel seven days back from the starting locations shown in Figure 4.3. The moisture carried along these air masses are represented once again in these diagrams with the use of colour with the reds corresponding to a higher specific humidity and blues to lower values.

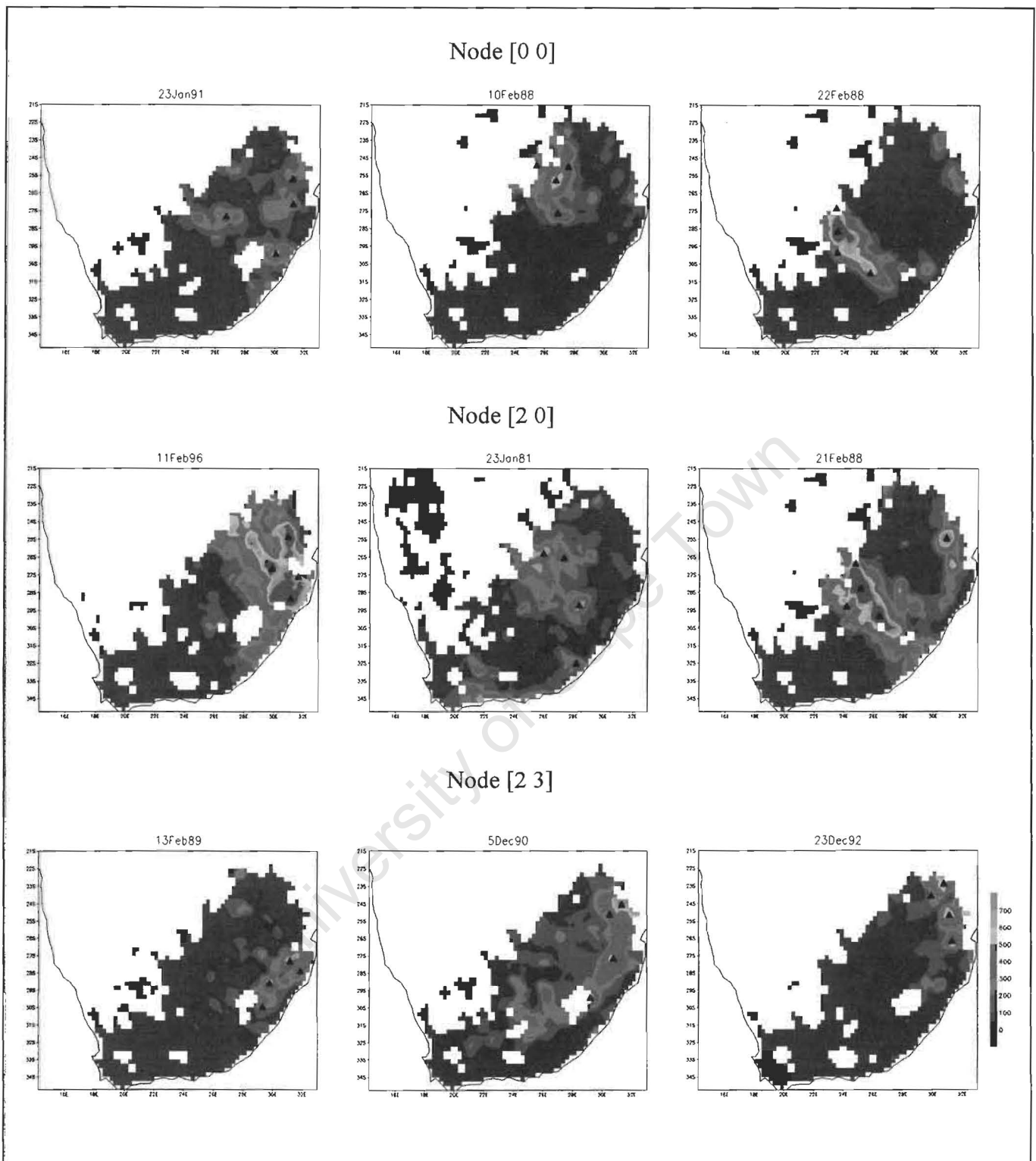


Figure 4.3: Starting locations of the trajectories for each day chosen from nodes [0 0], [2 0], and [2 3], shown using solid triangles, on the daily accumulated precipitation (in mm) maps of those days.

The event days mapped to node [0 0] display two possible sources of moisture; the south Atlantic and the south Indian Oceans (see Fig 4.4). Trajectories on the 23rd January 1991 show that both of these sources may have contributed to the rainfall over the interior. Two of the trajectory paths originating in the south Atlantic show relatively high values of moisture. This value reduces drastically once the air mass is over the land. This loss may have been as a result of precipitation. Increases in moisture was also observed whilst the air mass was just south of Cape Agulhas, at approximately 35°S; 20°E, before reaching the continent. The influence of the Agulhas current is suspected for such increases and will be discussed later. For the trajectory originating over the south Indian Ocean, increases in the moisture content was observed east of Madagascar, at around 24°S; 77°E and 21°S; 55°E. The path of this trajectory was also seen to move across the island of Madagascar and the Mozambique Channel before entering the country from Mozambique in the north-east. An increase in moisture was also observed when crossing the Madagascan island.

On the two other days in this category however, no trajectories were found to originate from the Atlantic. The trajectories calculated for the 10th February 1988, showed a close proximity with each other in their paths. Such observations lead to more confidence in the calculated trajectory as the occurrence of a random trajectory was minimised in this case. The trajectories were all located in an area between 25°S and 35°S and between longitudes 60°E and 70°E, at the end of the seven-day back-trajectory. They all follow a coherent path to the northeastern part of South Africa and were found to have travelled south of the Madagascan island. Moisture increases along the path were seen just south and southeast of island at approximately 28°S; 45°E.

On the 22nd of February 1988 the trajectories also displayed an easterly origin. They however travelled in a slightly different path to the ones seen on the 10th February 1988, with a more northeasterly approach into the interior. The paths were also seen to travel over southern Madagascar and the Mozambique Channel before reaching the interior of country via the Northern and Mpumalanga provinces. Increases in the moisture values were similarly seen for several of the trajectories to have occurred east of Madagascar at around 24°S and between 60°E and 80°E. Increases also occurred over the Mozambican Channel (25°S; 40°E).

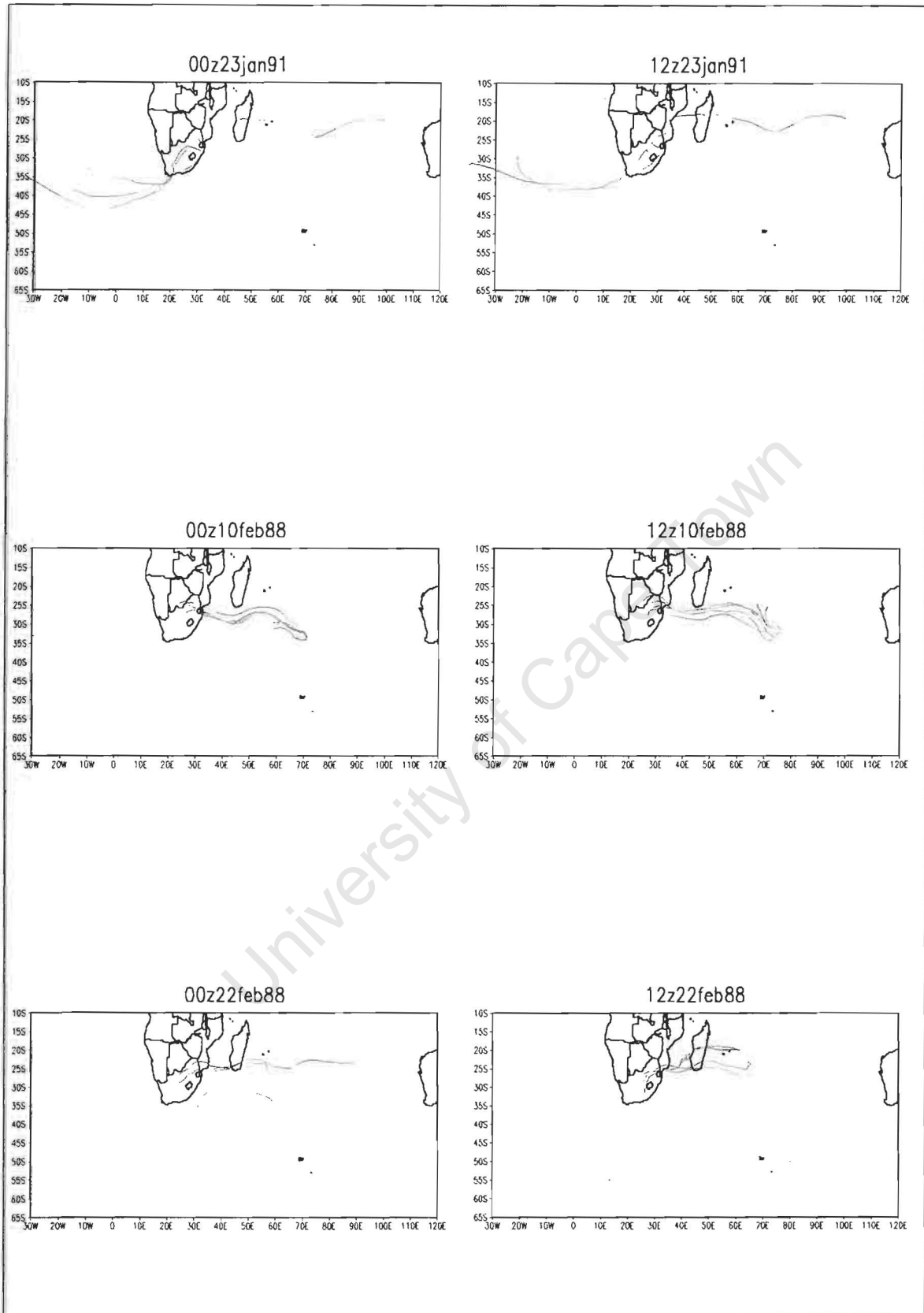


Figure 4.4: Trajectories for sample of days chosen from Node [0 0] with the colours representing relative moisture values. Each diagram is also given in Appendix B in a larger format.

Observations of the trajectories for the days from node [2 0] also show paths from both the Atlantic and Indian Oceans (see Fig 4.5). The paths of the air masses for the 11th February 1996 and the 21st February 1988 show a predominantly south Indian Ocean origin. The paths for the 21st February 1988 were more coherent with most of the trajectories originating southeast or just east of Madagascar (between 23-34°S and 50-75°E). The paths of the trajectories for the 11th February 1996 span further east than this, to about 90°E. Increases in moisture in both cases were seen just east of Madagascar at around 60°E and also in the Mozambique Channel. One trajectory from 11th February 1996 is seen to originate from the South Atlantic Ocean and travel around the south of the continent towards the south Indian Ocean. The moisture carried by this air mass remained very low until it was over the south Indian Ocean (around 28°S; 70°E) where increases were observed. The path was also seen to recurve from this point and follow a path similar to the other trajectories from the south Indian Ocean.

The calculations carried out for the 23rd January 1981 however show a different pattern to either of the other two days in this sample for node [2 0]. One trajectory calculated at 00h00 SAST was also seen to have travelled from the Indian Ocean but further north than the other trajectories examined thus far in this sample. It crossed over Madagascar at about 17°S and travel south over Mozambique into Zimbabwe before entering South Africa. The moisture along the trajectory was seen to be high whilst it was over the Indian Ocean at around 80°E; 15°S, but lost most of it as it approached Africa. Moisture was once again seen to increase whilst the air mass was just entering South Africa over the Northern Province. This moisture was lost as the air travels further south towards Lesotho. This was again suspected to be as a result of precipitation in this area. Another trajectory calculated at the same starting time show a recirculated path through the interior of the continent. The air mass originating from southern Zambia travels westwards over the Atlantic before turning round and moving over Namibia at around 22°S and then moving south over Zimbabwe. The air mass, which carried very little moisture up to this point, was seen to increase its moisture load just before moving over South Africa to the point of the trajectory's origin. For the trajectories calculated at the 12h00 SAST time step, all were seen to have travelled from the south Atlantic and the southern seas. One of these trajectories was seen to have travelled northwards along the west coast before moving inland over Namibia at around 25°S. Its path in-land thereafter, over Namibia and Zimbabwe follows in a similar manner to the one described previously.

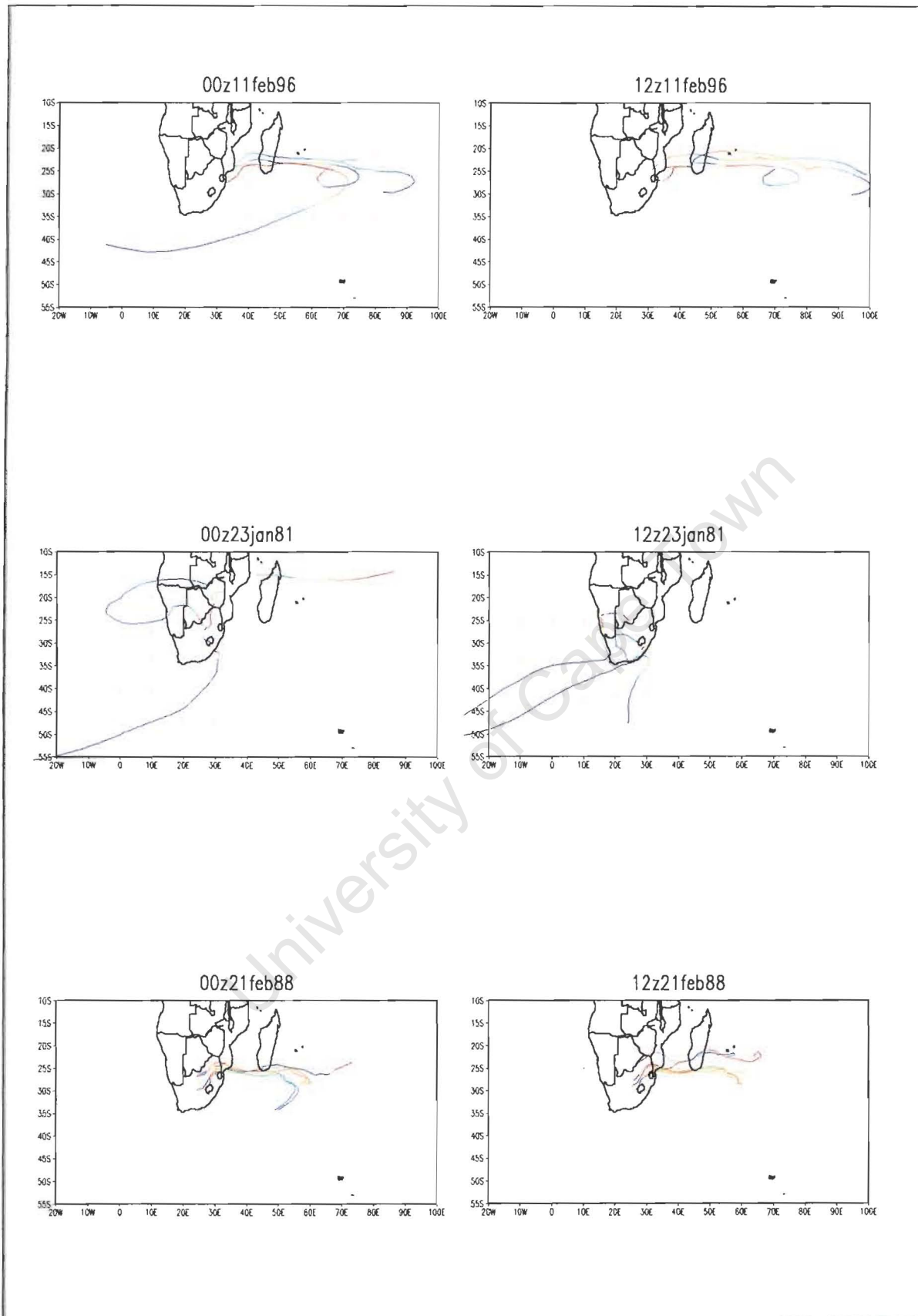


Figure 4.5: Trajectories for sample days chosen from Node [2 0] with colours represent relative moisture values. Each diagram is also given in Appendix C in a larger format.

Similarly, examination of the results of the days corresponding to node [2 3] showed that trajectories travel from both the south Indian as well as the south Atlantic Oceans (see Fig 4.6). However, the trajectories in this group were seen to have origins very far south compared to the samples from the previous two nodes. Trajectories on both the 13th February 1989 and 5th December 1990 were observed to have travelled from an area south of 55°S. These trajectories were seen on the 5th December 1990 to follow a coherent path towards the Western Cape coast. Moisture along the path remained very low until the trajectory was just off the coast when an increase was observed. This may have been as a result of warmer sea surface temperatures that increased the moisture fluxes in the area. There may also have been a slight influence of the Agulhas current as well. On the 13th February 1989 the trajectories showed an eastward path that curves to the west at around 33°S; 60°E. When the air mass was just south of Madagascar it was seen to spiral and change direction once again and head in a northwesterly direction. The moisture of the air was seen to have increased over the south Indian ocean around 30°S and remained high as it approached the coast of South Africa at about 31°E; 27°S.

Comparisons of the trajectories for the 23rd December 1992 showed a definite easterly origin, of which all were seen to travel over Madagascar and cross the Mozambique Channel whilst heading in a more southerly direction before entering the country. Moisture along these air masses increased over the Indian Ocean at around 60°E, east of Madagascar. An increase in moisture was also seen whilst the air masses were over the Madagascan island. Again as speculated before, this could have been due to the influence of the vegetation and soil over the island.

After observing the results from the three nodes, it can be said that although there were influences of from the south Atlantic, the events here have shown a strong likelihood that the south Indian Ocean is the dominant origin of the air masses. The trajectories have also shown that the amount of water vapour carried by the air masses from the south Indian Ocean to be significant and it is therefore possible that moisture for the precipitation events inland was provided by them. The most likely location for moisture indicated by these trajectories is an area east of the Madagascar island at about 20-30S and 50-70E. Previous studies have indicated a different location to this and those studies and their findings, as well as those observed here are compared in the discussion section (section 4.4.4) that follows.

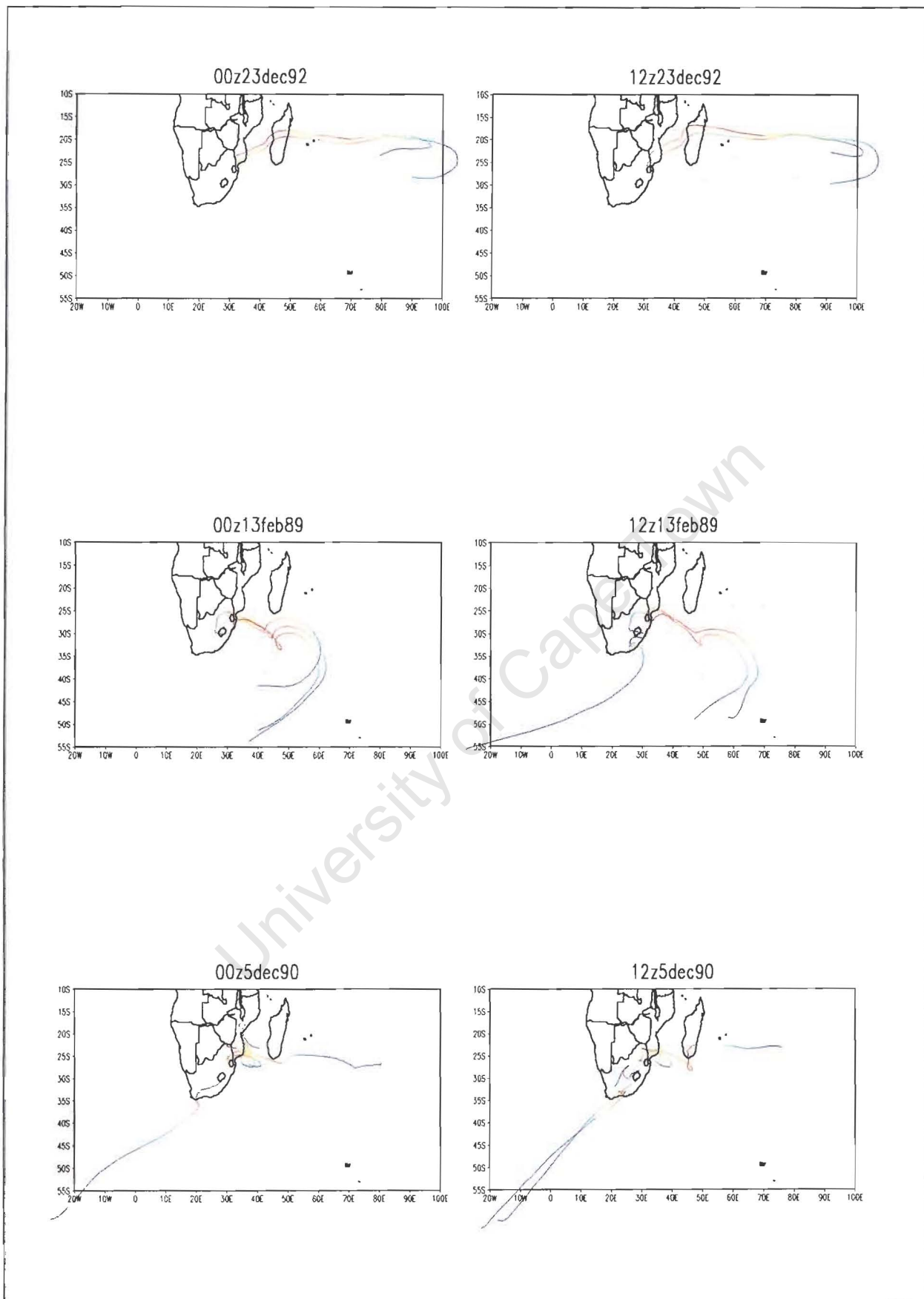


Figure 4.6: Trajectories for samples chosen from Node [2 3] with the colours representing relative moisture values. Each diagram is also given in Appendix D in a larger format.

4.4.3: Vertical Changes of the trajectories

In addition to changes in the path of the trajectories in the horizontal, changes in the vertical were also observed and are evaluated here. Figures 4.7, 4.8 and 4.9 show these changes in altitude for the sample days from each of the three selected nodes. Trajectories for both starting times of 00h00 and 12h00 SAST, are presented here and the differences between them are examined. The differences between the two starting times show small differences with the general patterns remaining the same but the actual magnitudes differing. These differences in altitude were often less than 0.05 sigma for the cases observed here.

For the days from node [0 0], the greatest vertical change was seen when the trajectory flows over the land (see Fig 4.7). From the results for the 22nd February 1988, a drop in altitude was seen when the air mass was over the island of Madagascar. Similar changes in altitude were observed when the trajectories move from the ocean onto land. This may be due to the topography of the area especially over the island of Madagascar where mountains are present over the eastern part of the country. The drop in altitude may thus correspond to the air moving over the lee of the mountains. However, the change may also be as a result of the resolution of NCEP data being used. The drop experienced for example in the case of trajectories moving inland from over the ocean, may be caused by the data being of low resolution and being unable to resolve this more accurately. This further emphasises the need for good quality and high resolution data for good modelling results.

During the remainder of the time, the air masses were all seen to remain below 0.86 sigma level (~850hPa). Figure 4.7b shows that the air mass remains fairly capped at 0.9 sigma level for a long period whilst the trajectories move over the ocean. Of the trajectory starting at 00h00 the trajectory calculated originating for the 23rd January 1991 was seen to originate from a higher altitude in the atmosphere compared to the other trajectories. This however did not appear for the same trajectory starting at 12h00. These changes could therefore be as a result of the changing synoptic conditions at the time.

Samples from node [2 0] in comparison showed that the air flow for these events originated from a higher altitude in the atmosphere than in the previous cases. Especially on the 23rd January 1981, the air mass was seen to have reached about 0.68 sigma level (~720hPa). The greatest increase in this case was seen between 10 and 17 hours after the start of the trajectory

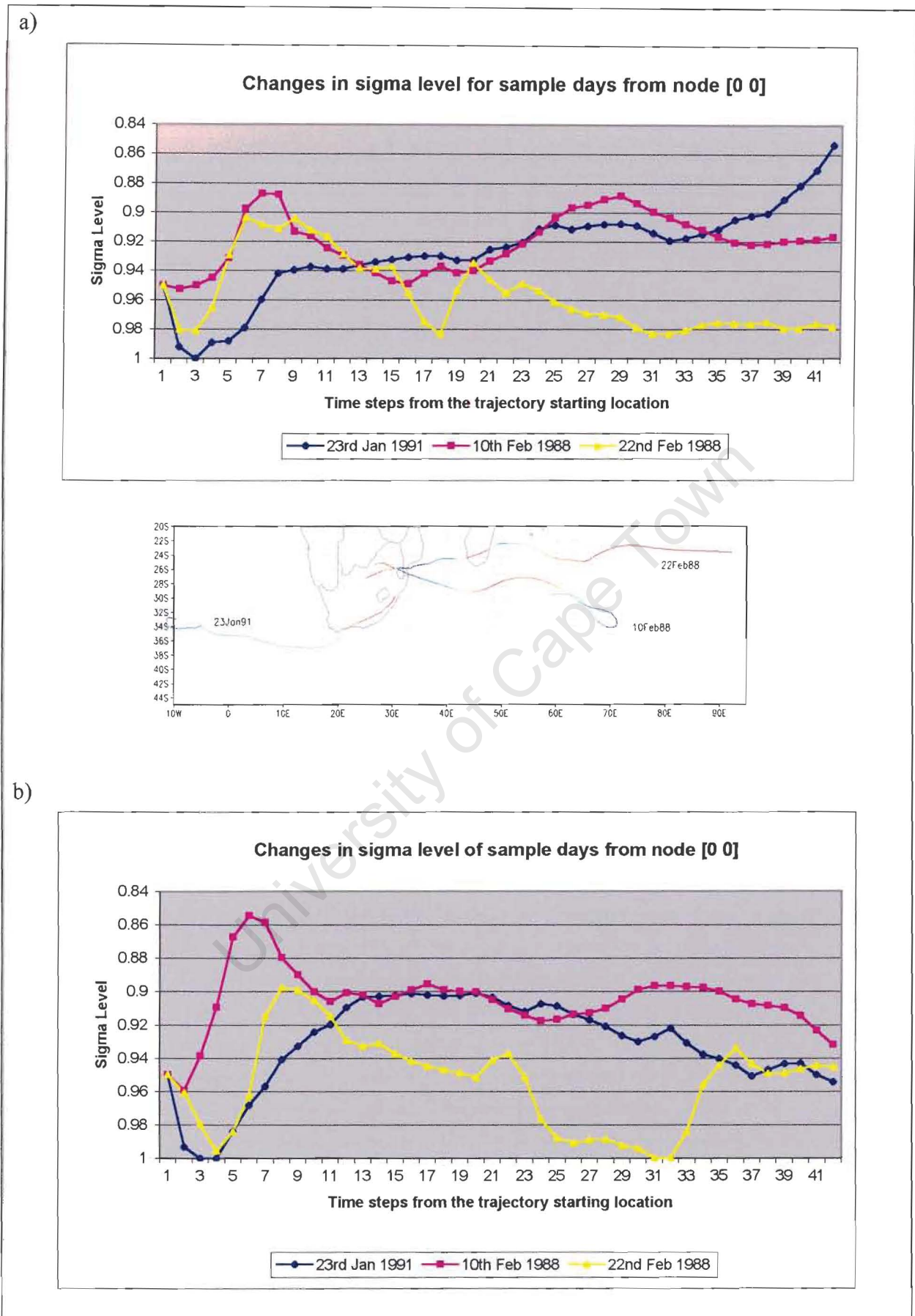


Figure 4.7: Sigma level changes of sample days in node [0 0] for trajectories starting at a) 00h00 and b) 12h00 from the starting locations shown in figure 4.3.

for the one started at 00h00 SAST (Figure 4.8a), whilst a more gradual increase was seen in the trajectory started at 12h00 SAST (Figure 4.8b). The changes in the other trajectories in this sample were much smaller.

Similarly in the examples from node [2 3], the vertical change was not extensive with the top height being 0.7 sigma on the 13th February 1989. Decreases were once again observed when the trajectory flow was over land. Other than this, the changes in the vertical were observed to remain small and gradual in this category.

The advantage of the use of the present model is that the vertical changes that occur along the trajectory paths can be observed easily. The three dimensional view of the movement of the air masses within the region can thus be obtained. With the use of the sigma levels instead of pressure levels, the occurrence of trajectories intersecting terrain is also eliminated. The analysis of the trajectories was also not confined to observations at a particular pressure level. The trajectories can be tracked along its path to observe the changes that occur in the altitude. This advantage allows easy visualisation of the air masses and their movement in the atmosphere.

The present model has also shown that the vertical changes of the trajectories were reasonable and not as high as expected from such kinematic models. Comparative studies done with isentropic models have revealed that kinematic models can be inferior with regards to the vertical changes (Stohl, 1998; Fuelberg *et al.*, 1996; D'Abreton, 1996). In this study however, as with the one done by D'Abreton (1996), the altitude levels attained by the trajectories have been seen to be reasonable and the changes also reasonable. The use of such models for moisture transport investigations is therefore thought to be acceptable.

In the following section, the existing literature on the trajectory modelling and water vapour transport in the region are reviewed, and comparisons of these previous findings to those made here is undertaken.

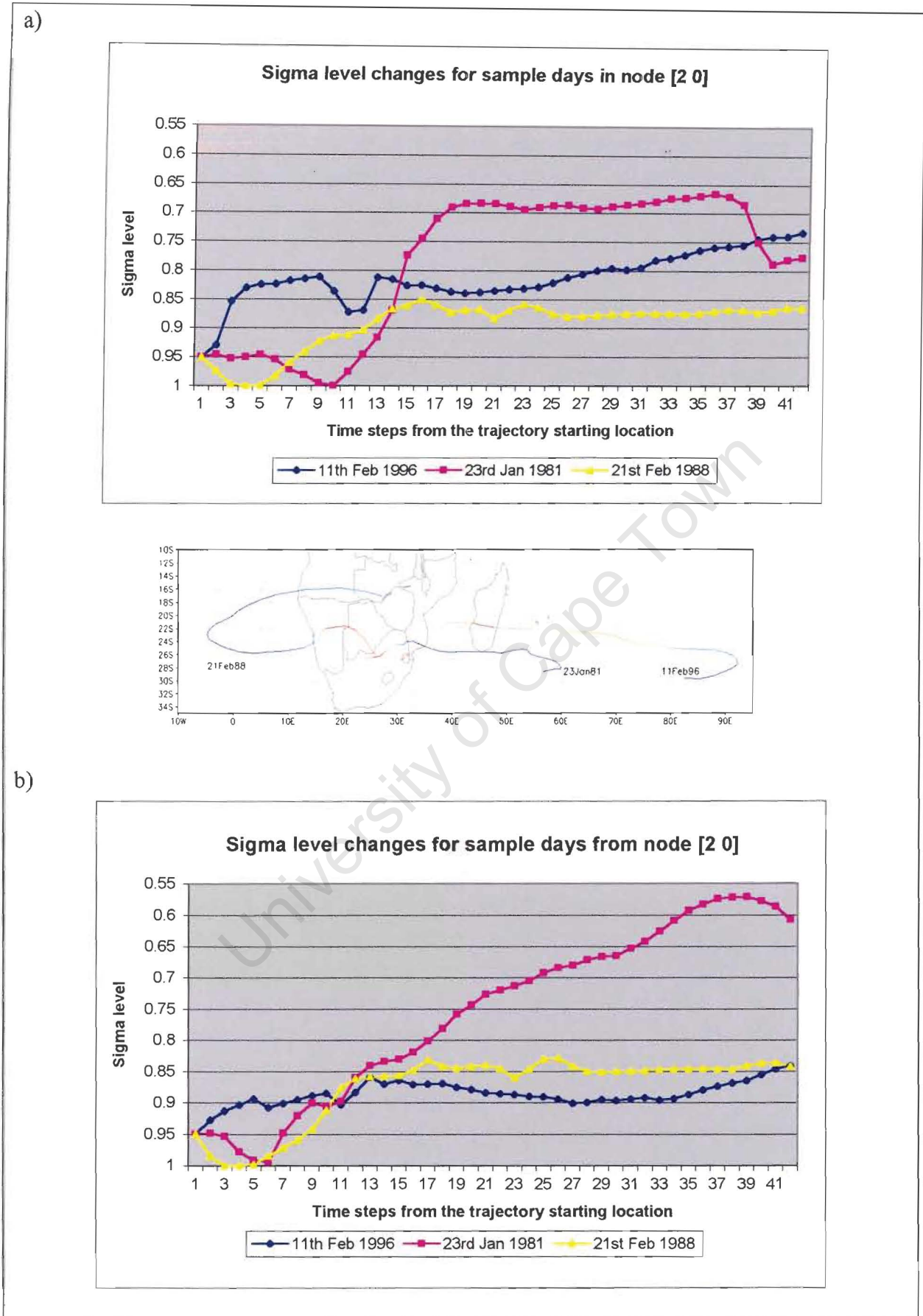
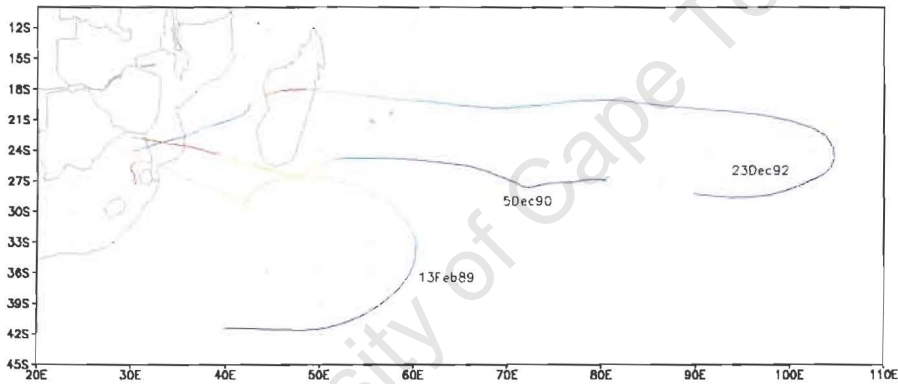
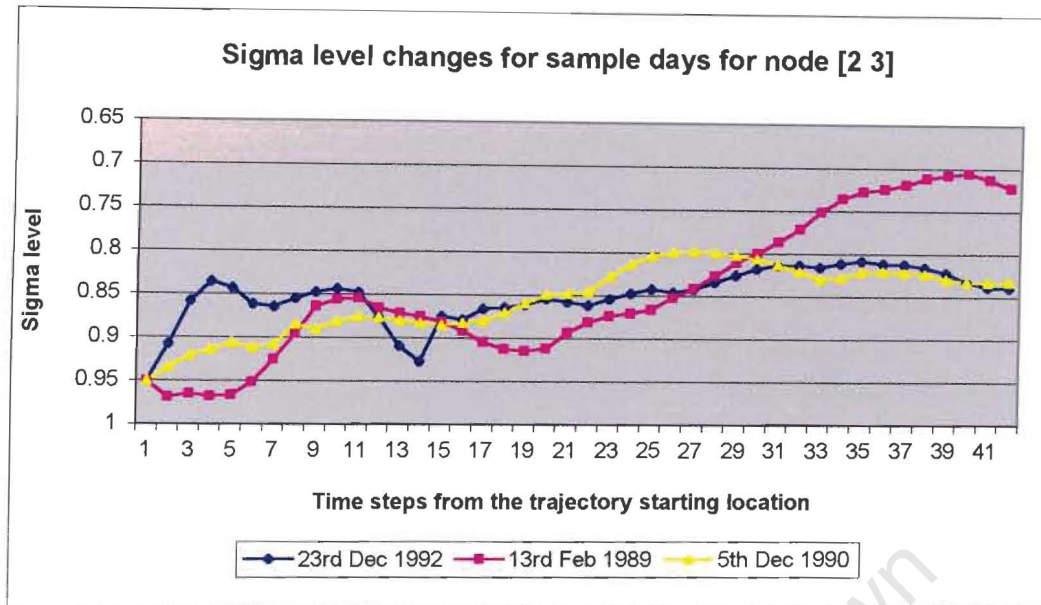


Figure 4.8: Sigma level changes of sample days in node [2 0] for trajectories starting at a) 00h00 and b) 12h00 from the starting locations shown in figure 4.3.

a)



b)

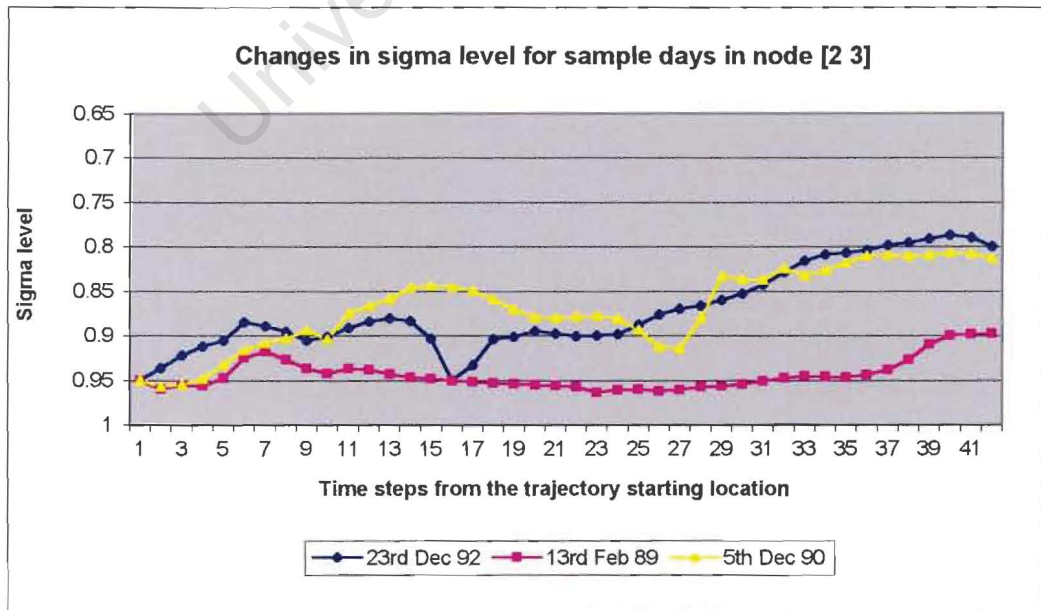


Figure 4.9: Sigma level changes for sample days in node [2 3] for trajectories starting at a) 00h00 and b) 12h00.

4.4.4: Discussion of Findings

The transport of air masses over southern Africa has been investigated in the past by Tyson and D'Abreton (1998), Tyson *et al.*, (1996a, 1996b), and Garstang *et al.*, (1996). These studies were predominantly interested in the transport of aerosols and pollutants, and used trajectory modelling to understand the possible movement and deposition of these in the region. Tyson *et al.* (1996a) identified the predominant synoptic types in the region and used these to classify the days under investigation. This allows for an analysis of the transport pattern of air under the different synoptic conditions. In the present study the classification of the days under investigation is done using the spatial pattern of the extreme precipitation events. Therefore the days classified into one group may still be influenced by different synoptic conditions. A summary of these synoptic conditions prevailing over the country during the different sample days investigated is given in the table below;

Table 4.1: Synoptic conditions prevailing during the days being investigated categorised according to Tyson's (1986) scheme.

NODE	DATE	SYNOPTIC CONDITION
Node [0 0]	23 rd Jan 1991	Ridging of anticyclone
	10 th Feb 1988	Cut-off low
	22 nd Feb 1988	Continental anticyclone
Node [2 0]	11 th Feb 1996	Cut-off low
	23 rd Jan 1981	Cut-off low developing
	21 st Feb 1988	Ridging Anticyclone
Node [2 3]	23 rd Dec 1992	Easterly wave disturbance
	13 th Feb 1989	Westerly wave
	5 th Dec 1990	Ridging anticyclone

Tyson *et al.* (1996a) describes the circulation of air in the region under these same synoptic conditions. Forward trajectories were calculated for this purpose using a Lagrangian model (Tyson *et al.*, 1996a). Under the continental highs, it was observed that two modes of transport are possible; one exiting into the Atlantic Ocean via Angola and the other to the Indian Ocean via Natal (Tyson *et al.*, 1996a). The easterly flow into the subcontinent is seen to dominate in this case, with the transport being spatially continuous and coherent (Tyson *et al.*, 1996a). Observations of the trajectory field calculated for the 22nd February 1988, in

which the influence of continental highs are present, show such a pattern. The conditions on the 10th February 1988, which showed the presence of the south Indian Anticyclone, also showed trajectories from the south-east. Moisture carried along this path was seen to be relatively high and would thus have fed the low pressure over the interior of the country. Tyson et al. (1996a) also pointed out that recirculation of air over the region especially under anticyclonic conditions is very likely. In the examination of the present sample, some anticyclonic curvature was evident for days in all three nodes. However the recurvature occurred some distance to the east of the continent, between 60°E and 105°E. This curvature also seemed to correlate well with the presence and location of the high pressure system over the south Indian Ocean.

By contrast during ridging anticyclonic conditions, Tyson et al. (1996a) showed that the flow is predominantly out into the Atlantic Ocean with a recirculated transport occurring in the south to the Indian Ocean. Examination of the days in the sample with this synoptic condition revealed trajectories originating from the south Atlantic Ocean. The passing of a baroclinic system prior to the ridging of the anticyclone explains this. The moisture being carried by the air mass was also seen to be less than those trajectories with an easterly origin. By contrast however, on the 23rd January 1991, the moisture of the trajectories was seen to be much greater than in the previous cases even though the flow was from the south Atlantic. The origin of these trajectories was seen to be further north than the others and may have been part of the recirculated air from the continent. The moisture content may be expected to be higher in this case, as there has been a more tropical influence. South easterly flow of air into the subcontinent was also expected to occur under ridging anticyclonic conditions. Samples in this study however showed a rather more easterly flow. The moisture content of these trajectories was also seen to be high.

The westerly wave disturbances are also associated with easterly flow and flow from the south Atlantic. The easterly flow is expected ahead of the frontal system whilst cold air from the south will follow the front. Such flows were observed on some trajectories calculated for the 13th February 1989, 11th February 1996, and 23rd January 1981. Observation of the changes in the vertical for these same trajectories also showed that there was a gradual descent from higher up in the troposphere towards the surface (see Figure 4.10). Trajectories originating from the south Atlantic and following a south-westerly flow was seen to be those that originated from higher up in the atmosphere. Examples from the 23rd January 1981

showed these air masses to have reached above the 0.4 sigma level. This event has been classified here as having been influenced by a cut-off low, and as Tyson et al. (1996a) noted, such systems are seen to perturb through the whole troposphere. By comparison neither of the flows from the east or the west were seen to have originated from such heights (Figure 4.10).

The moisture content of all these trajectories was also seen to increase whilst near the southern coast (see 5th Dec 90, 23rd Jan 91 and 23rd Jan 81). The warm Agulhas current is seen in this same area, following the continental shelf to about 15°-22°E when it is seen to retroflect back towards the south Indian Ocean. The heat flux has been found to be high along this current and especially over the retroflection region (Mey *et al.*, 1990; Walker & Mey, 1988). Turbulent heat fluxes have been found to average over 150Wm^{-2} over a year (Walker & Mey, 1988) with maximum losses of between $175\text{-}200\text{Wm}^{-2}$ in the core of the retroflection region. However the heat fluxes are observed to decrease northwards, towards the continental shelf areas, where they average between 75 and 125Wm^{-2} (Walker & Mey, 1988). Latent heat flux is seen to account for more than 90% of the total turbulent flux (Walker & Mey, 1988). The increase in moisture for the trajectories crossing over this current could therefore have been as a result of this high latent heat flux.

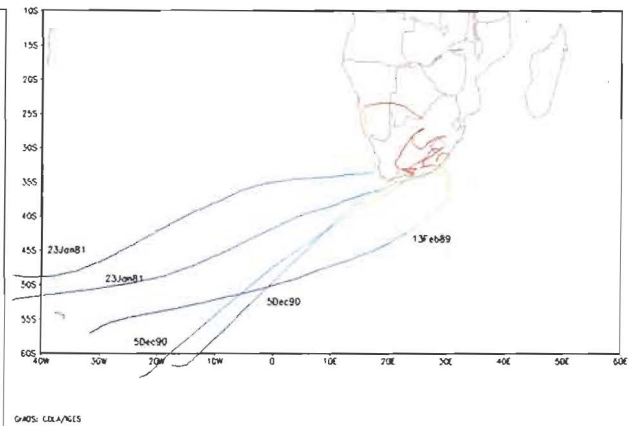
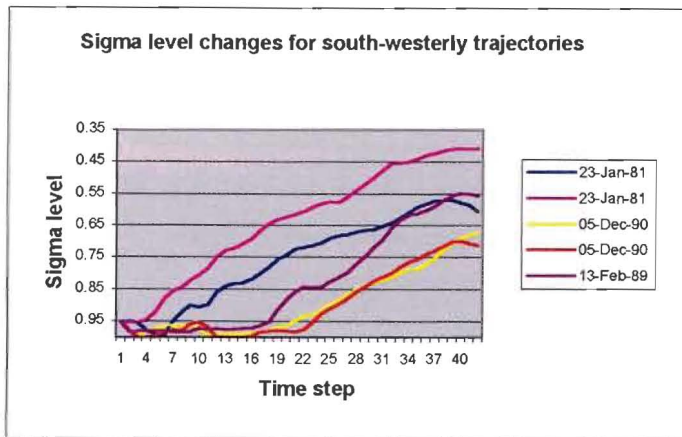
In addition to the air transport studies, water vapour transport in the region have also been investigated to understand the differences that occur between predominantly wet and dry seasons as well as the differences observed between early and late summer (D'Abreton & Tyson, 1995; D'Abreton & Lindesay, 1993). Significant differences were seen in both of these cases. During the early summer season (Oct-Dec), important moisture sources are found in both the tropical south Atlantic and the south Indian Oceans (D'Abreton & Tyson, 1995; D'Abreton & Lindesay, 1993), but during the late summer (Dec-Feb), the south Indian Ocean is seen to play the major role as a moisture source (D'Abreton & Tyson, 1996; 1995; D'Abreton & Lindesay, 1993). D'Abreton and Lindesay (1993) showed how during the early wet season influx of water vapour is from the north-west, but that during a much drier season, this flow is absent and is rather replaced by a south-easterly flux. D'Abreton and Tyson (1995) confirmed this and showed that the north-westerly flow is aided by eddy divergence which is effected by westerly disturbances present during the early summer. They also observed that during the dry early summer, transport of available moisture from the south Indian Ocean is northwards. Eddy divergent transport occurs further to the east in this case,

as the upper tropospheric wave is also displaced in this direction (D'Abreton and Tyson, 1995).

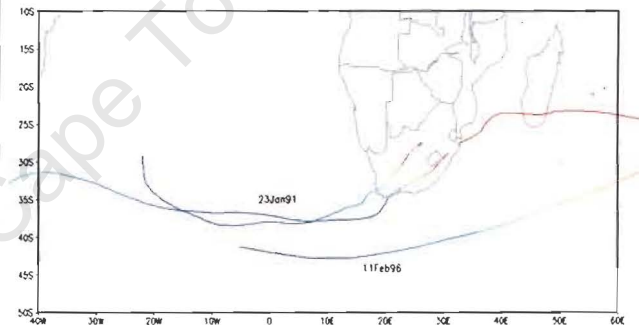
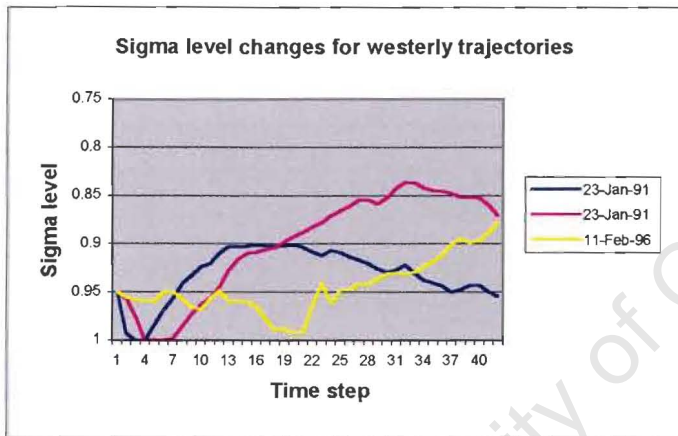
Much of the rainfall in South Africa during the summer is experienced during the later part of the season. In this study, extreme precipitation events were selected from the months of December, January and February. All the events therefore fall under the late summer category. For this time period, it has been found, as mentioned before, that the south Indian Ocean forms the major source of moisture for the region's rainfall. The vertically integrated vapour fluxes for mean January show a maxima over southern Angola/northern Namibia as well as over the island of Madagascar, showing a zonal pattern over the subtropics, in the south and west (D'Abreton and Lindesay, 1993). The pattern over South Africa is seen to be westerly, southwesterly to northwesterly. Vapour fluxes in the north near the equator and tropical regions are not seen to change drastically between wet and dry Januaries. However, during wet Januaries over Madagascar and subtropical southern Africa, large northeasterly vapour fluxes are observed (D'Abreton & Lindesay, 1993). Strong divergence also occurs over the western tropical Indian Ocean north of Madagascar, whilst convergence is seen over tropical Africa (D'Abreton & Tyson, 1995). Divergent transport of water vapour thus occurs to the south into the eastern parts of the southern African region (D'Abreton & Tyson, 1995). The non-divergent component of the circulation shows a southward shift of the Indian Ocean cyclonic cell. At the same time, an anticyclonic cell from the western tropical Indian Ocean extends southwards into the Mozambique Channel. Over the sub-continent, a north-south cyclonic cell develops which facilitates the transport of moisture from the tropics to the south (D'Abreton & Tyson, 1995).

By contrast during the drier Januaries, the divergence over west Indian Ocean decrease in magnitude as well as spatial extent (D'Abreton & Tyson, 1995). The convergence over tropical Africa increases whilst an area of divergence over eastern southern Africa develops and results in southerly divergent transport out of the region (D'Abreton & Tyson, 1995; D'Abreton & Lindesay, 1993). The non-divergent transport for the dry late summer season sees the cyclonic cell, which was over the interior displaced westwards into the Atlantic Ocean (D'Abreton & Tyson, 1995). The anticyclonic cell over the Mozambique Channel is also seen to weaken and change to cyclonic. The water vapour is thus observed to move from tropical Africa eastwards to northern Madagascar as well as an easterly to southeasterly transport over northern South Africa (D'Abreton & Tyson, 1995).

a)



b)



c)

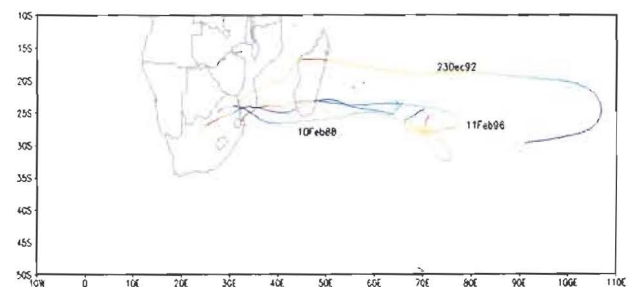
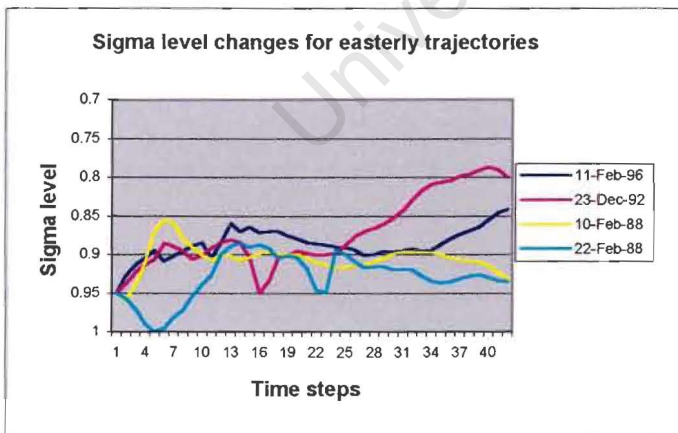


Figure 4.10: Comparison of sigma level changes for trajectories originating from different directions.

For the sample cases examined here the moisture increases and decreases were seen to correlate well with the horizontal divergence fields of the same time periods. Horizontal divergence fields for the trajectories in Figures 4.4, 4.5 and 4.6 were calculated using NCEP reanalysis data. These divergence fields were calculated for four days prior to the dates of the events, so that any possible uptake of moisture whilst the trajectories were over the oceans can be observed. These are shown in Figure 4.11.

The general pattern of divergence of water vapour is such that there is strong divergence over the south Indian Ocean just north and east of Madagascar as well as over the eastern part of the country. Convergence is seen over southern Madagascar and the Mozambique Channel. There is also convergence for certain days over the southern parts of the country. A north-south band of strong convergence is also evident. Moisture is therefore believed to be transported both from the tropics in the north to the subcontinent as well from an easterly direction from the south Indian Ocean.

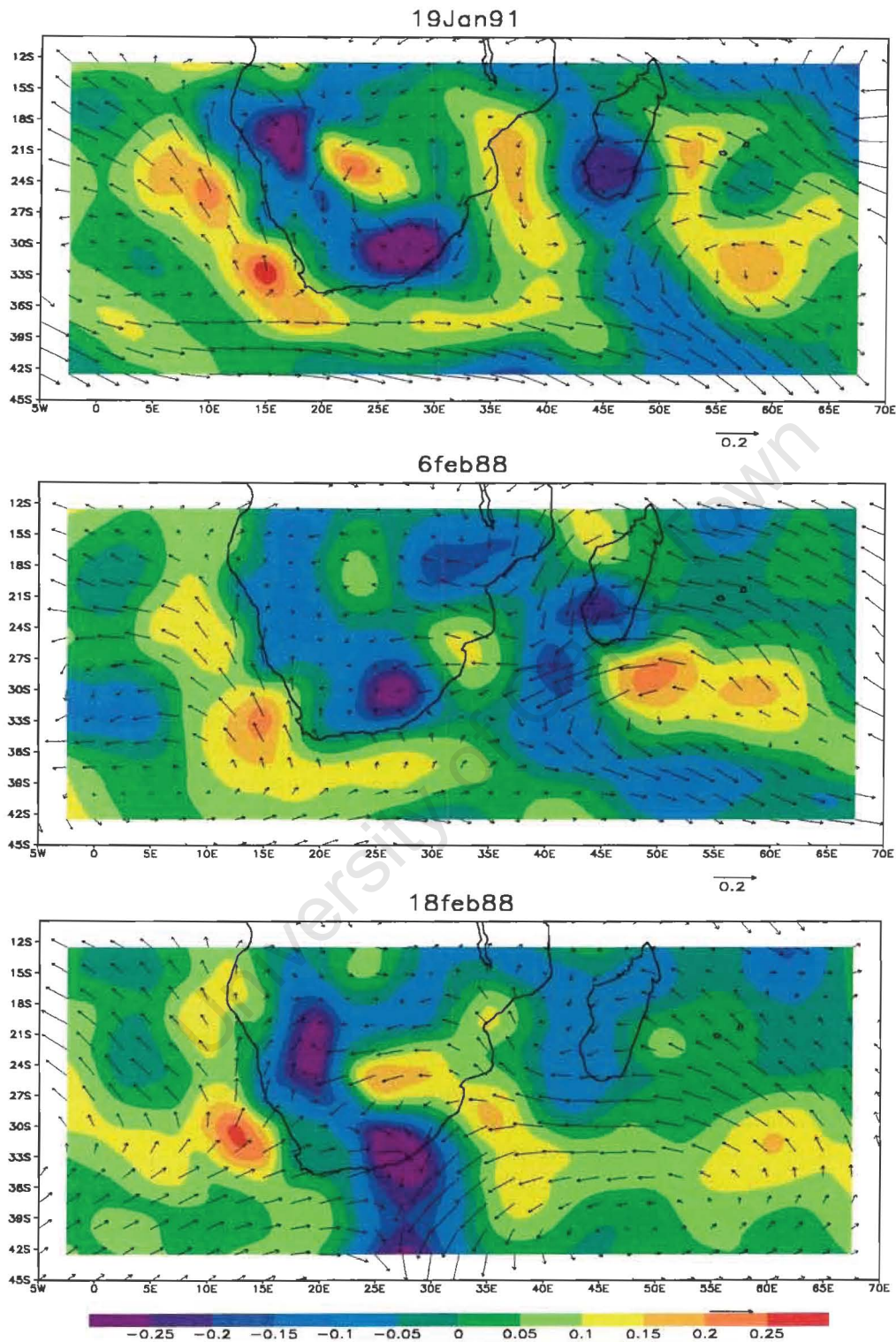
Horizontal divergence ($\times 1000000$) for Node [0 0] events

Figure 4.11(a): Horizontal divergence fields for four days prior to the events examined from Node [0 0]. Positive values indicate divergence

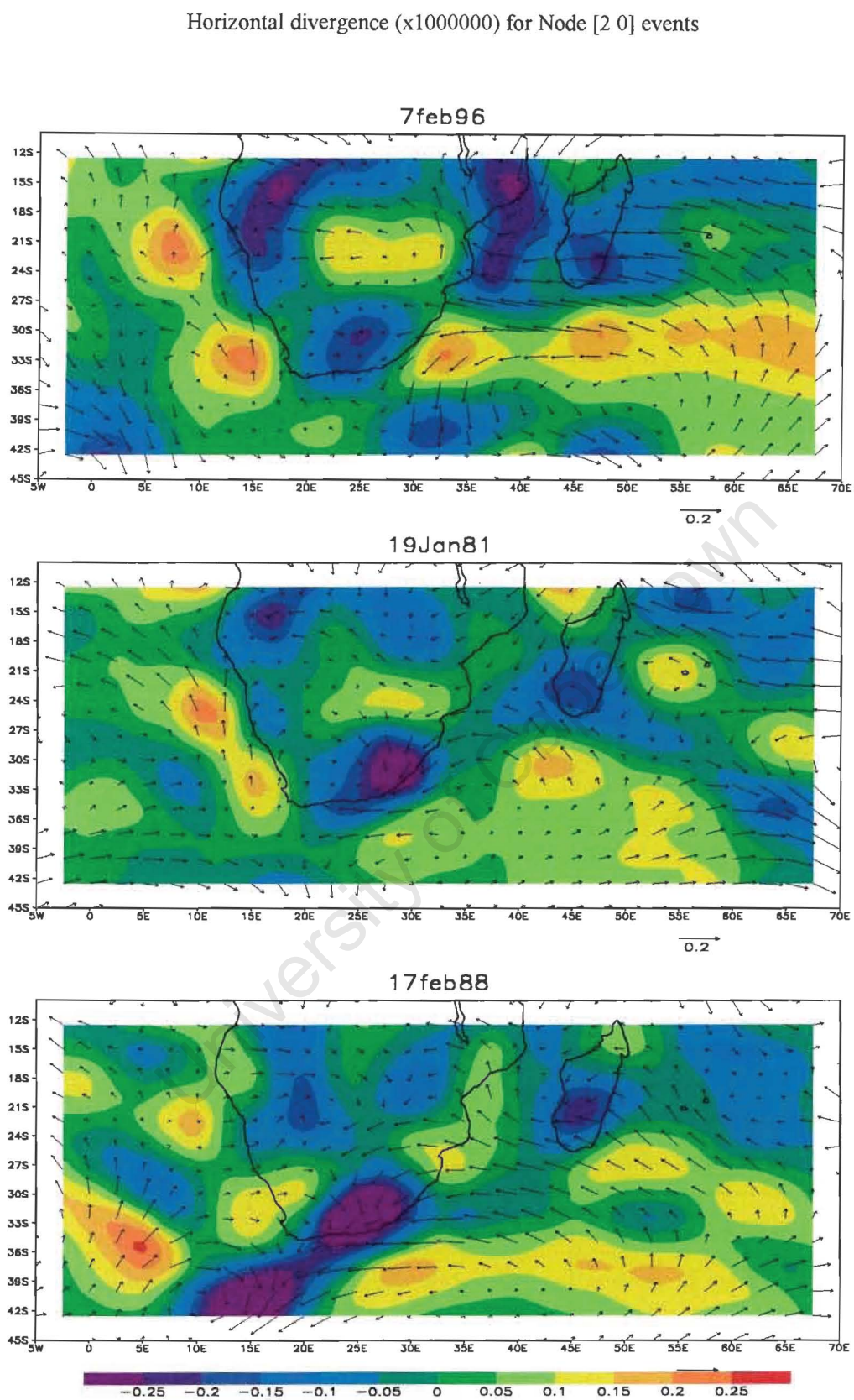


Figure 4.11(b): Horizontal divergence fields four days prior to the events examined from Node [2 0]. Positive values indicate divergence

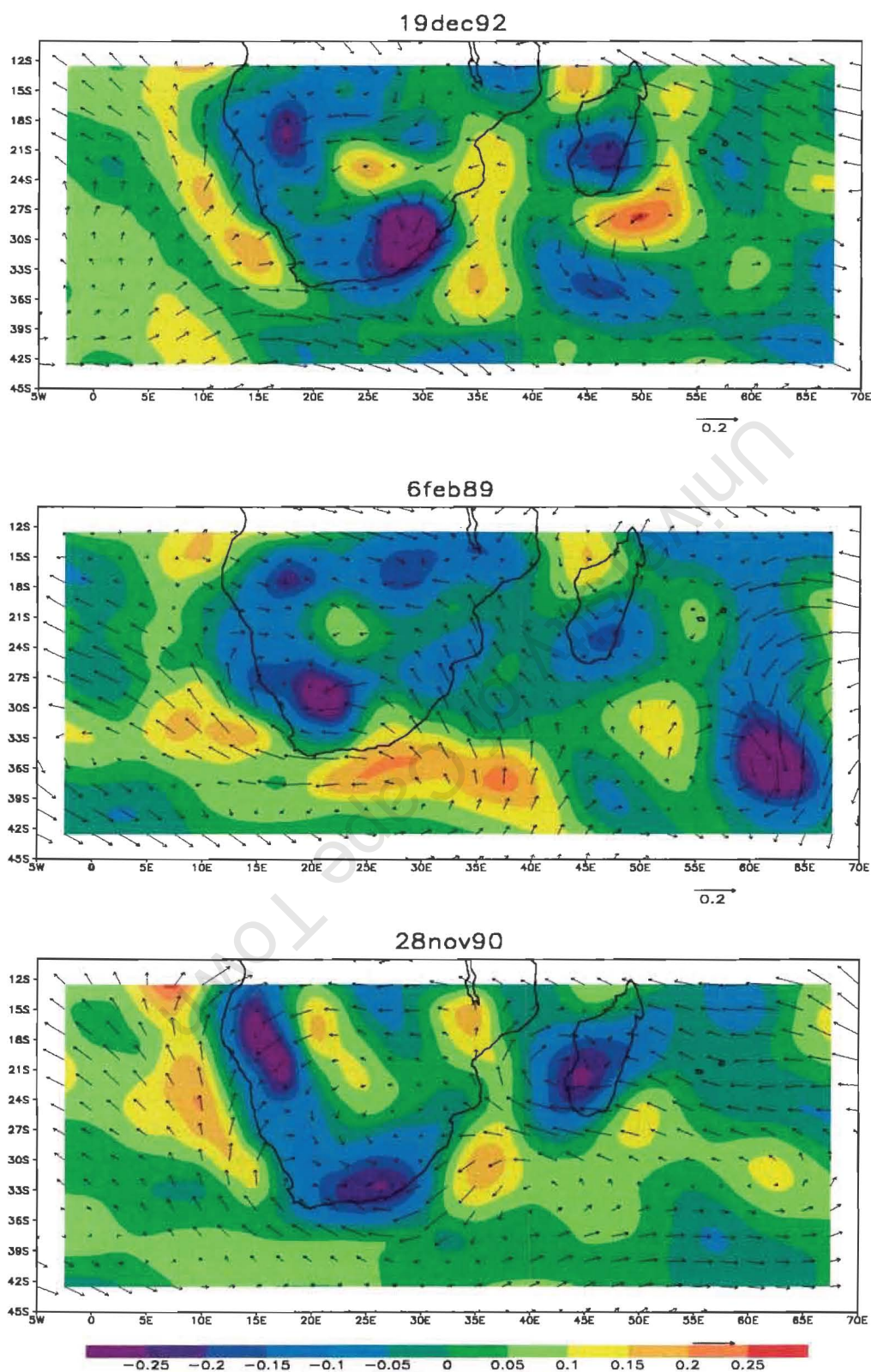
Horizontal divergence ($\times 1000000$) for Node [2 3] events

Figure 4.11(c): Horizontal divergence fields four days prior to the events examined from Node [2 3]. Positive values indicate divergence

4.5: Conclusion

Trajectory modelling has in the past been undertaken in South Africa for various different reasons, most notably for the study aerosol transport (Tyson & D'Abreton, 1998; D'Abreton, 1996; Garstang *et al.*, 1996; Tyson *et al.*, 1996a; 1996b). The investigation of moisture and its transport in the region has recently become an important addition to this area of research. The region's vulnerability to drought and the scarcity of water itself maybe motivating the growth and importance of these investigations. These studies follow the analysis of the rain bearing synoptic systems and their occurrences that were investigated by various authors including Harrison (1986), Tyson (1986) and Taljaard (1995a; 1995b; 1994; 1987; 1986). D'Abreton and Lindesay (1993) and D'Abreton and Tyson (1995) both looked at the transport of water vapour in the region between wet and dry summer months. The investigations also looked at the differences that exist between the early summer and late summer seasons.

By contrast in this investigation trajectory analysis was carried out for a sample of days as a preliminary analysis of moisture pathways related to spatially extensive extreme events identified through the selection process described in Chapter Three. It must be borne in mind that this is a limited investigation of a small number of trajectories. Nonetheless, these are representative of the generalised modes of circulation as represented by the SOM analysis, and as such provide some insight into the processes involved, and offer additional direction for further study.

The calculated trajectories indicated that the major source of moisture lies in an area east of Madagascar in the south Indian Ocean. Previous findings by D'Abreton and Tyson (1996; 1995) and D'Abreton and Lindesay (1993), showed possible moisture source areas for precipitation over the southern African region to lie further north. However these investigations did not concentrate specifically on extreme precipitation events but rather on the general rain events over the summer rainfall region. In contrast a case study of an extreme event by Joubert *et al.* (1999) indicated that the area east of Madagascar might be a source of moisture. These investigations have also shown that the synoptic condition under which the event is observed plays an important role as the circulation under these conditions provides a means by which the moisture from the source area can be supplied to the interior of the subcontinent.

The results from the present investigation also indicated that the Agulhas current to the south of the continent might play a significant role in provision of moisture for some events. The fluxes from this current have been seen to be high (Mey *et al.*, 1990; Walker & Mey, 1988). The scope of the present study does not allow for the indepth investigation of any contribution that this current has on extreme events over the country. However, past studies investigating case events have shown significant contributions of the current to events of high precipitation over the Eastern Cape close to the coast (Rouault *et al.*, 2002). In addition the possible sea surface-atmosphere interaction was not directly investigated in this study. Sea surface temperature changes in the adjacent oceans are believed to have a significant impact on the rainfall pattern over the subcontinent. This as well as the influence of ENSO events has been examined in the past. These non-local changes are known to cause variability in the precipitation pattern over the region. These issues were discussed previously in Chapter Two. Their possible influence on these events examined here were however, not investigated.

Other issues of concern for this study is with regards to the use of the trajectory model itself. There are several different methods and models employed in calculating trajectories used in climatology today. It is not possible in this study to examine all of these or compare them in order to assess their abilities. D'Abreton (1996) however, compared the performance of an isentropic and kinematic model in calculating trajectories for aerosols and trace gases in the region. Another comparison was done by Kahl *et al.* (1989) between isobaric, isentropic and kinematic models on trajectories calculation over the Arctic region (in Fuelberg *et al.*, 1996). These studies note that the kinematic model has a disadvantage over the isentropic one, as the vertical displacement in the first may be substantially higher especially for trajectories at higher altitudes (differences can be double that of isentropic trajectories). Fuelberg *et al.* (1996), however notes that if suitable vertical velocities are provided this problem is minimised and realistic results are obtained. The present study used the kinematic model as it was designed specifically for moisture trajectory transport investigations in the region. Since direct comparisons between the model and others have not been attempted here, it is not possible to assess its performance to other trajectory models. However previous work done using the model and comparisons of these results have been positive (Hewitson *et al.*, 2001; 2000).

It should also be noted here that any results obtained through modelling work is very much dependant on the reliability and accuracy of the source data provided. As has been noted before, the use of NCEP reanalysis data in this thesis does limit the accuracy of the obtained results to a certain extent due to the errors that may exist within the data set. However, this data set is one of the most comprehensive and freely available global climate data sets and is acceptable for use in the work attempted here. The resolution of the data however also introduces possible inaccuracies into the results. The 2.5° X 2.5° grid resolution means that some smaller features would not have been resolved. Events such as thunderstorms, which are associated with high convective processes, are thus not incorporated. This can therefore compromise the specific humidity values in the data and therefore also along the trajectories. However, as the study does focus on spatially extensive events, the use of the data set is still thought to be reasonable and the results acceptable for the preliminary examination.

In the analysis of modelling results, trajectories are often taken as representing the absolute truth. However this is not the case. There is always a margin of error associated with the trajectories. Position errors of up to 20% of the travel distance are still considered to be typical (Stohl, 1998) and more is likely with poorer source data for the models. This leads to varying degrees of uncertainty with the result obtained (Stohl, 1998). This margin of error must always be kept in mind when analysing the results obtained from the model. In this present study however, the margin of error for the trajectories were not calculated. Instead the probability of error is reduced by calculating trajectories for multiple grid points around a single location of interest, for multiple starting times. This reduces the bias that may be associated in deducing conclusions from one single trajectory. The number of trajectories calculated for this present investigation was still however, relatively small. The calculation of more trajectories is possible but the visualisation of a large number of these is a problem. The analysis of a huge number of trajectories then becomes much more complicated. For this reason, the number of trajectories being calculated was kept small but for the greater accuracy of the path, a number of starting points and times were chosen.

The results obtained from the work done in this chapter are encouraging. However as has been pointed out here, there are a number of issues that have not been examined. The analysis of the trajectory results did not reveal distinct differences between the different samples from the three nodes being investigated. However all three nodes have shown that some of the moisture for the event has originated in the south Indian Ocean. An individual

case event is further investigated in the following chapter to see if further information may be attained. This and other case studies from the past will be examined and discussed in Chapter Five.

University of Cape Town

CHAPTER FIVE: CASE STUDY OF AN EXTREME EVENT

5.1: Introduction

The scope of this project does not allow for the thorough analysis of all the days selected for each of the nodes from the SOM analysis. In order to further investigate the moisture transport process and the sources of moisture for these events, the trajectory analysis must be done in multiple locations and time frames. As an example of this process a single large-scale precipitation event is chosen and analysed in greater depth. Although this examination does not serve as conclusive evidence to the non-local sources of moisture for all extreme events in the country, it will serve as a demonstration and stepping-stone for further analysis in this field.

The selection of the case event was done after the inspection of the precipitation records for the selected summer years. The selection of the case event in this manner was done so as to see what similarities if any would occur between this event and those examined in nodes [0 0], [2 0] and [2 3]. This selected event of 23-27 January 1996 was also noted to have occurred during a wet spell period. The literature also shows that this particular event had been previously examined (Edwards, 1997; de Coning, 1997) due to the extensive and heavy precipitation associated with it. When these days were checked against the results of the SOM analysis from Chapter Three, it was found that they mapped against three different SOM nodes, which represent transition states relative to each other (these being nodes [0 2], [1 2] and [2 2]). These features made it an appropriate event to be further analysed. In addition the synoptic conditions for these five days were examined, to help understand the processes that were responsible for the heavy precipitation that followed.

5.2: Synoptic analysis of the event

The summer season of 1995-1996 was one of the wettest seasons in the decade. It followed a long drought period and brought with it flooding to various parts of the country. During this summer period, there were four separate short heavy precipitation events that produced the

high amounts of rainfall (Edwards, 1997). These were the 20-29 December 1995; 16-27 January 1996; 13-17 February 1996 and 22-26 February 1996 (Edwards, 1997). During this entire period it was noted by Edwards (1997) that there was strong southerly horizontal flux of water vapour from over the Indian Ocean north of Mozambique. Of particular interest is the period between the 23rd and 27th of January 1996, throughout which exceptionally heavy rainfall was experienced over a large section of the country (Edwards, 1997). NCEP reanalysis data, in addition to existing literature on this event, is used here to examine the synoptic conditions prevailing over these days¹⁰. This period has also been identified, through the selection process in Chapter Three, as consisting of spatially extensive heavy precipitation days. The results from the subsequent SOM categorization process shows that these days mapped onto three successive nodes; [0 2], [1 2] and [2 2] (Fig 5.1). This progressive change in the mapping of these days by the SOM process may illustrate the gradual change in the synoptic system with time. The source of moisture for the event is investigated here for the duration of the event through trajectory modelling. Any change in the path or source of moisture to the affected areas as the system progresses can thus be identified and examined.

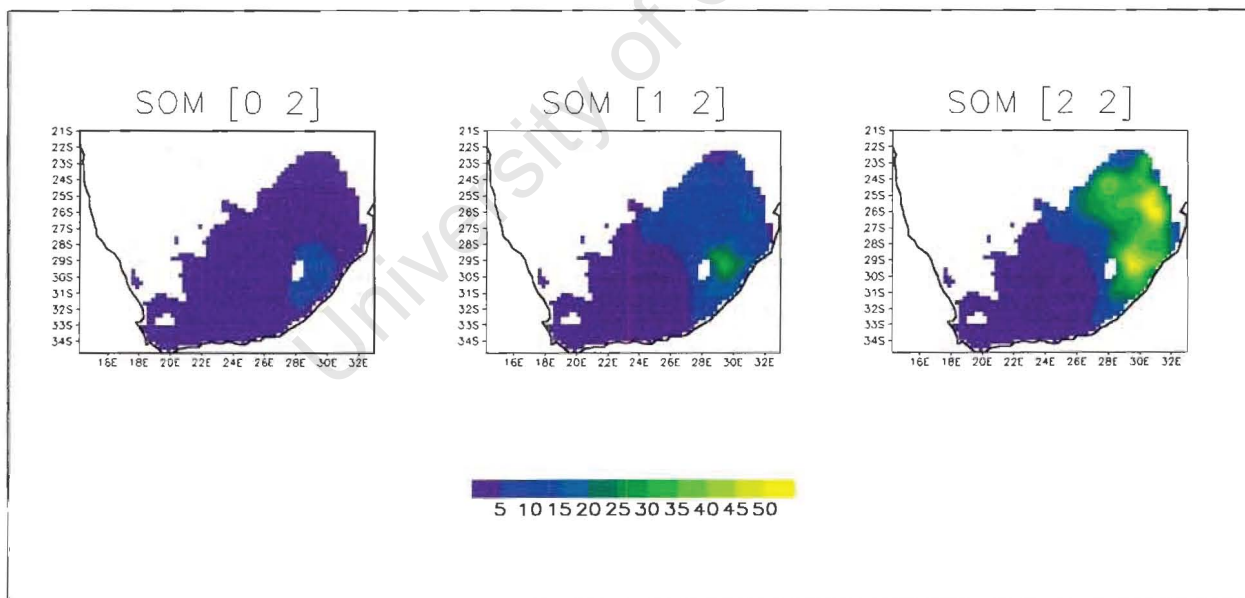


Figure 5.1: The SOM nodes [0 0], [2 0] and [2 3] to which the event of 22Jan1996 to 27Jan1996 mapped to. The precipitation values are given in millimetres.

¹⁰ The relevant synoptic data for the duration of this event, 22Jan1996 to 27Jan1996, is given in the Appendix A. This data is the NCEP reanalysis data for the region.

It has already been found that during this wet season much of the area was under the influence of the maritime equatorial air mass, which typically has a large vertical extent of moisture (Edwards, 1997). The establishment of an upper air trough at an early stage of the season resulted in heavy rain through convective processes. This was followed on the 11th January 1996 by tropical cyclone 'Bonita', which affected the north-eastern and eastern regions of the country. The system quickly dissipated into a low pressure system once inland over Zambia. This low pressure remained quasi-stationary over the area well until the 28th January 1997. Edwards (1997) also notes that the maritime equatorial air flowed southwards to the east of this low pressure system and that the precipitable water vapour increased during this time.

Examinations of the conditions during the 22nd and 27th January 1996 show that the country was affected by a number of factors that in combination produced the heavy rainfall. The south Indian Anticyclone was seen during this time to be strong and present just south of Madagascar between 35°E and 70°E and 30°S and 45°S. The presence of this allowed for the easterly flow of warm, moist air into the interior of the country. On the 22nd January such conditions were seen to be present and an easterly flow was seen crossing the country's boundary at around 29°S. Once inland the flow changed to move southwards into the interior where much of the rainfall during that day was experienced. A cold front was also seen moving east along the east coast of South Africa. A southern flow of more drier and colder air was present behind this front as it progressed. The south Atlantic Anticyclone to the west of the country was seen to ridge eastward behind this front over the next few days. This brought with it a south to south-easterly flow of air to the Cape coastal regions.

The low pressure system over Zambia that was mentioned earlier was seen to intensify during this same time period. A southward flow of tropical air was evident on the eastern side of this low as was observed by Edwards (1997). This system was seen on the 25th January to extend from Zambia down to the western parts of South Africa, forming what is known as a tropical-temporal trough. At the same time a strong baroclinic system was also seen to be present to the south of Cape Town. Easterly flow of air into the interior of the country also continued at this time. The cold front, which intensified as it moved in an easterly direction, was seen to affect the low pressure trough that was prevalent over the interior. A continuous low pressure system extending in a northwest to southeast axis was seen to emerge through this. The passing of the cold front also resulted in the moist equatorial air prevalent over the

previous days being replaced by a much drier air mass from the south-west. The rainfall that was experienced over much of the interior as a result of the extensive tropic temporal trough got progressively confined to the eastern parts of the country as the cold front moved in this direction. On the 27th January the low pressure was seen to be confined to the eastern part of the country with a strong low pressure area present over the north-eastern part of the country.

The paths of the trajectories calculated for this event using the kinematic model should reflect some of these synoptic conditions. Through the tracking of the moisture along the trajectories, the non-local sources of moisture may also be located for this particular event. Previous work done on moisture transport within the region will also then be compared to the findings of this chapter. This is presented in the discussion section after the description of the results of the trajectory analysis that follows.

5.3: Results of the trajectory analysis and discussion

5.3.1: Trajectory results

D'Abreton and Tyson (1996), in their study of the water vapour transport over southern Africa, examined the moisture pathways of an extreme event caused by a cut-off low. The Lainsburg event of January 1981 caused much damage through major flooding to this semi-arid region of the country. In their investigation, D'Abreton and Tyson calculated backward trajectories with the use of a Lagrangian trajectory model to examine the movement of air masses around the core of this storm at the 700hPa level. Through this it was shown that two different and opposite paths of moisture were present. From the tropical region two different sources of moisture was evident. One originated in the equatorial Indian Ocean just off Kenya and the second over Angola (D'Abreton and Tyson, 1996). These two conveyers were seen to merge over southern Zambia before moving south over northern Botswana into South Africa. The cold conveyer on the other hand originated in the Atlantic Ocean south-west of Cape Town. Moisture for the event was also found to have been predominantly supplied by the warm conveyers in this case (D'Abreton and Tyson, 1996).

In the present case study, a similar analysis was attempted with the use of the kinematic model. The specifications of this model and the method employed in obtaining the trajectories were explained in the previous chapter. For the case event chosen here, seven-

day back trajectories were calculated from the 22nd January to the 27th January 1996. The starting locations or grid points were selected in the area of greatest precipitation over each of these days. These locations are shown on the precipitation diagrams for each day in Figure 5.2. Trajectories were calculated from these points for two different starting times; one at 00h00 SAST and the other at 12h00 SAST on each of the stated days. The results of the trajectory calculations are presented in Figure 5.3.

The trajectories represent the paths of the air masses and the amount of moisture associated with them along these paths. As was observed the horizontal extent of the trajectories vary considerably from the different starting grid points. It was also apparent that there were three different locations from which the air masses may have originated for the localities indicated in Figure 5.2 above. These are the South Atlantic Ocean, the tropical Atlantic Ocean and the South Indian Ocean.

The trajectories from three locations calculated for the 22nd January 1996, showed air masses originating from the south Atlantic and the southern sea. Similarly on the 23rd January, air flow from very far south (greater than 55°S) was also observed. However, trajectories calculated from the northeastern part of the country on these same days showed a more tropical origin to the air masses. This source was seen to be in the Indian Ocean, just north of Mauritius (~ 15°S; 57°E), and the flow travelled over Madagascar before reaching the starting point of the trajectory. On the 23rd January, calculations done from a similar location in the northeast show the air mass to have originated from southwestern Zimbabwe. The amount of moisture being carried along this path remained very low up to the starting point of the trajectory. Similar trajectories were also seen on the 27th January, also from starting locations in the northeastern part of the country.

The trajectories for the 24th, 25th and 26th January showed a definite input from the south Indian Ocean and the changes in moisture along these trajectories are also more distinguishable. The paths of the trajectories from the three different locations for the 24th January share a high coherence. Increases in the moisture content of the trajectories were observed to occur in the South Indian Ocean close to Mauritius. On the 25th and 26th however, the paths did not stretch eastward to the same extent. The tracks were mainly confined to the Mozambique Channel except for once on the 26th when a trajectory was

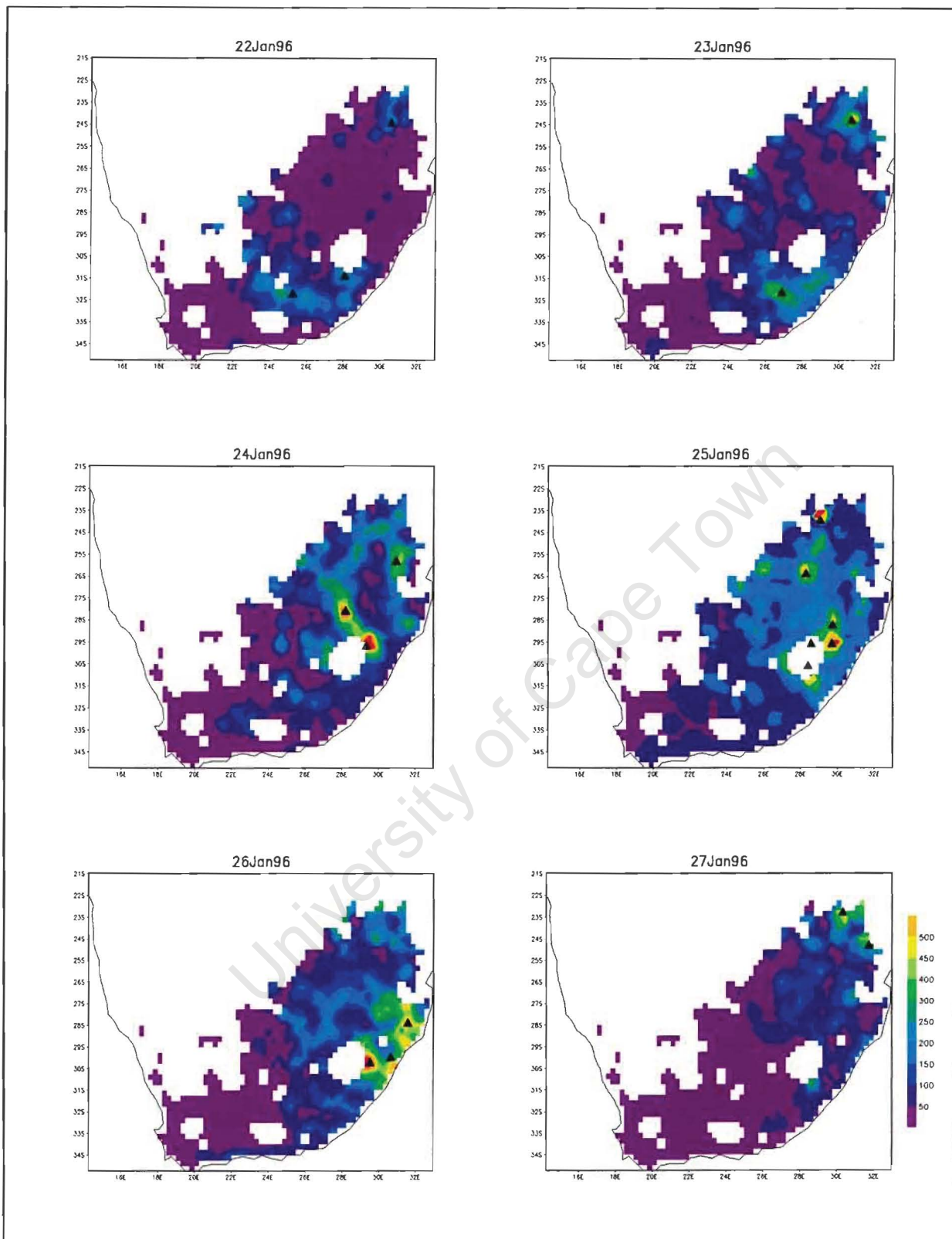


Figure 5.2: Locations of the starting points of the trajectories for the case study event (22-27Jan1996), shown by solid black triangles on the daily accumulated precipitation (in mm) maps for each individual day.

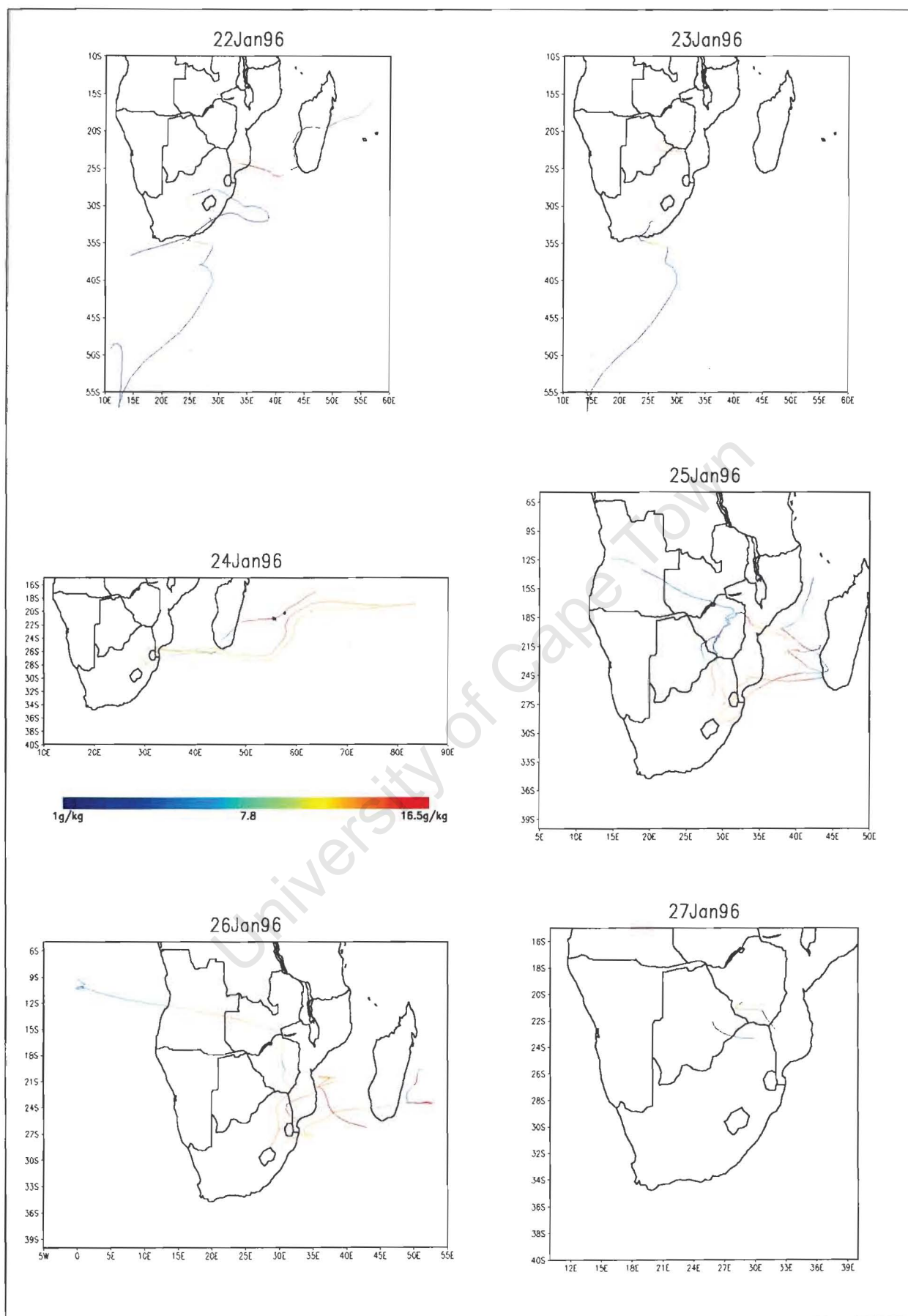


Figure 5.3: Trajectories for each day of the case study event of 22-27Jan 1996, at the starting time of 00h00.

observed just east of Madagascar. During this particular day, air mass was also seen to have originated in the Atlantic Ocean. The path of this air mass was observed to move across central Angola, Democratic Republic of Congo, and southwards over Zimbabwe before moving further south towards the point of origin, just east of Lesotho. Along this track the moisture level was seen to have increased and decreased. The conditions over the interior of the continent during this time were such that a low pressure trough was observed as was mentioned previously. This may be contributing to the increase in moisture along the path of this trajectory as it travelled through the continent.

5.3.2: Discussion of results

As was discussed in the previous chapter, some water vapour studies have been carried out in the region. These have indicated that the source of moisture for rain events in South Africa is primarily located in the western tropical Indian Ocean (D'Abreton & Tyson, 1996). The continental regions around this area are also thought to provide some moisture that is brought down to South Africa by a warm conveyor. This is thought to have been the situation for the Laingsburg flood event of Jan 1981, which D'Abreton and Tyson (1996) investigated.

The findings of the present study are such that similar warm and cold conveyors were observed as was found by D'Abreton and Tyson (1996). The case event shows that air masses may originate in the south Atlantic or the tropical regions of the South Indian Ocean. The trajectories originating from the tropical regions were observed to carry more moisture. This may be attributed to the difference in the sea surface temperatures of the two regions. High sea surface temperatures contributes to higher latent heat fluxes and allow the air over the region to carry more water vapour. By comparison the colder air from the poles carry less water vapour.

Comparisons of the paths of the trajectories from this study and those of D'Abreton and Tyson (1996) show that those calculated in this case study originated much further south as oppose to those of D'Abreton and Tyson (1996). During the seven-day back trajectories from various locations, the paths were not seen to move further north than 15°S whilst other trajectories were seen as far east as 58°E. The calculated trajectory fields for rain days by D'Abreton and Tyson (1996) showed that the easterly flow from the tropical Indian Ocean was from north of Madagascar, and the onshore flow into Africa was at around 10°S. The

case studies in their paper also showed that for the Laingsburg event, the trajectory paths originated from even further north in the Indian Ocean, off the coast of Kenya, whilst the trajectories of the tropical-temperate trough case study, indicated origins more similar to those of the present study. These trajectories were observed to the east of Madagascar and some from over the Island itself. In both of these studies clockwise curvature of trajectories was observed south of Madagascar. In the present case study however, the curvature occurred further east than in those observed in D'Abreton and Tyson (1996). This curvature and change in the path was probably due to the presence of the South Indian Anticyclone in the same region.

The differences seen here between the present study and those of the case studies of D'Abreton and Tyson (1996) may be due to the use of different trajectory models for the investigations. The kinematic model used by D'Abreton and Tyson (1996) also uses a different set of source data, that of the European Centre for Medium Range Weather Forecasts (ECMWF). This data set, which gives twice daily data, is then interpolated to obtain hourly data. In addition vertical interpolation is also done from the standard seven pressure surfaces to ten equally spaced pressure levels (1000-100hPa) for the model. In contrast this study's model uses six hourly data on 12 sigma levels that are placed such that there are more levels at the surface than at the top of the atmosphere. Such differences in the models, in addition to any synoptic differences between the events investigated, may be a reason for the differences seen in these results. In addition, the changes in moisture for these events were also investigated in both studies.

The location where moisture content was seen to increase the greatest in this study was in a region of the south Indian Ocean, just east of Madagascar. The average specific humidity value of the air masses over this region was around 13gkg^{-1} . Other regions of high moisture increases for the air mass trajectories calculated were in the Mozambique Channel. The maximum moisture values in these regions can reach about 17gkg^{-1} . The changes in the moisture content along each of these trajectories were quite different. Some of these changes can be seen in Figure 5.4(a), which represents the water vapour values for a number of calculated trajectories shown in Figure 5.4(b).

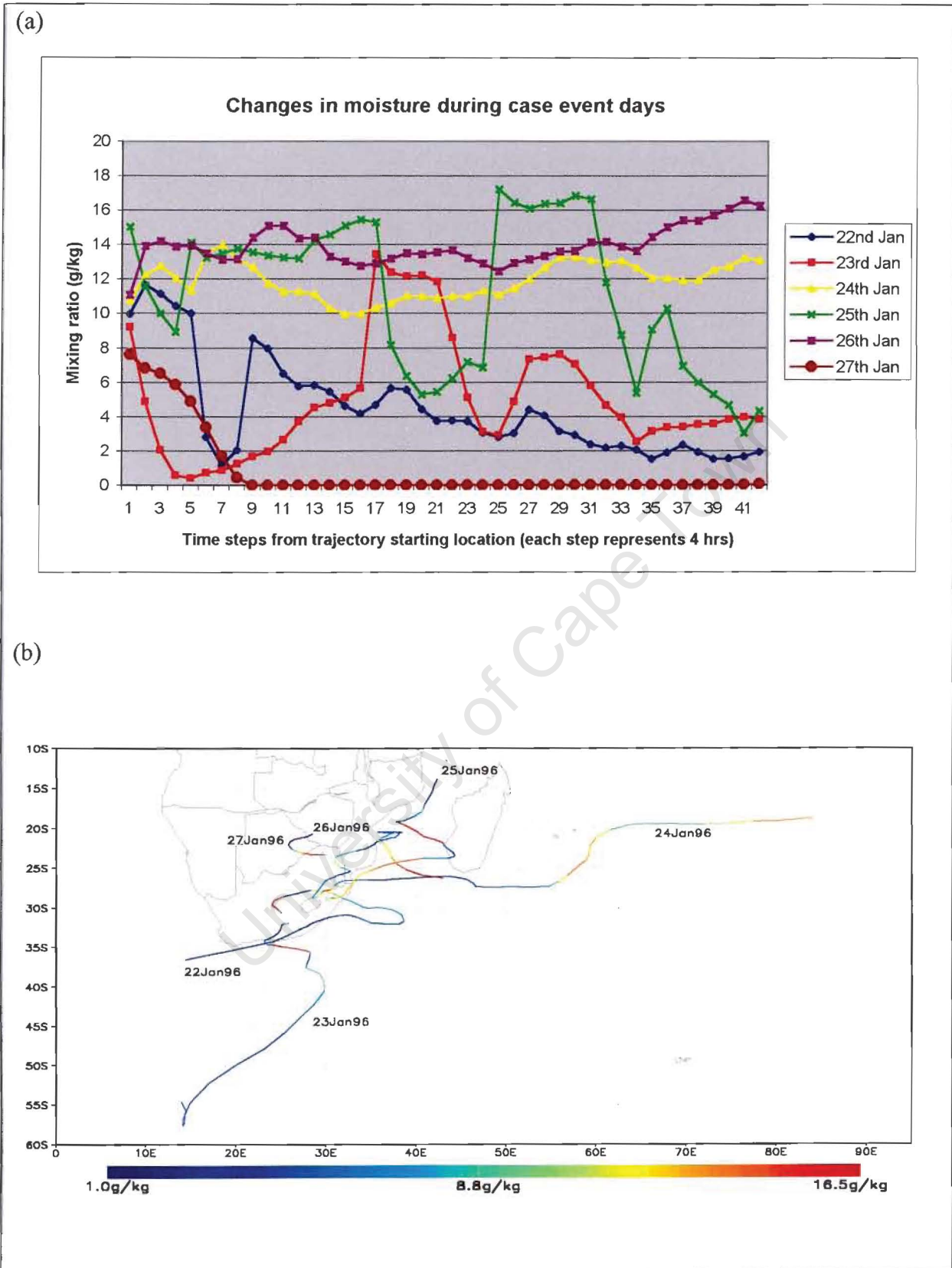


Figure 5.4: Changes in the moisture content (a) of the trajectories represented in (b).

The horizontal divergence fields were also calculated for this period using NCEP data (see Appendix A). These show positive values south and east of Madagascar, in the south Indian Ocean. Negative values, or divergence was seen over the subcontinent and over much of the Madagascan Islands. D'Abreton and Tyson (1995) studied water vapour transport in dry and wet Januaries and found that for the wet January, strong divergence to occur over western tropical Indian Ocean north of Madagascar. This is also seen for the duration of the present case event. However in this case in addition, strong divergence fields were seen to the south of Madagascar as stated.

Convergence of water vapour was also seen to occur over the tropical region and over the eastern part of the country. This was thought to be associated with the Walker cell and Hadley cell as explained by Harrison (1984a). D'Abreton and Tyson (1995) also notes, that the divergent transport of water vapour occur to the south, into the eastern parts of the region. This was also observed in the present case event. These observations were in agreement with the conditions that are observed during predominantly wet summer seasons into which this case study falls.

It is evident from the graph in Figure 5.4(a) that the trajectories originating in the south Indian Ocean carry more moisture than those from the south Atlantic Ocean. The trajectories represented in the Figure 5.4(a) for the 24th, 25th and 26th January, have specific humidity values on average of around 12gkg^{-1} . These values were seen to fluctuate more on the 25th January than in the other two cases. The trajectory for this day showed that it moved through a region of greater horizontal divergence in the Mozambique Channel, at which point an increase in the specific humidity from around 5.5gkg^{-1} to over 16gkg^{-1} was observed. The flow was then seen to move further south passing over southern Madagascar, which was seen to have a strong horizontal convergence developing. This may be attributed to the decrease of moisture seen in the air mass. Some of this moisture was recovered once the trajectory moves across the warm Channel.

In the case of the 23rd January, it was observed that the specific humidity value increased drastically from around 6gkg^{-1} to around 13gkg^{-1} at time step 17, or 68 hours after the start of the trajectory. The values were then seen to decrease again. This increase may be attributed to the Agulhas Current that is located near the region where the increase was observed. As mentioned in the previous chapter, latent heat flux over the Agulhas Current is very high.

This may contribute to an increase in the water vapour content being carried by the air mass as it travels over this current. Observations of latent heat fluxes were done using NCEP reanalysis data for the event period. It showed high values of 150-250 Wm^{-2} in this region to the southeast of the country. Such high latent heat flux values were also observed to the east of the country at 25°S; 35°E. This may be contributing to the increase in moisture seen for trajectory of the 22nd January (see Figure 5.3). In addition high flux values were also seen south and east of Madagascar, in the region where moisture increases are also observed. Very high values along the coast of the South Africa were also seen to develop from the 26th January. The pattern corresponds well with the ridging anticyclone that was also observed at the same time.

High latent heat fluxes were also present over the interior of the continent, particularly over Zambia and Angola. This may also be a contributing factor to the increase in moisture seen for the trajectory calculated for the 26th January, especially as the area has been under heavy precipitation for a considerable number of days. Soil inundated with rainfall may contribute to a certain extent to an increase in the moisture of the air in a localised area. As was discussed in the previous chapter, contribution by vegetation and soil to these events have not been studied to a large extent in this region.

The changes in altitude were also investigated as was done in the previous chapter. Observation of the trajectories for this case event showed, as for the trajectories in the previous chapter, changes in the altitude to be small. These vertical changes along the trajectories represented in Figure 5.5 (b) are given in Figure 5.5 (a).

For most of these trajectories vertical movement was confined to below the 0.85 sigma level. Only in the case of the 22nd January did the trajectory show movement above this, to around 0.67 sigma. This trajectory was seen to have descended from this level after travelling around a low pressure system just east of the country. This trajectory was not seen to carry much moisture along the way, with the maximum value of 10gkg^{-1} seen only at the start of the trajectory (Fig 5.4(a)). The average value for the rest of the time is around 4gkg^{-1} . Similar observations were made by D'Abreton and Tyson (1996), where the average moisture content of the cold conveyor was also found to be in the same order of magnitude.

The comparison of the differences in the vertical changes in the isentropic and the kinematic models done by D'Abreton (1996) show the difference to be smaller than in previous investigations like those of Fuelberg et al. (1996). These results have encouraged the use of kinematic models such as the present one, in the region especially as the conditions prevailing does not always allow for the use of isentropic models. D'Abreton (1996) concludes that at the 500hPa level the difference remains small, with the absolute difference being about 400m for trajectories up to 2 days.

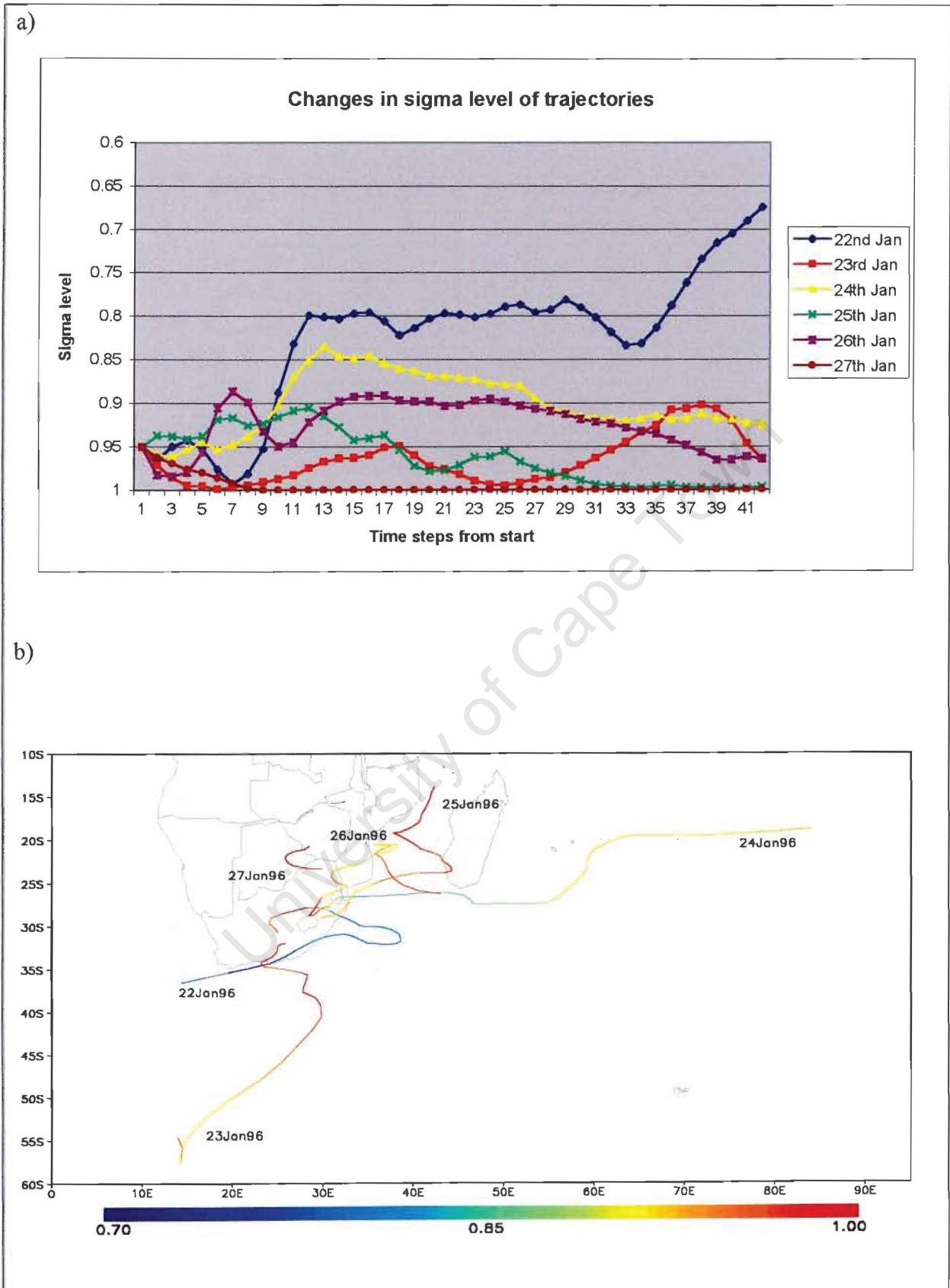


Figure 5.5: Sigma level changes (a) of the trajectories (b) during the event days.

The use of the kinematic model such as the one used here often helps in not only locating the non-local sources of moisture but also to understand the underlying processes responsible for the precipitation events over the country. In conjunction with other climatic data, the model helps to visualise the movement of air masses and moisture in the atmosphere.

5.4: Conclusion

The observations made through the examination of the case event in this chapter revealed that moisture for this spatially extensive precipitation event had more than one source location. The trajectories calculated at the beginning of the event showed that the air flow was from the extreme southern sea and the south Indian ocean. The passing of a cold front and the presence of a strong anticyclone to the east of the country can be attributed to these. During the next few days a tropical-temporal trough is observed to develop and intensify. At the same time, a strong baroclinic system to the south of the country was also seen approaching from the west. The moisture for precipitation during these days was seen to be originating mainly from the tropical regions, both in the Atlantic and south Indian Oceans. The amounts of moisture were however seen to be higher from the south Indian Ocean than from the Atlantic Ocean.

The most likely source of moisture for rain days in the country has been pointed out through previous studies to be the south Indian Ocean (D'Abreton & Tyson, 1996; 1995; Joubert et al., 1999). However, the trajectories calculated in the present case study indicate the source of moisture to be further south than these findings. D'Abreton and Tyson (1995) in their examination of the divergent and non-divergent water vapour transport in the region, indicated that the region north of Madagascar in the western tropical Indian Ocean to be of great importance for predominantly wet summers. This is also confirmed through trajectory modelling done by D'Abreton and Tyson (1996). However the area of increased moisture for the trajectories calculated in this study was found to be just east of Madagascar in the south Indian Ocean. It must be noted that the investigation here is of spatially extensive precipitation events. A number of previous studies have focused on looking at predominantly wet and dry months and comparing the differences in these (D'Abreton & Tyson, 1996; 1995). The case studies of extreme events that have been studied are limited and future investigations like the present one will only benefit in understanding of these events.

The findings of the trajectory calculation for this case study event showed that the source of moisture for these extreme events might indeed be different from what has previously been proposed. However, only a limited number of trajectories were calculated in this case study and it is therefore difficult to form a strong conclusion from them. The results are only valid for this particular event and other extreme events may produce different results. Analysing vast numbers of trajectories was indeed one of the major challenges of this project and future studies of this kind. A better visualisation technique than the present one needs to be developed for the understanding of the events that produce huge quantities of rainfall in the country.

Another point of consideration is the existence of a natural variability in the rainfall pattern of the region. This has been the focus of many studies and has shown that in the southern African region, the precipitation may be closely linked to non-local forces. Fluctuations in the sea surface temperatures of the adjacent oceans have been attributed to have a large impact on the rainfall of the region (Rocha & Simmons, 1997a; 1997b; Mason & Jury, 1997). Investigation in this direction was not attempted for this study as the topic was beyond the scope of this study. In addition large-scale forces such as ENSO, which has effects on a global scale are also responsible for a portion of the variability of the region's rainfall (Rocha & Simmons, 1997a; 1997b; Lindesay et al, 1986; Nicholson & Kim, 1997). These effects, the rainfall pattern and its variability were introduced in Chapter Two. They are important issues that must be investigated in conjunction with any study of extreme events in the future.

CHAPTER SIX: SUMMARY AND CONCLUSIONS

The primary aim of this thesis was to locate the possible non-local moisture sources for spatially extensive heavy precipitation events over South Africa. For this purpose it was necessary to firstly define the spatially extensive precipitation days in terms that would allow for a method to extract them from the data set as well as keeping within the pre-define terminology for such events. This was successfully done and the events selected and classified into different groups or nodes, through the use of the Self Organizing Map method.

6.1: Findings of the Study

A review of the SOM method as well as the basic ANN principles is provided in Chapter Three. The use of the method for the categorising process proved to be helpful in identifying the spatial patterns that existed in extreme precipitation events over the region. As was pointed out, one of the key advantages of using this method of classification was the ability to view the relationship that each of the patterns or groups has with one another. This was evident in the results of the summer SOM (Fig. 3.6). The possible synoptic systems responsible for some of the precipitation patterns were speculated to be tropical-temperate troughs. These systems have been previously identified as being the primary synoptic systems providing much of the summer rainfall over the country (Lindesay, 1998; Tyson 1986; Harrison, 1984a).

Three of the dominant nodes identified by the SOM method were then investigated further with the aid of a kinematic trajectory model. The specifics of this model are given in Chapter Four. The trajectories from several locations for sample days from each of the selected nodes were calculated and the results discussed. Trajectories were seen to originate from the south Atlantic or south Indian Oceans. Of these two locations, trajectories originating from the south Indian Ocean were seen to carry substantially more water vapour than those from the south Atlantic.

Of the trajectories seen to originate in the south Indian Ocean, the location of highest moisture uptake was observed to lie east of Madagascar. This finding is different to previously thought locations for moisture sources in the Indian Ocean. The earlier studies

had indicated that areas further north to be possible source areas of moisture for rainfall over South Africa (D'Abreton & Tyson, 1996; 1995; D'Abreton & Lindesay, 1993). More recent study by Joubert *et al.*, (1999) has also found different source of moisture to this previously thought location. In their study it was also found that the south Indian Ocean is the most important source of moisture and unlike the earlier findings also identified a region further south as the possible location. Although the region located by this present study and that of Joubert *et al.*, (1999) is still not exactly the same, it does appear that the non-local source of moisture for heavy precipitation is most likely located further south and possibly further east than previously believed.

The trajectory results were also analysed to see what vertical changes may have occurred and the differences between them. The change in the altitude was found to be small in most of the cases. It was often seen that the trajectories from the south Indian Ocean did not attain great heights during the course of transport. Those from the south Atlantic however were seen in some cases to reach about 0.6 sigma level. Changes were also seen when trajectories crossed the island of Madagascar where mountains are present over the eastern side. This could have been a possible reason for the changes in altitude seen for along these trajectories. Although it has also been noted that kinematic models have greater vertical changes than their isentropic counterparts (Fuelberg *et al.*, 1996), during this investigation the altitude changes observed were found to be small and reasonable. Similar findings were also found by D'Abreton (1996) in his comparison of these models.

A case event was also chosen and investigated further in Chapter Five with the use of the kinematic model. Such a study allowed for more trajectories to be calculated for a single event that had been possible in the initial investigation. The high precipitation event chosen for this purpose had produced flooding in parts of South Africa and had been discussed before by Edwards (1997) and de Coning (1997).

The trajectories were calculated for this event over several days and the results showed that the predominant direction from which air was seen to be originating was from the south Indian Ocean. Increases in moisture were once again observed to occur in an area just east of Madagascar and also in the Mozambique Channel. Moisture increases were also observed near the southern coast of the country. This is believed to be due to the presence of the warm Agulhas current. It has been noted that the availability of moisture from this current has a

great influence on the rainfall over the country especially over the coastal areas (Walker & Mey, 1988; Mey *et al.*, 1990; Mason & Jury, 1997). The influence of vegetation and soil moisture was also speculated as changes in moisture content were observed for the trajectories travelling inland. Much research is still needed in this field in order to better assess the influence of the local vegetation in providing some moisture for rain events. The vertical changes of the trajectories were also observed to be small in this case except for the trajectory travelling from the south Atlantic Ocean.

As this is a preliminary study of the source and movement of moisture for events in South Africa, the results obtained are insufficient for a firm conclusion to be established. As was mentioned earlier, the number of trajectories calculated was fairly small and more work needs to be done before a conclusive answer may be provided. It is also important to address some of the issues that have arisen during this study that may be improved in any future work carried out.

6.2: Some Caveats of this Study

Every research project tries to ensure that it is as objective as possible in all methodologies used. Even with the help of computers, some decisions have to be made and a degree of subjectiveness is introduced. This was experienced mostly in the initial process of determining the extreme event days in this project. The threshold method was chosen to try and capture those days that had a substantial amount of precipitation over a region so that it was climatologically significant. Similarly an area criterion was introduced to facilitate the selection of spatially extensive events only. Both of these values were chosen after a simple examination of the data. No statistical tests were carried to attribute that the values would be appropriate ones. As the threshold chosen (20mm) is expected to be above the 90th percentile for rainfall in most parts of the country, the use of this method was thought to be reasonable. However, if further comparative work is attempted then a standard method may be necessary in determining extreme rainfall days. Such a standard method does not however seem to exist at present. There have been some attempts made in using indices when studying these kinds of events. This has not been looked at in great detail in this study and will perhaps be an opportunity for other similar studies in future. The use of such indices makes the comparison of work from different regions much easier. This should therefore be

encouraged. However, precipitation is a rather difficult variable to standardise and care should be taken when adopting such an index.

Another aspect that this study was unable to investigate was the rainfall events occurring over more than one single day. As Shulze (1980) points out, in area such as Kwa-Zulu Natal and Eastern Cape, floods occur as a result of rain falling over several days. The probability of a two-day extreme event exceeding the one-day extreme rain by more than 50% is only 1 to 2 years out of 10 in most parts. However, in the case of a seven-day event, the probability increases to 6 to 9 years out of 10 years (Shulze, 1980). The possibility of great floods and soil erosion in this situation is much greater than in the one-day event case. It is therefore important to also analyse the data for two-day and seven-day events in a similar manner as the daily events have been done here.

One of the other issues that is of concern in this study is the length of the data record. The analysis of the heavy precipitation event is only done over approximately 50 years (i.e. 1950-1998). The examination of the results should therefore be done with some caution, as the time frame may not be significantly long enough for firm conclusions to be made. There is also a need for good quality higher resolution data. As has been noted by Joubert *et al.*, (1999), the study of extremes requires such high quality data in order for a reasonable outcome to be achieved. In this study the CCWR data that was used is thought to have been reasonable for the task of categorization that was attempted. However for modelling purposes in future and for analysis of the trends in extreme events, a better quality data may be necessary.

The time constraint of this study has meant that only some aspect of extreme precipitation events could be examined. There still remain an enormous amount of work left to do and these possibilities are examined here.

6.3: Future Research Directions

6.3.1: The importance of investigating extreme events

As was emphasised in the introduction, the social impacts of heavy rainfall can be enormous. The losses sustained by the agricultural sector alone can be devastating. The compounded effects are such that it is not necessarily only a small community that is affected by the

events, but rather an entire region and sometimes an entire nation. The third IPCC report published recently (Houghton *et al.*, 2001) states how the understanding of extreme events is important especially as the sensitivity of ecosystems and society to them is larger than to changes in the means.

The rise in global mean temperatures caused by increasing greenhouse gases is believed to have an effect on regional precipitation. The actual amount and variability of the rainfall is expected to change with the temperature change. There is sufficient indication now that the change in the mean of the variables including precipitation will bring about a change in extreme events. In the southern African region, an increase in rainfall is expected in the summer rainfall region with a decrease in the winter rainfall region (Houghton *et al.*, 2001). The increase in the summer rainfall region is also expected to be caused to a great extent due to an increase in extreme events. Along with this increase in the frequency of heavy precipitation events, the intensity is also believed to increase. This is likely to make more people vulnerable to flooding events such as those experienced over the past two years.

Water is however an extremely valuable resource in this semi-arid part of the world. Compared with how much water is needed for sustainable living, most countries in the southern African region fall short. This is the situation without taking into account any changes that may be experienced in the future. The possible changes in precipitation amounts in the country effectively means that there is a need for policies to be developed, so that those regions that are expected to suffer losses might be able to mitigate and access this resource from elsewhere. It may also mean that there may be a need for better planning on the use of water and its distribution. In order for this to occur, better understanding of precipitation events is needed. Only then will hopefully better policies will be made.

6.3.2: *Directions for future research*

Since it is still a fairly new topic of research, especially in southern Africa, the possible options for further research are substantial. The present initial study of moisture transport has observed that the non-local source of moisture of heavy precipitation events over South Africa to be different to previous findings. This needs to be further investigated with the use of trajectory models as well as more in depth analysis on the synoptics associated with the

events. Recent work with the use of regional climate models may also help in this direction in enabling the three dimensional visualisation of events such as these.

The present study also notes that the frequency and intensity changes of extreme events have not been investigated here. This is another area of importance that leads to possible further work. With a possible increase in the frequency of extreme events in the region, the impact on the intensity of these events must be investigated.

During the analysis of the trajectory results, increases of moisture of the air masses were observed over the subcontinent. Although in some of these cases, such as when a tropical-temporal trough is present, this may be attributed to moisture being brought in from the tropics, in certain cases the increases were observed without any apparent moisture fluxes from these regions. Contribution of moisture is therefore believed to have been made by the vegetation in the region as well as from the evaporation of soil moisture. These issues have been largely neglected in the past and are only now being investigated over the region. The influence that the diverse vegetation in the subcontinent may have is thought to be much more significant than previously believed. However, this avenue of investigation was not a primary aim of this project and the limited time does not allow for further examination of this issue.

One of the other important avenues of research is also on assessing the impact that these events have on both society and ecosystems. Such work will help in implementation of better policies and also in planning various aspects of development (e.g. settlements, roads). The number of people vulnerable to extreme events may be increasing and therefore it is essential to assess this and the various other impacts that may be caused by the movement of populations in developing countries such as South Africa.

6.4: Conclusion

This thesis addresses one of the most important issues that face climate studies today. Extreme events have in the last couple of years been receiving much more attention by the research communities. This can be attributed to the understanding that changes in the mean is likely to be of more importance when it comes to considering the impacts they cause.

Heavy precipitation events experienced in the country has the potential to cause floods in many regions, affecting thousands of residents. This study has attempted to see the spatial patterns that exist within these events and to explore the moisture transports for these events.

It must be made clear that the events examined in this study may not have necessarily caused floods. There are many contributory factors for flooding and heavy rainfall is but one of them. It has however been noted in several studies worldwide that the number of people and communities that are vulnerable to such disasters has increased. This may have been caused by people inhabiting areas on floodplains and sandbank islands within large rivers. The number of people living in urban cities has also been increasing especially in developing countries. Some of these cities are vulnerable to events such as tropical cyclones. The number of people in total that are therefore at risk is much higher. These factors also need to be considered when thinking about the impacts that an increase in frequency of extreme events might have on the country.

There are still many aspects of the topic of extreme events that has not been discussed here. The introduction that this study has brought will hopefully be continued through other studies to improve our knowledge of these events. In this manner the forecasting of these events will be more accurate. Mitigation for these events will therefore be a sincerely possibility rather than disaster relief that we have seen far too often in the region.

REFERENCES

University of Cape Town

REFERENCES

- Andres M., Tomas C. and De Pablo F., 2000. Spatial patterns of the daily non-convective rainfall in Castilla y Leon (Spain). *International Journal of Climatology*, **20**, 1207-1224.
- Badran F. and Thiria S., 1991. Wind ambiguity removal by the use of neural network techniques. *Journal of Geophysical Research*, **92**, 20,521-20,529.
- Bankert R.L., 1994. Cloud classification of AVHRR imagery in maritime regions using a probabilistic neural network. *Journal of Applied Meteorology*, **33**, 909-918.
- Cavazos T., 2000. Using Self-Organizing Maps to investigate extreme climate events: An application to wintertime precipitation in the Balkans. *Journal of Climate*, **13**, 1718-1732.
- Christie F. and Hanlon J., 2001. *Mozambique and the Great Flood of 2000*. Oxford University Press, United Kingdom, 176pp.
- Clothiaux E.E and Bachmann C.M., 1994. Neural networks and their applications. In: *Neural Nets: Applications in Geography*. Hewitson B. C. and Crane R. G. (Eds.). Kluwer Academic Publishers, Dordrecht, The Netherlands, p.35-50.
- Crimp S.J., van der Heever S.C., D'Abreton P.C., Tyson P.D. and Mason F.E., 1997. *Mesoscale modelling of tropical-temperate troughs and associated systems over Southern Africa*. Report No 595/1/97, Water Research Commission, Pretoria, 395pp.
- D'Abreton P.C., 1996. Lagrangian kinematic and isentropic trajectory models for aerosol and trace gas transport studies in Southern Africa. *South African Journal of Science*, **92**, 157-160.
- D'Abreton P.C. and Lindesay J.A., 1993. Water vapour transport over Southern Africa during wet and dry early and late summer months. *International Journal of Climatology*, **13**, 151-170.
- D'Abreton P.C. and Tyson P.D., 1995. Divergent and non-divergent water vapour transport over Southern Africa during wet and dry conditions. *Meteorology and Atmospheric Physics*, **55**, 47-59.
- D'Abreton P.C. and Tyson P.D., 1996. Three-dimensional kinematic trajectory modelling of water vapour transport over Southern Africa. *Water SA*, **22** (4), 297-306.

- Dayhoff J.E., 1990. *Neural Network Architectures: An Introduction*. Van Nostrand Reinhold, New York, 259pp.
- de Coning E., 1997. *Heavy rains and Floods in South Africa During January February 1996: An isentropic Perspective*. Fifth International Conference on Southern Hemisphere Meteorology and Oceanography. The American Meteorology Society, Boston, 400pp.
- Diaz H.F. and Kiladis G., 1992. Atmospheric teleconnections associated with the extreme phases of the Southern Oscillation. In *El Niño: Historical and Paleoclimatic Aspects of the Southern Oscillation*. Diaz H.F. and Markgraf V. (Eds), Cambridge University Press, Australia, 476pp.
- Diaz H.F. and Markgraf V. (Eds), 1992. *El Niño: Historical and Paleoclimatic Aspects of the Southern Oscillation*. Cambridge University Press, Australia, 476pp.
- Easterling D.R., Diaz H., Douglas A.V., Hogg W.D., Kunkel K.E., Rogers J.C. and Wilkinson J.F., 1999. Long-term observations for monitoring extremes in the Americas. *Climatic Change*, **42**, 285-308.
- Easterling D.R., Evans J.L., Groisman P.Ya., Karl T.R., Kunkel K.E. and Ambenje P., 2000. Observed variability and trends in extreme climate events: A brief review. *Bulletin of the American Meteorological Society*, **81(3)**, 417-425.
- Edwards M, 1997. *Heavy rain and Floods in South Africa During January-February 1996: Synoptic Review*. Fifth International Conference on Southern Hemisphere Meteorology and Oceanography. American Meteorology Society, Boston, 400pp.
- Ehrendorfer M., 1987. A regionalization of Austria's Precipitation climate using Principal Component Analysis. *Journal of Climatology*, **7**, 71-89.
- Eliassen A., 1980. A review of long-range transport modelling. *Journal of Applied Meteorology*, **19**, 231-240.
- Fausett L., 1994. *Fundamentals of Neural Networks: Architectures, Algorithms, and Applications*. Prentice-Hall Inc., New Jersey, 461pp.
- Fuelberg H.E., Loring R.O., Watson M.V., Sinha M.C, Pickering K.E., Thompson A.M., McNamara D.P., Sachse G.W., Blake D.R. and Schoeberl M.R., 1996. Trace A trajectory intercomparison: Part 2. Isentropic and kinematic methods. *Journal of Geophysical Research*, **101**, 23,927-23,939.
- Gardner M.W. and Dorling S.R., 1998. Artificial neural networks (the multilayer perceptron)- a review of applications in the atmospheric sciences. *Atmospheric Environment*, **32(14/15)**, 2627-2636.

- Garstang M., Kelbe B.E., Emmitt G.D. and London W.B., 1987. Generation of convective storms over the escarpment of northeastern South Africa. *Monthly Weather Review*, **115**, 429-443.
- Garstang M., Tyson P.D., Swap R., Edwards M., Kållberg P. and Lindesay J.A., 1996. Horizontal and vertical transport of air over southern Africa. *Journal of Geophysical Research*, **101**, 23,721-23,736.
- Gondwe M.P. and Jury M.R., 1997. Sensitivity of vegetation (NDVI) to climate over southern Africa: Relationships with summer rainfall and OLR. *The South African Geographical Journal*, **79(1)**, 52-60.
- Gordon H.B., Whetton P.H., Pittock A.B., Fowler A.M. and Haylock M.R., 1992. Simulated changes in daily rainfall intensity due to the enhanced greenhouse effect: implications for extreme rainfall events. *Climate Dynamics*, **8**, 83-102.
- Groisman P.Ya, Karl T.R., Easterling D.R., Knight R.W., Jamason P.F., Hennessy K.J., Suppiah R., Page C.M., Wibig J., Foruniak K., Razuvaev V.N., Douglas A., Førland E. and Zhai P., 1999. Changes in the probability of heavy precipitation: Important indicators of climatic change. *Climatic Change*, **42**, 243-283.
- Gutowski, W. J., 2001: Self-Organizing Maps (SOMs): Proposed RMIP Analysis. Regional Model Intercomparison Project. Science Team Meeting, Kobe, Japan, 11-13 December 2001.
- Harrison M.S.J., 1984a. A generalized classification of South African summer rain-bearing synoptic systems. *Journal of Climatology*, **4**, 547-560.
- Harrison M.S.J., 1984b. The annual rainfall cycle over the central interior of South Africa. *The South African Geographical Journal*, **66**, 46-47.
- Hewitson B.C., 2002. *The Climatology of water vapour sources, sinks, and transport in southern Africa*. Project K5/1012. Interim report for the Water Research Commission, Pretoria, unpublished.
- Hewitson B.C. and Crane R.G., 2002. Self organizing maps: Applications to synoptic climatology. *Climate Research*, in press.
- Hewitson B. C. and Crane R. G (eds.), 1994. *Neural Nets: Applications in Geography*. Kluwer Academic Publishers, Dordrecht, The Netherlands, 194pp.
- Hewitson B. C. and Crane R. G., 1992. Large-scale atmospheric controls on local precipitation in tropical Mexico. *Geophysical Research Letters*, **19(18)**, 1835-1838.

- Hewitson B.C., Hudson D., Jack C. and Reason C., 2000 *The Climatology of water vapour sources, sinks, and transport in southern Africa*. Project K5/1012. Interim report for the Water Research Commission, Pretoria, unpublished.
- Hewitson B.C., Hudson D., Jack C., Reason C. and Walawege R., 2001. *The Climatology of water vapour sources, sinks, and transport in southern Africa*. Project K5/1012. Interim report for the Water Research Commission, Pretoria, unpublished.
- Houghton J.T., Ding Y., Griggs D.J., Noguer M., van der Linden P.J., Dai X., Maskell K. and Johnson C.A., 2001. *Climate Change 2001: The Scientific Basis*. The Press Syndicate of the University of Cambridge, United Kingdom, 881pp.
- Houghton J.T., Meira Filho L.G., Callander B.A., Harris N., Kattenberg A. and Maskell K., 1996. *Climate Change 1995: The Science of Climate Change*. Cambridge University Press, Great Britain, 572pp.
- Hudson D. A., 1998. Antarctic Sea-Ice Extent, Southern Hemisphere Circulation and South African Rainfall. Unpublished Ph.D Thesis. University of Cape Town, Cape Town, 308pp.
- Hulme M., 1992. Rainfall changes in Africa 1931-1960 to 1961-1990. *International Journal of Climatology*, **12**, 685-699.
- Hulme M. (Ed.), Arntzen J., Downing T., Leemans R., Malcom J., Reynard N., Ringrose S., Rogers D., Chiziya E., Conway D., Joyce A., Jain P., Magadza C., Markham A. and Mulenga H., 1996. *Climatic Change and Southern Africa: an exploration of some potential impacts and implications in the SADC region. Report to WWF International*. Climatic Research Unit, University of East Anglia, UK, 104pp.
- IPCC, 2001. *Climate Change 2001: The Scientific Basis: Summary for Policymakers and Technical Summary of the Working Group I Report*. Cambridge University Press, United Kingdom, 98pp.
- Joubert A.M., Crimp S.J., and Mason S.J., 1999. *Modelling Extreme Rainfall over Southern Africa*. Report No 805/1/99. Water Research Commission, Pretoria, 87pp.
- Joubert M.A. and Hewitson B.C., 1997. Simulating present and future climates of southern Africa using general circulation models. *Progress in Physical Geography*, **21**(1), 51-78.
- Joubert M.A., Mason S.J. and Galpin J.S., 1996. Droughts over southern Africa in a doubled-CO₂ climate. *International Journal of Climatology*, **16**, 1149-1156.

- Jury M.R and Levy K.M., 1993. The climatology and characteristics of drought in the Eastern Cape of South Africa. *International Journal of Climatology*, **13**, 629-641.
- Kalnay E., Kanamitsu M., Kistler R., Collins W., Deaven D., Gandin L., Iredell M., Saha S., White G., Woollen J., Zhu Y., Leetmaa A., Reynolds R., Chelliah M., Ebisuzaki W., Higgins W., Janowiak J., Mo K.C., Ropelewski C., Wang J., Jenne R., and Joseph D., 1996. The NCEP/NCAR 40-Year Reanalysis Project. *Bulletin of the American Meteorological Society*, **77**, 437-471.
- Karl T.R. and Easterling D.R., 1999. Climatic extremes: selected review and future research directions. *Climatic Change*, **42**, 309-325.
- Karl T.R. and Knight R.W., 1998. Secular trends of precipitation amount, frequency and intensity in the United States. *Bulletin of the American Meteorological Society*, **79**(2), 231-241.
- Katz R.W. and Brown B.G., 1992. Extreme events in a changing climate: variability is more important than averages. *Climatic Change*, **21**, 289-302.
- Kistler R., Kalnay E, Collins W., Saha S., White G., Woolen J., Chelliah M., Ebisuzaki W., Kanamitsu M., Kousky V., van den Dool H., Jenne R. and Fiorino M., 2001. The NCEP-NCAR 50-Year Reanalysis: Monthly Means CD-ROM and Documentation. *Bulletin of the American Meteorological Society*, **82**(2), 247-267.
- Kohonen T., 1997. *Self-Organizing Maps*. Springer-Verlag, Berlin, 426pp.
- Kohonen T., Hynninen J., Kangas J., and Laaksonen J., 1995. SOM_PAK: The Self-Organizing Map Program Package. Technical Report A31, Helsinki University of Technology, Laboratory of Computer and Information Science, Finland.
- Krishnamurti T.N., Fuelberg H.E., Sinha M.C., Oosterhof D., Bensman E.L., and Kumar V.B., 1993. The meteorological environment of the tropospheric ozone maximum over the tropical South Atlantic Ocean. *Journal of Geophysical Research*, **98**, 10,621-10,641.
- Liebmann B., Jones C. and De Carvalho L.M.V., 2001. Interannual variability of daily extreme precipitation events in the state of São Paulo, Brazil. *Journal of Climate*, **14**, 208-218.
- Lindsay J.A., 1984. Spatial and temporal rainfall variability over South Africa, 1963 to 1981. *South African Geographical Journal*, **66**, 168-175.
- Lindsay J.A., 1988. Southern African rainfall, the Southern Oscillation and a Southern Hemisphere semi-annual cycle. *Journal of Climatology*, **8**, 17-30.

- Lindsay J.A., 1998. Present climates of southern Africa. In: *Southern Hemisphere Climates: Present, Past and Future*, Hobbs J.E., Lindsay J.A. and Bridgman H.A. (Eds). John Wiley and Sons, England, 297pp.
- Lindsay J.A., Harrison M.S.J. and Haffner M.P., 1986. The Southern Oscillation and South African rainfall. *South African Journal of Science*, **82**, 196-198.
- Lindsay J.A. and Jury M.R., 1991. Atmospheric circulation controls and characteristics of a flood event in central South Africa. *International Journal of Climatology*, **11**, 609-627.
- Lund I.A., 1963. Map-pattern classification by statistical methods. *Journal of Applied Meteorology*, **2**, 56-65.
- Main J., 1997. Seasonality of Circulation in Southern Africa using the Kohonen Self-Organising Map. Unpublished M.Sc. Thesis, University of Cape Town, Cape Town, South Africa, 84pp.
- Marzban C. and Stumpf G.J., 1996. A neural network for tornado prediction based on doppler radar derived attributes. *Journal of Applied Meteorology*, **35**, 617-626.
- Mason S.J., 1996. Rainfall trends over the Lowveld of South Africa. *Climatic Change*, **32**, 35-54.
- Mason S.J. and Joubert A.M., 1997. Simulated changes in extreme rainfall over southern Africa. *International Journal of Climatology*, **17**, 291-301.
- Mason S. J. and Jury M. R., 1997. Climatic variability and change over Southern Africa: a reflection on underlying processes. *Progress in Physical Geography*, **21**(1), 23-50.
- Mason S.J. and Lindsay J.A., 1993. A note on the modulation of Southern Oscillation-southern African rainfall associations with the Quasi-Biennial Oscillation. *Journal of Geophysical Research*, **98**, 8847-8850.
- Mason S.J. and Tyson P.D., 1992. The modulation of sea surface temperature and rainfall associations over southern Africa with solar activity and the Quasi-biennial Oscillation. *Journal of Geophysical Research*, **97**, 5847-5856.
- Mason S.J., Waylen P.R., Mimmack G.M., Rajaratnam B. and Harrison M., 1999. Changes in extreme rainfall events in South Africa. *Climatic Change*, **41**, 249-257.
- McGowan H.A., McTainsh G.H., Zawar-Reza P. and Sturman A.P., 2000. Identifying regional dust transport pathways: application of kinematic trajectory modelling to a trans-Tasman case. *Earth Surface Processes and Landforms*, **25**, 633-647.

- Mearns L.O., Katz R.W. and Schneider S.H., 1984. Extreme high-temperature events: Changes in their probabilities with changes in mean temperature. *Journal of Climate and Applied Meteorology*, **23**, 1601-1613.
- Meehl G.A., Zwiers F., Evans J., Knutson T., Mearns L. and Whetton P., 2000. Trends in extreme weather and climate events: Issues related to modelling extremes in projections of future climate change. *Bulletin of the American Meteorological Society*, **81(3)**, 427-436.
- Mey R.D., Walker N.D. and Jury M.R., 1990. Surface heat fluxes and marine boundary layer modification in the Agulhas retroreflection region. *Journal of Geophysical Research*, **95**, 15,997-16,015.
- Miron O. and Lindesay J.A., 1984. A note on changes in airflow patterns between wet and dry spells over South Africa, 1963 to 1979. *The South African Geographical Journal*, **65**, 141-147.
- Miron O. and Tyson P.D., 1984. Wet and dry conditions and pressure anomaly fields over South Africa and the adjacent oceans, 1963-79. *Monthly Weather Review*, **112**, 2127-2132.
- MMMD, 2000. *PSU/NCAR Mesoscale Modeling System Tutorial Class Notes and User's Guide: MM5 Modeling System Version 3*. Mesoscale and Microscale Meteorology Division, National Center for Atmospheric Research.
- Navone H.D. and Ceccatto H.A., 1994. Predicting Indian monsoon rainfall: A neural network approach. *Climate Dynamics*, **10**, 305-312.
- Nicholls N., Landsea C. and Gill J., 1998. Recent trends in Australian region tropical cyclone activity, *Meteorology and Atmospheric Physics*, **65**, 197-205.
- Nicholson S. E., 1986. The nature of rainfall variability in Africa south of the equator. *Journal of Climatology*, **6**, 515-530.
- Nicholson S. E., 1989. African drought: Characteristics, causal theories and global teleconnections. In: *Understanding Climate Change*, Berger A., Dickinson R.E., and Kidson J.W (Eds). Geophysical Monograph 52, American Geophysical Union, Washington DC, p79-100.
- Nicholson S.E., 1993. An overview of African rainfall fluctuations of the last decade. *Journal of Climate*, **6**, 1463-1466.
- Nicholson S. and Kim J., 1997. The relationship of the El Nino-Southern Oscillation to African rainfall. *International Journal of Climatology*, **17**, 117-135.

- Openshaw S., 1994. Neuroclassification of spatial data. In: *Neural Nets: Applications in Geography*. Hewitson B. C. and Crane R. G. (Eds.). Kluwer Academic Publishers, Dordrecht, The Netherlands, p53-70.
- Patterson D. W., 1996. *Artificial Neural Networks: Theory and Applications*. Simon & Schuster (Asia), Singapore, 477pp.
- Rocha A. and Simmonds I., 1997(a). Interannual variability of South-eastern African summer rainfall. Part 1: Relationships with air-sea interaction processes. *International Journal of Climatology*, **17**, 235-265.
- Rocha A. and Simmonds I., 1997(b). Interannual variability of South-eastern African summer rainfall. Part 2: Modelling the impact of sea-surface temperatures on rainfall and circulation. *International Journal of Climatology*, **17**, 267-290.
- Rouault M., White S.A., Reason C.J.C., Lutjeharms J.R.E. and Jobard I., 2002. Evidence for the influence of the Agulhas Current on a South African extreme weather event. *Weather and Forecasting*, in press.
- Sammon J.W., 1969. A nonlinear mapping for data structure analysis. *IEEE Transactions on Computers*, **C18(5)**, 401-409.
- Stohl A., 1998. Computation, accuracy and application of trajectories – A review and bibliography. *Atmospheric Environment*, **32(6)**, 947-966.
- Stohl A., and Trickl T., 1999. A textbook example of long-range transport: Simultaneous observation of ozone maxima of stratospheric and North American origin in the free troposphere over Europe. *Journal of Geophysical Research*, **104**, 30,445-30,462.
- Shulze R.E., 1980. *Potential Flood Producing Rainfall of Medium and Long Duration in Southern Africa*. Water Research Commission, Pretoria, 37pp.
- Sturman A.P., Tyson P.D., and D'Abreton P.C., 1997. A preliminary study of the transport of air from Africa and Australia to New Zealand. *Journal of The Royal Society of New Zealand*, **27(4)**, 485-498.
- Swap R., Garstang M., Macko S.A, Tyson P.D., Maenhaut W., Artaxo P., Källberg P. and Talbot R., 1996. The long-range transport of southern African aerosols to the tropical south Atlantic. *Journal of Geophysical Research*, **101**, 23,777-23,793.
- Taljaard J. J., 1972. Synoptic meteorology of the Southern Hemisphere. In: *Meteorology of the Southern Hemisphere*. Newton C.W. (Ed), American Meteorological Society, Boston, 139-213.

- Taljaard J. J., 1986. Change of rainfall distribution and circulation patterns over southern Africa in summer. *Journal of Climatology*, **6**, 579-592.
- Taljaard J. J., 1987. *The anomalous climate and weather systems over South Africa during summer 1975-1976*. South African Weather Bureau Technical Paper, No 16, 80pp.
- Taljaard J. J., 1994. Atmospheric Circulation Systems, Synoptic Climatology and Weather Phenomena of South Africa. Part 1: Controls of the Weather and Climate of South Africa. *South African Weather Bureau Technical Paper*, **27**, 45pp.
- Taljaard J. J., 1995a. Atmospheric Circulation Systems, Synoptic Climatology and Weather Phenomena of South Africa. Part 2: Atmospheric Circulation Systems in the South African Region. *South African Weather Bureau Technical Paper*, **28**, 65pp.
- Taljaard J. J., 1995b. Atmospheric Circulation Systems, Synoptic Climatology and Weather Phenomena of South Africa. Part 3: Synoptic Climatology of South Africa in January and July. *South African Weather Bureau Technical Paper*, **29**, 64pp.
- Tarassenko L., 1998. *A Guide to Neural Computing Applications*. John Wiley & Sons Inc., New York, 139pp.
- Tennant W.J., 2002. *Event Characteristics of Intra-Seasonal Climate Circulations*. Unpublished Ph.D Thesis. University of Cape Town, Cape Town, 185pp.
- Tennant W.J. and Hewitson B.C., 2002. Intra-seasonal rainfall characteristics and their importance to the seasonal prediction problem. *International Journal of Climatology*, in Press.
- Triegaardt D.O., Terblanche D.E., van Heerden J. and Laing M.V., 1988. *The Natal flood of September 1987*. South African Weather Bureau Technical Paper No. 19, Pretoria, 62pp.
- Tyson P. D., 1981. Atmospheric circulation variations and the occurrence of extended wet and dry spells over southern Africa. *Journal of Climatology*, **1**, 115-130.
- Tyson P. D., 1984. The atmospheric modulation of extended wet and dry spells over South Africa, 1958-1978. *Journal of Climatology*, **4**, 621-635.
- Tyson P. D., 1986. *Climatic Change and Variability in Southern Africa*. Oxford University Press, South Africa, 220pp.
- Tyson P.D., 1991. Climatic change in southern Africa: Past and present conditions and possible future scenarios. *Climatic Change*, **18**, 241-258.

- Tyson P.D., and D'Abreton P.C., 1998. Transport and recirculation of aerosols off Southern Africa – macroscale plume structure. *Atmospheric Environmental*, **32(9)**, 1511-1524.
- Tyson P.D., Garstang M. and Swap R., 1996(b). Large-scale recirculation of air over southern Africa. *Journal of Applied Meteorology*, **35**, 2218-2235.
- Tyson P. D, Garstang M., Swap R., Kållberg P., and Edwards M., 1996(a). An air transport climatology for subtropical Southern Africa. *International Journal of Climatology*, **16**, 265-291.
- Tyson P. D. and Preston-Whyte R. A., 2000. *The Weather and Climate of Southern Africa*. Oxford University Press, Cape Town, 396pp.
- Vines R.G., 1980. Analyses of South African rainfall. *South African Journal of Science*, **76**, 404-409.
- Vines R.G., 1982. Rainfall patterns in Southern South America, and possible relationships with similar patterns in South Africa. *South African Journal of Science*, **78**, 457-459.
- Walker N. D., 1990. Links between South African summer rainfall and temperature variability of the Agulhas and Benguela current systems. *Journal of Geophysical Research*, **95**, 3297-3319.
- Walker N.D. and Lindesay J.A., 1989. Preliminary observations of oceanic influences of the February-March 1988 floods in central South Africa. *South African Journal of Science*, **85**, 164-169.
- Walker N.D and Mey R.D., 1988. Ocean/atmosphere heat fluxes within the Agulhas retroflection region. *Journal of Geophysical Research*, **93**, 15,473-15,483.
- Yarnal B., 1993. *Synoptic climatology in Environmental Analysis: A Primer*. Belhaven Press, London, 195pp.
- Yonetani T. and Gordon H.B., 2001. Simulated changes in the frequency of extremes and regional features of seasonal/annual temperature and precipitation when atmospheric CO₂ is doubled. *Journal of Climate*, **14**, 1765-1779.

APPENDICES

University of Cape Town

APPENDIX A: Atmospheric variables for each day of the case study event of 22Jan1996 to 27Jan1996 described in Chapter Five

- Precipitation values
- Sea level pressure
- Geopotential heights at 700hPa
- Specific humidity at surface
- Specific humidity at 700hPa
- Surface winds
- Wind vectors at 700hPa
- Latent heat flux

APPENDIX B: Trajectory figures for sample events from node [0 0]

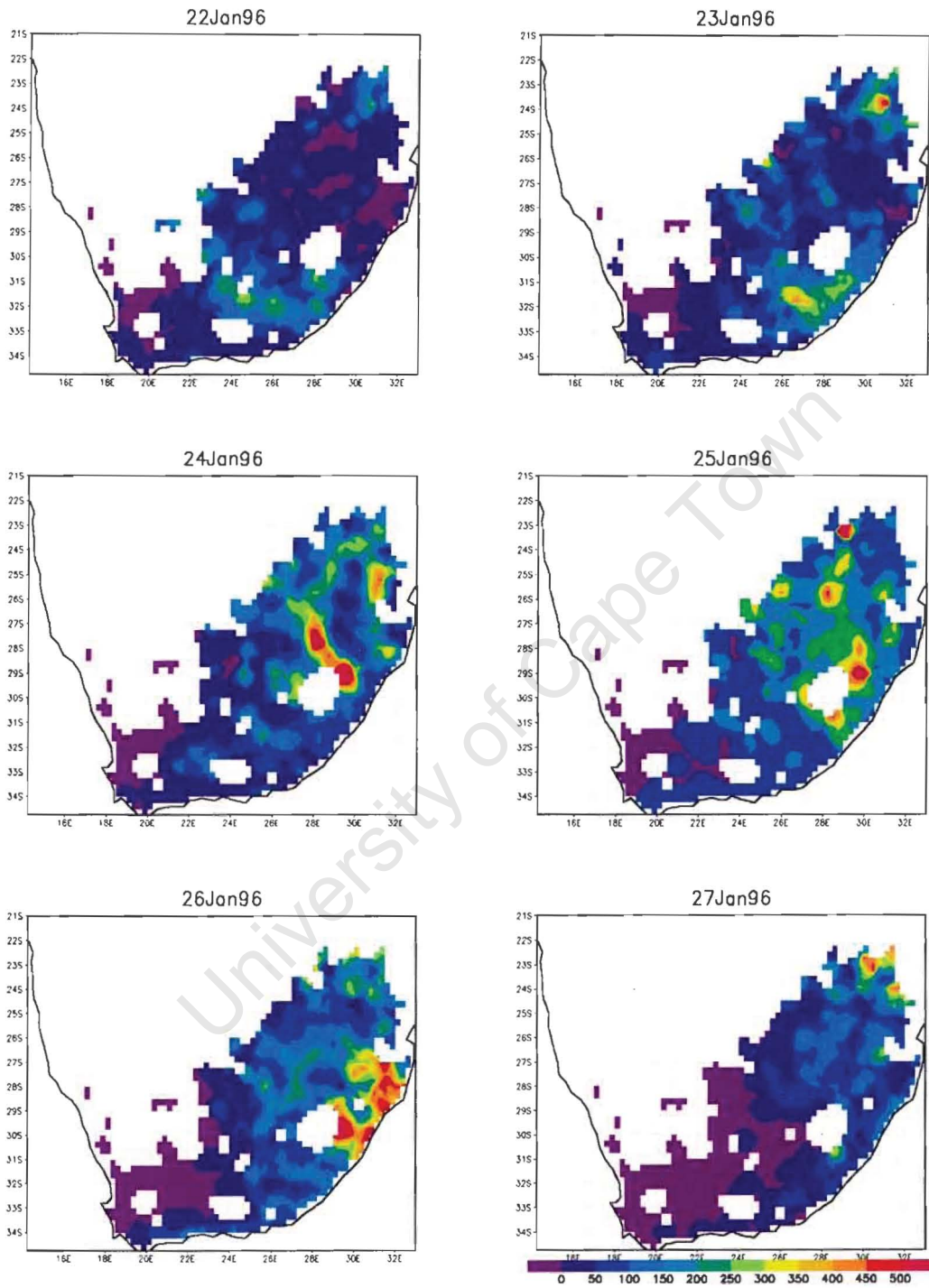
APPENDIX C: Trajectory figures for sample events from node [2 0]

APPENDIX D: Trajectory figures for sample events from node [2 3]

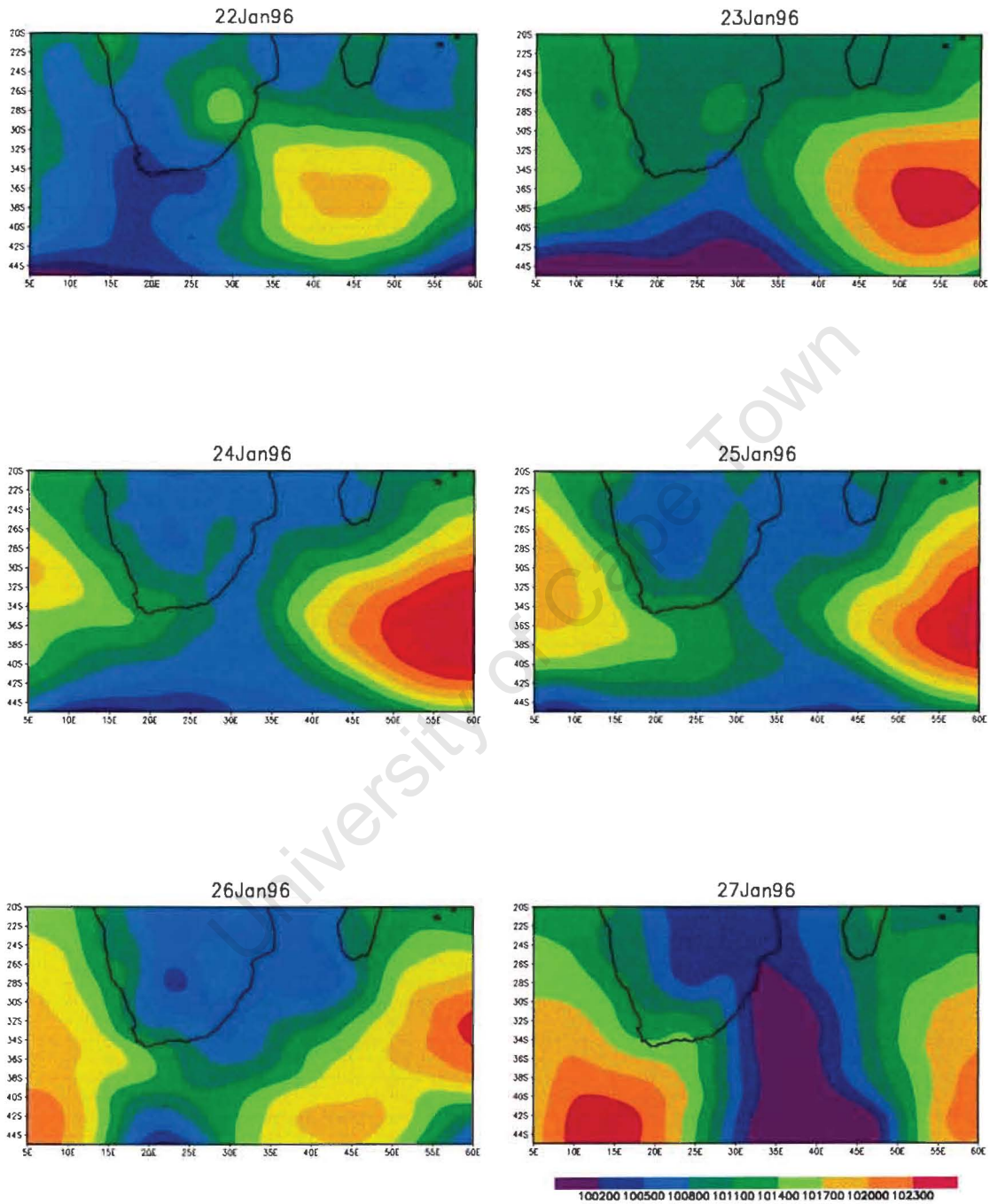
APPENDIX A

University of Cape Town

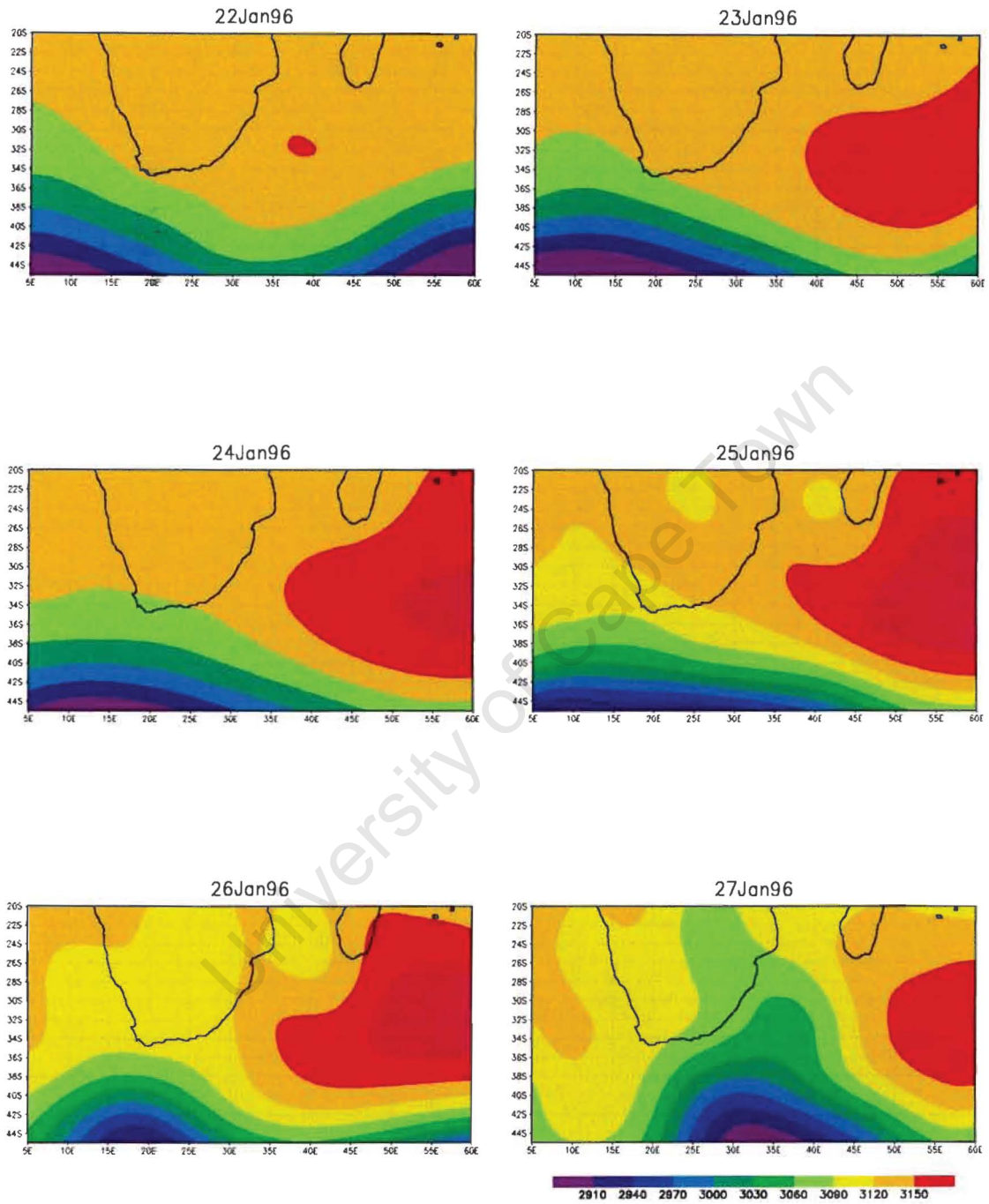
Precipitation values



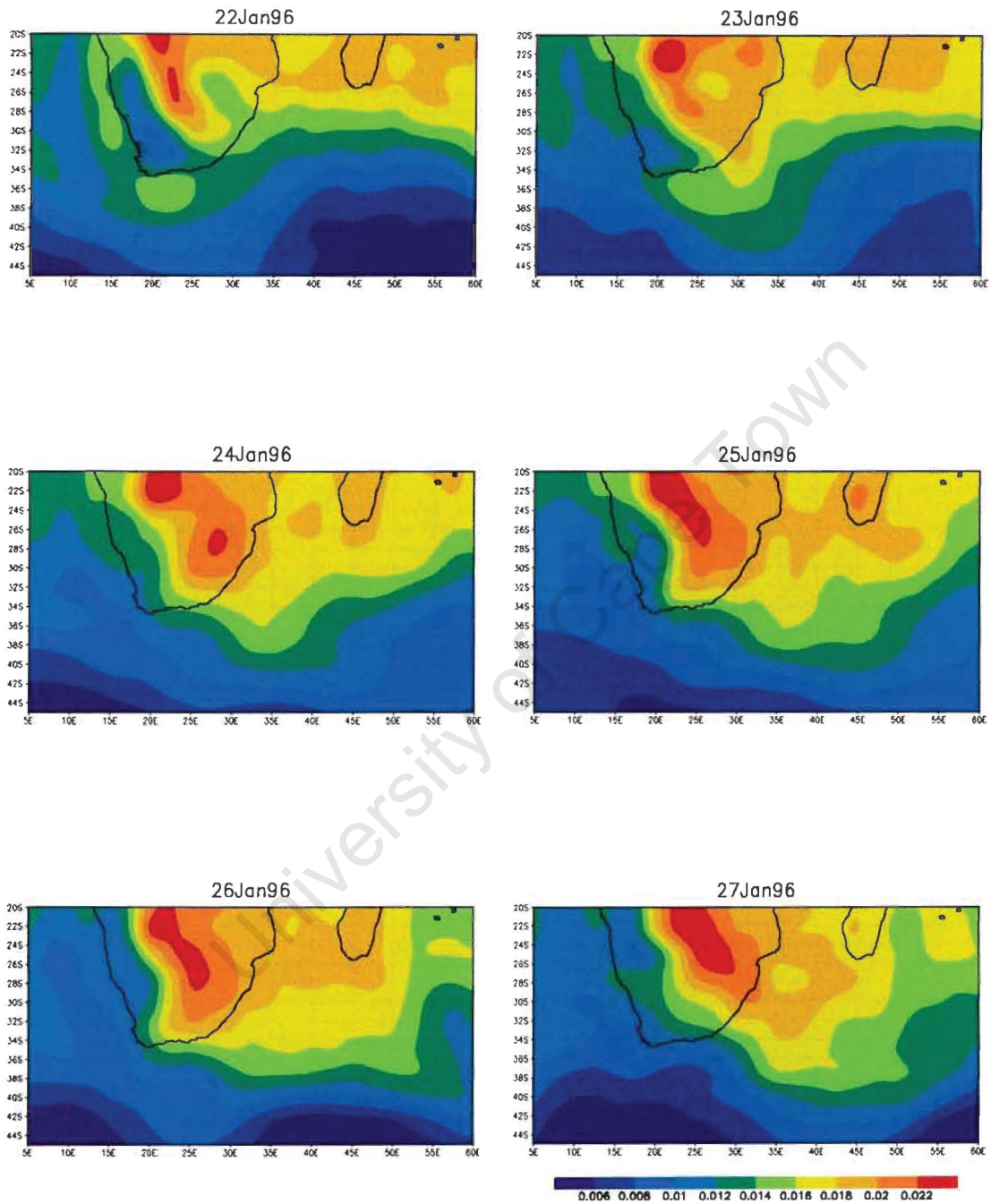
Sea Level Pressure values



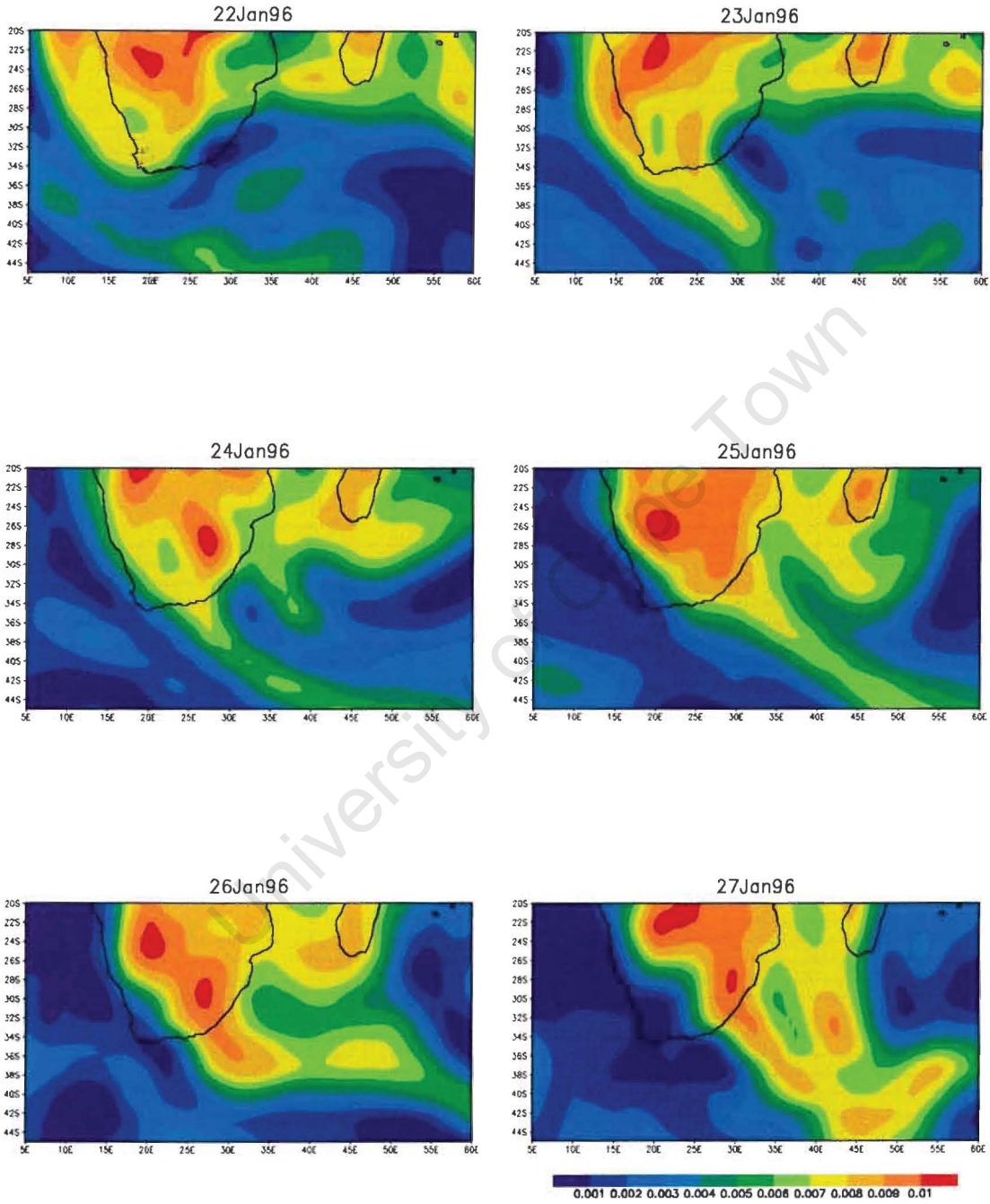
Geopotential heights at 700hPa



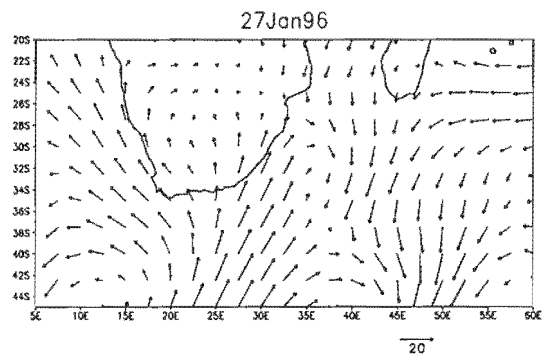
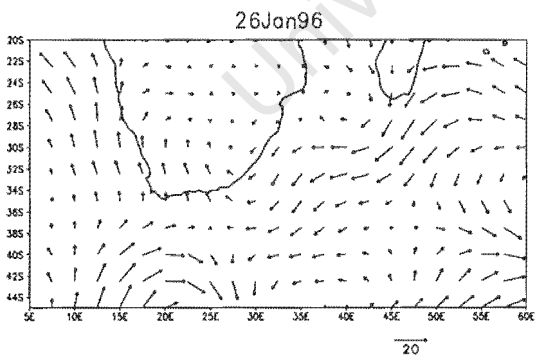
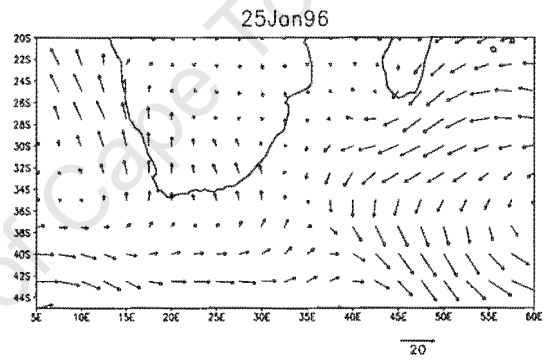
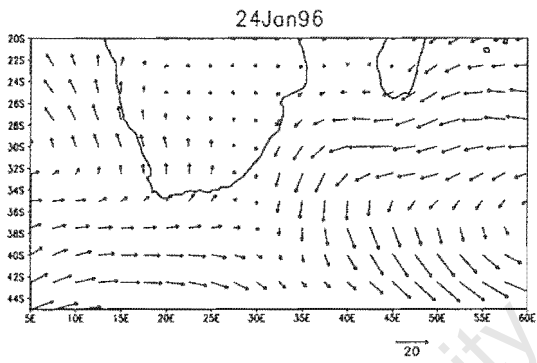
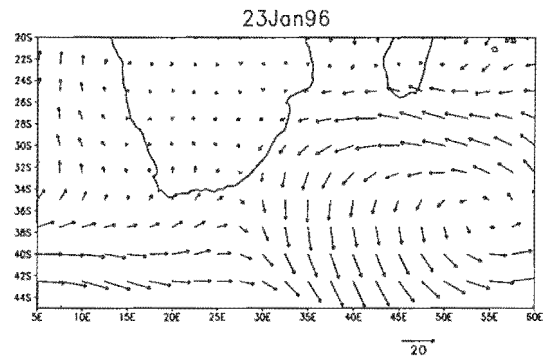
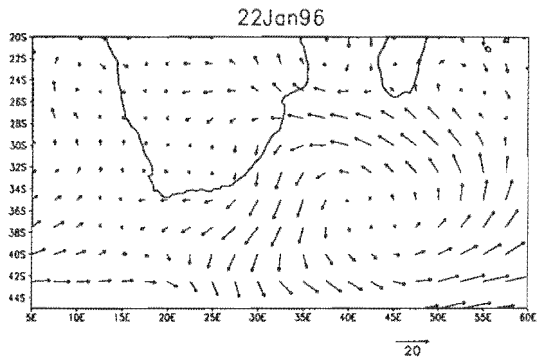
Specific humidity at surface



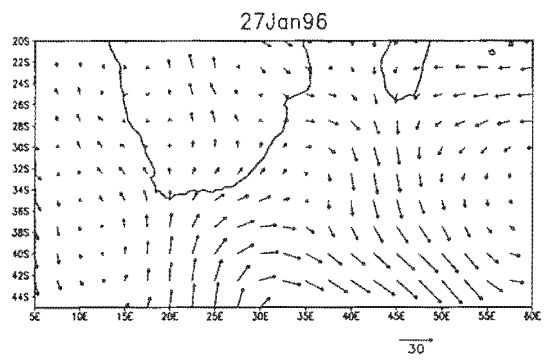
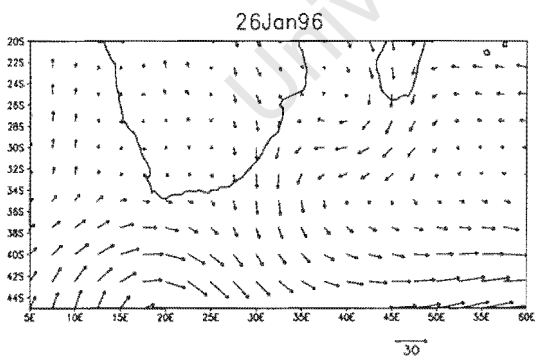
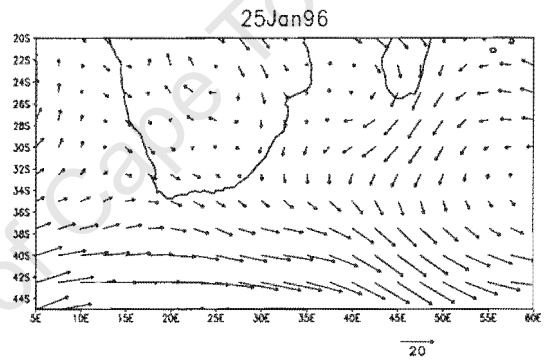
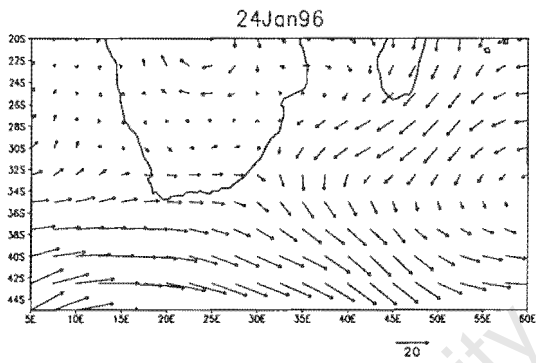
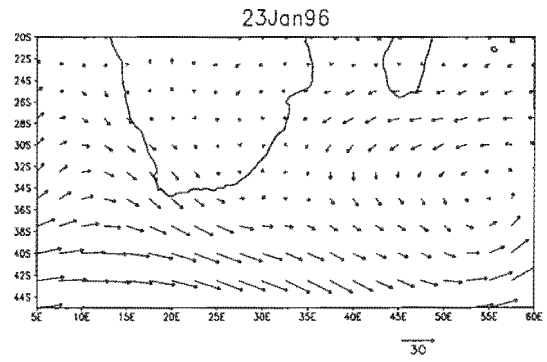
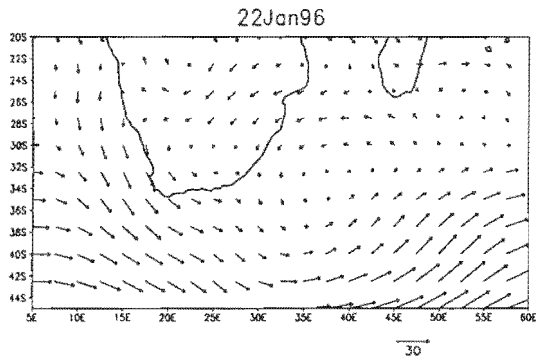
Specific Humidity at 700hPa



Surface Winds

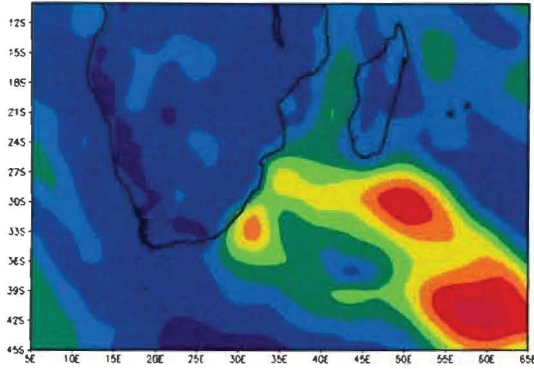


Winds at 700hPa

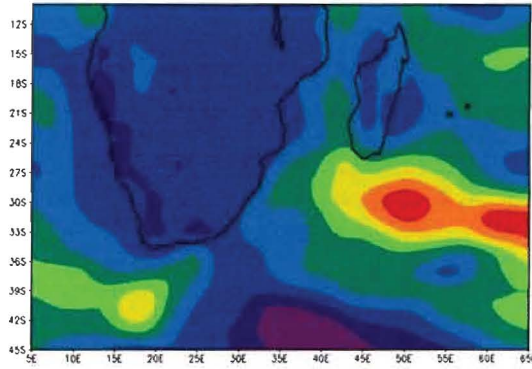


Latent heat flux

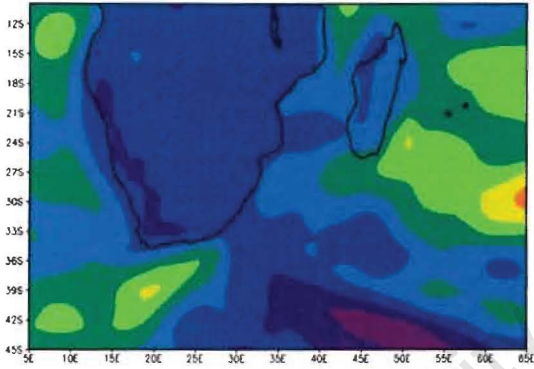
22Jan96



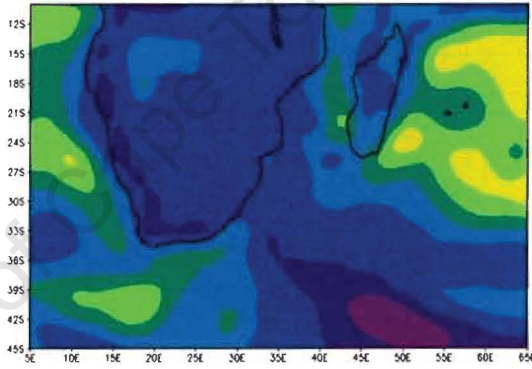
23Jan96



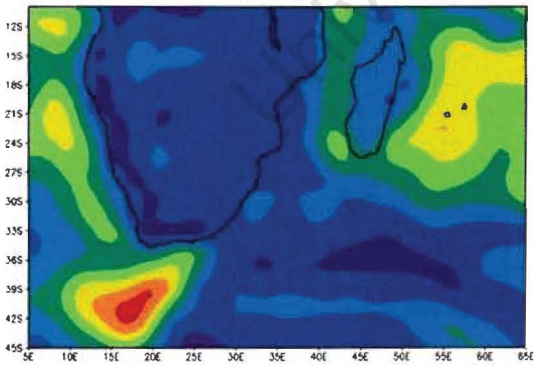
24Jan96



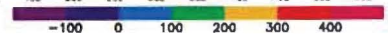
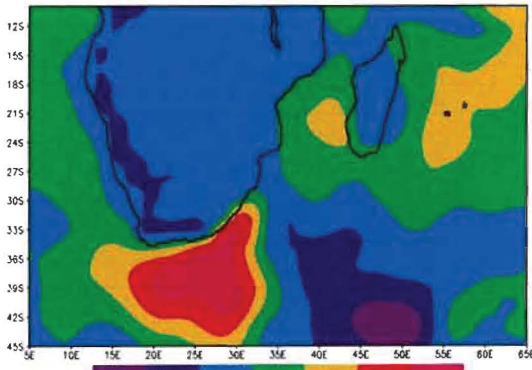
25Jan96



26Jan96



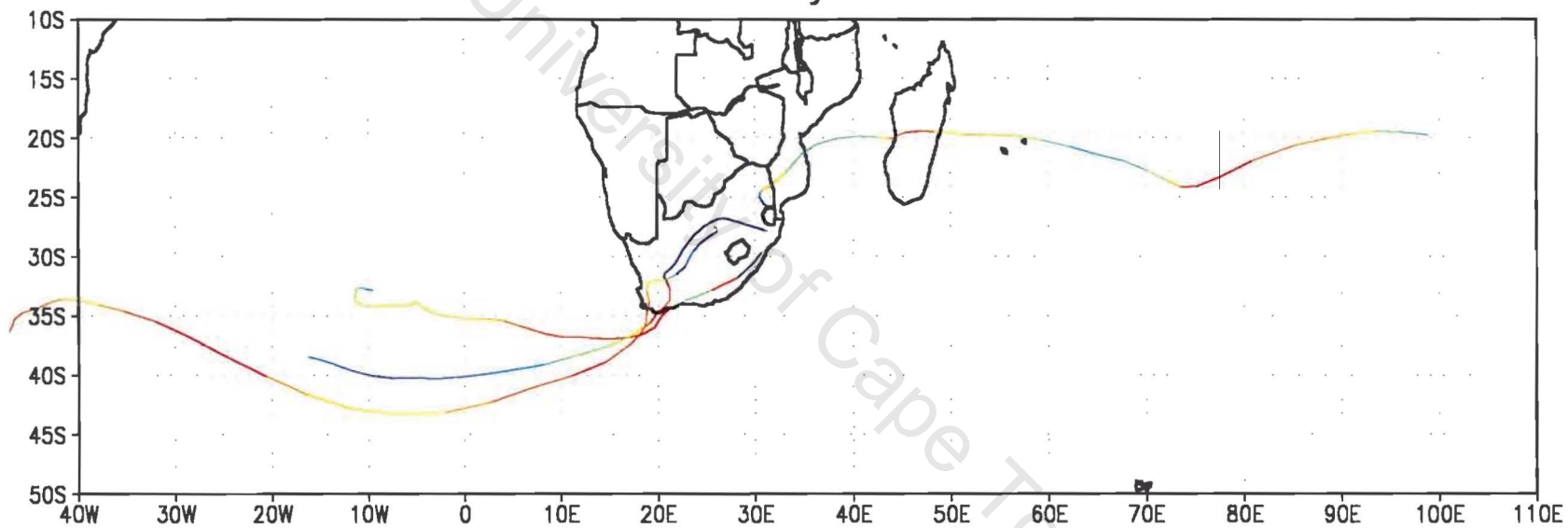
27Jan96



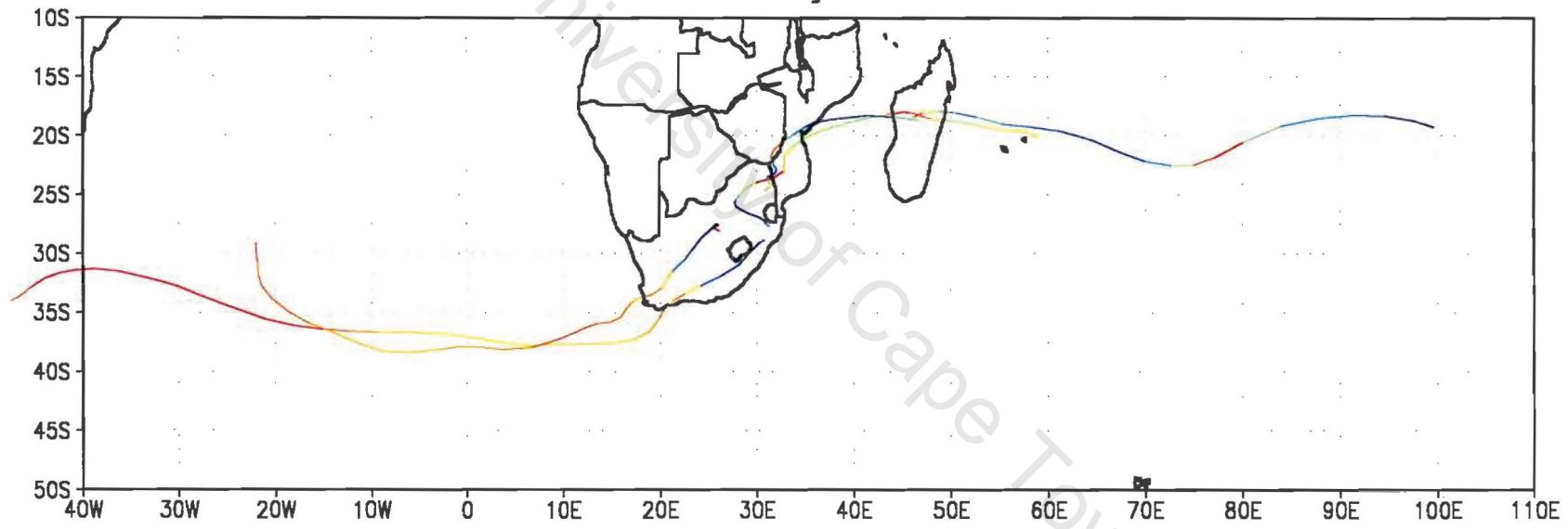
APPENDIX B

University of Cape Town

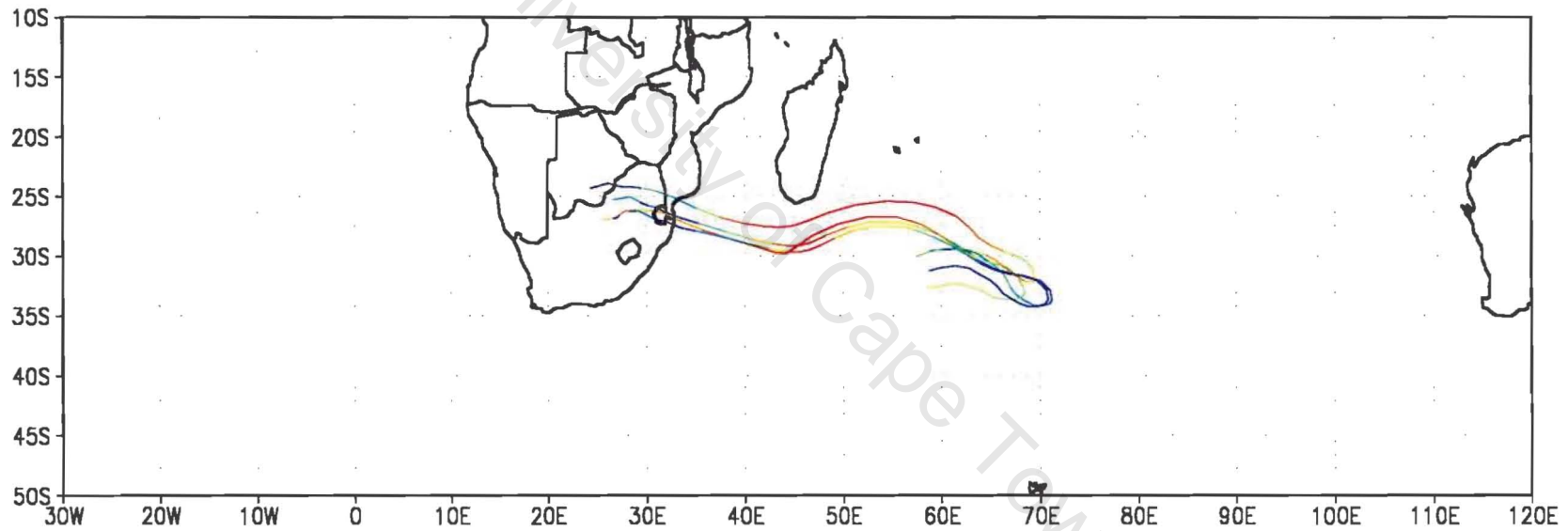
00z23jan91



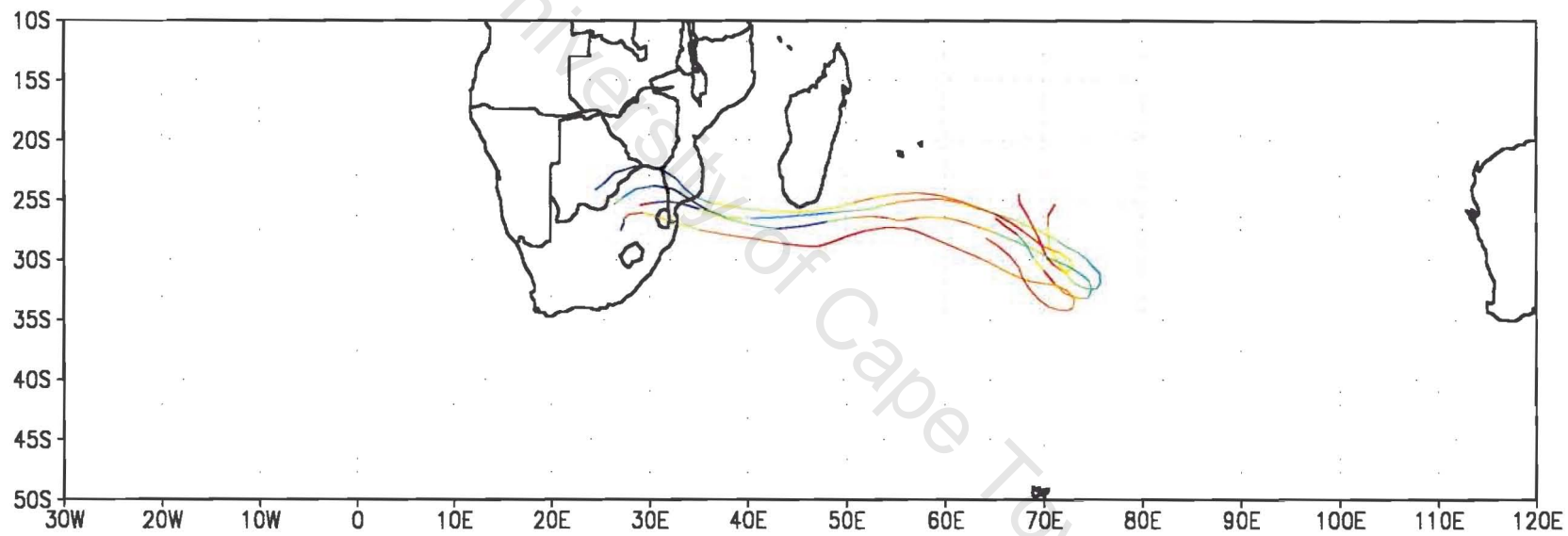
12z23jan91



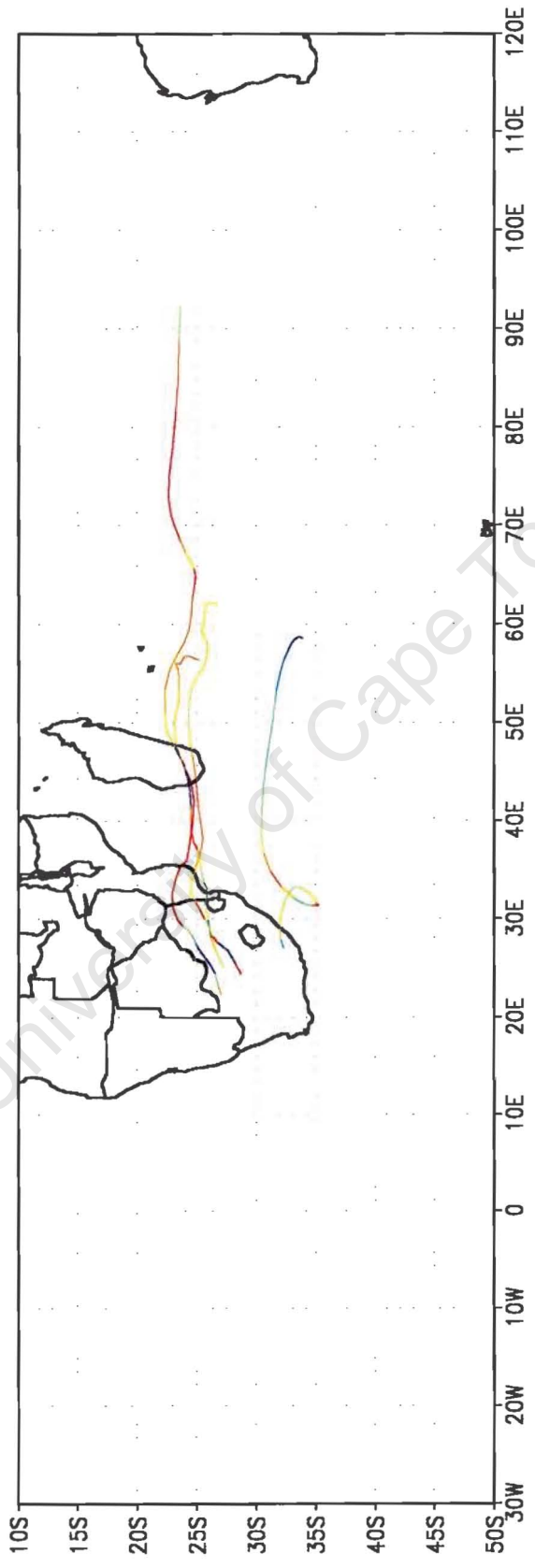
00z10feb88



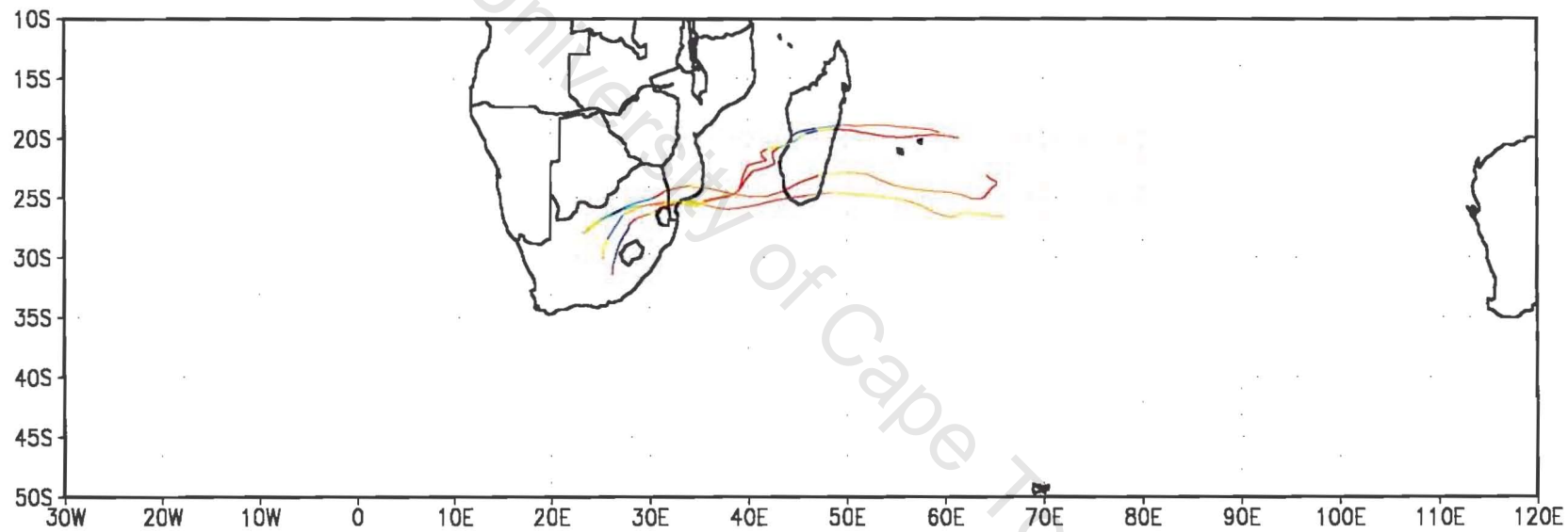
12z10feb88



00z22feb88



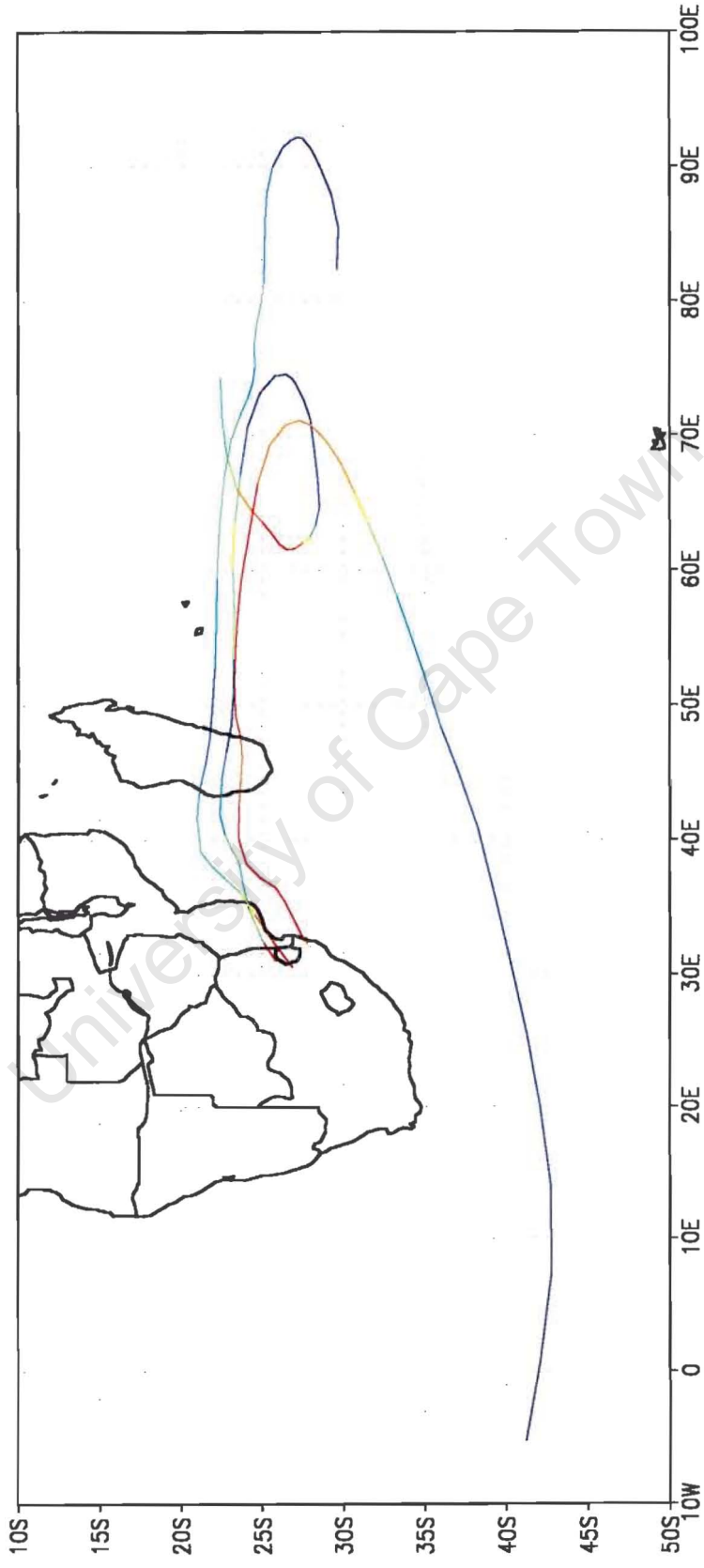
12z22feb88



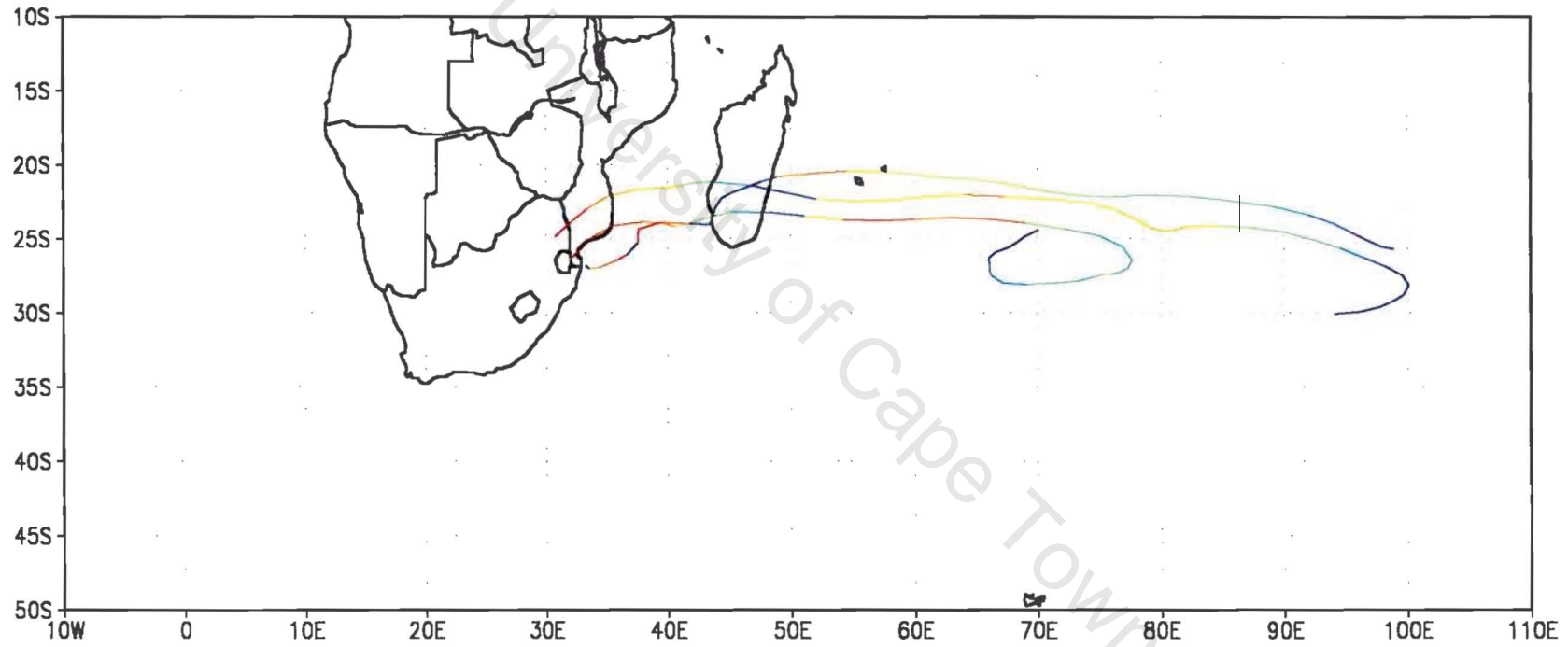
APPENDIX C

University of Cape Town

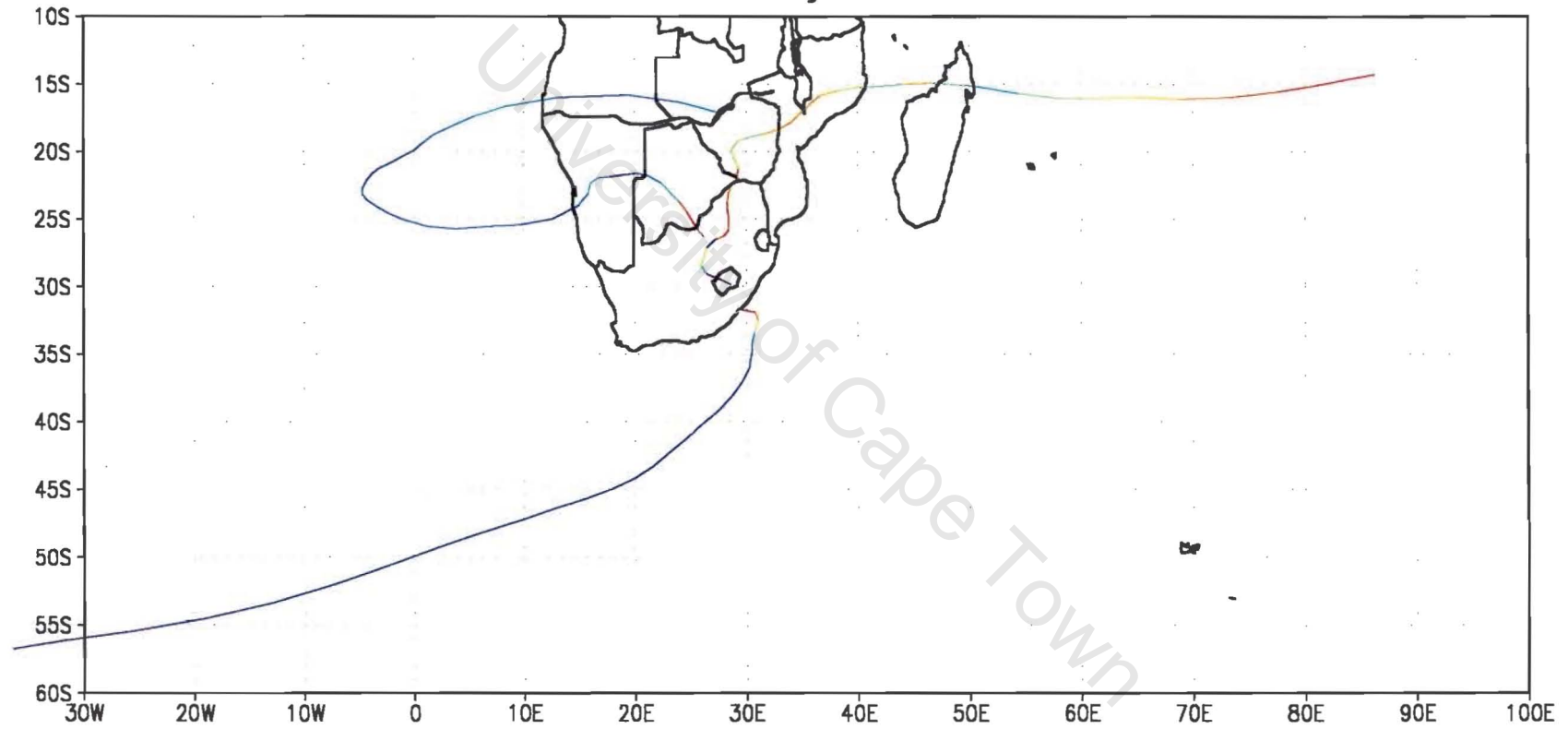
00z11feb96



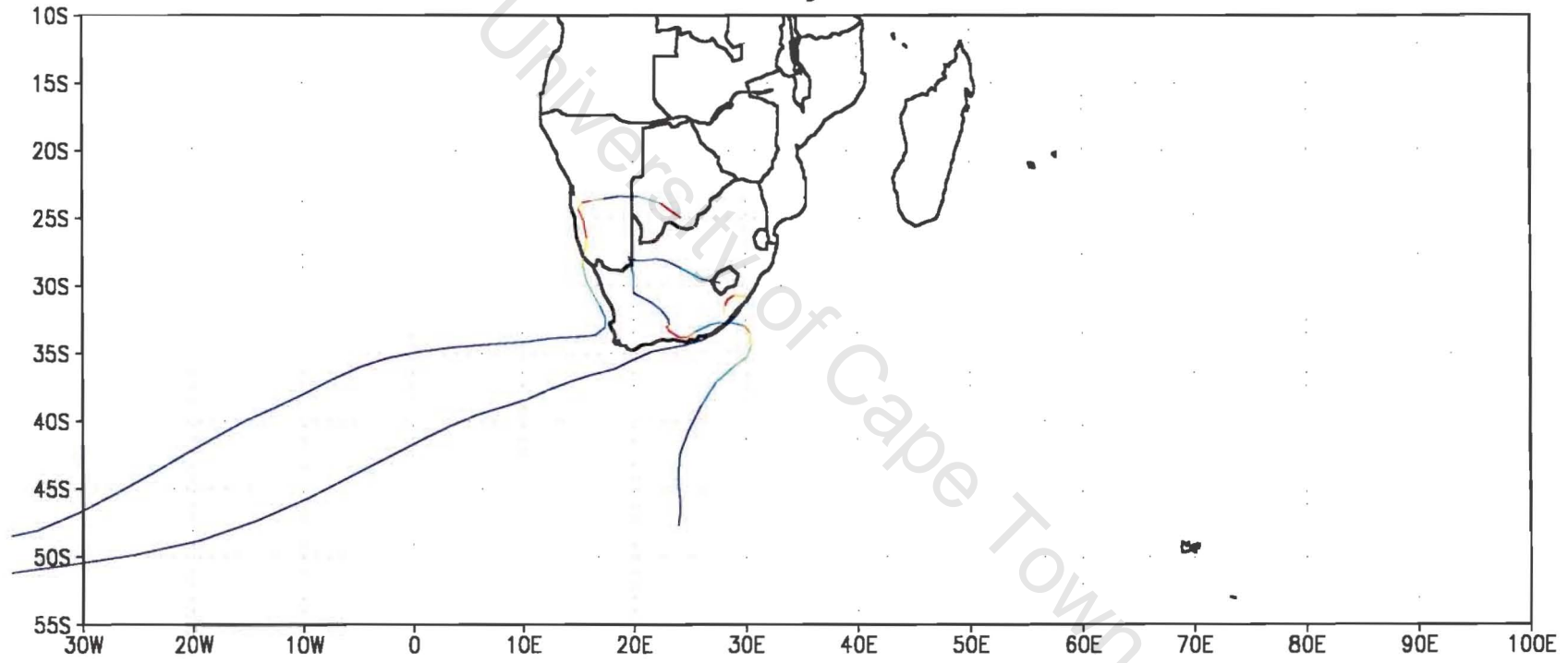
12z11feb96



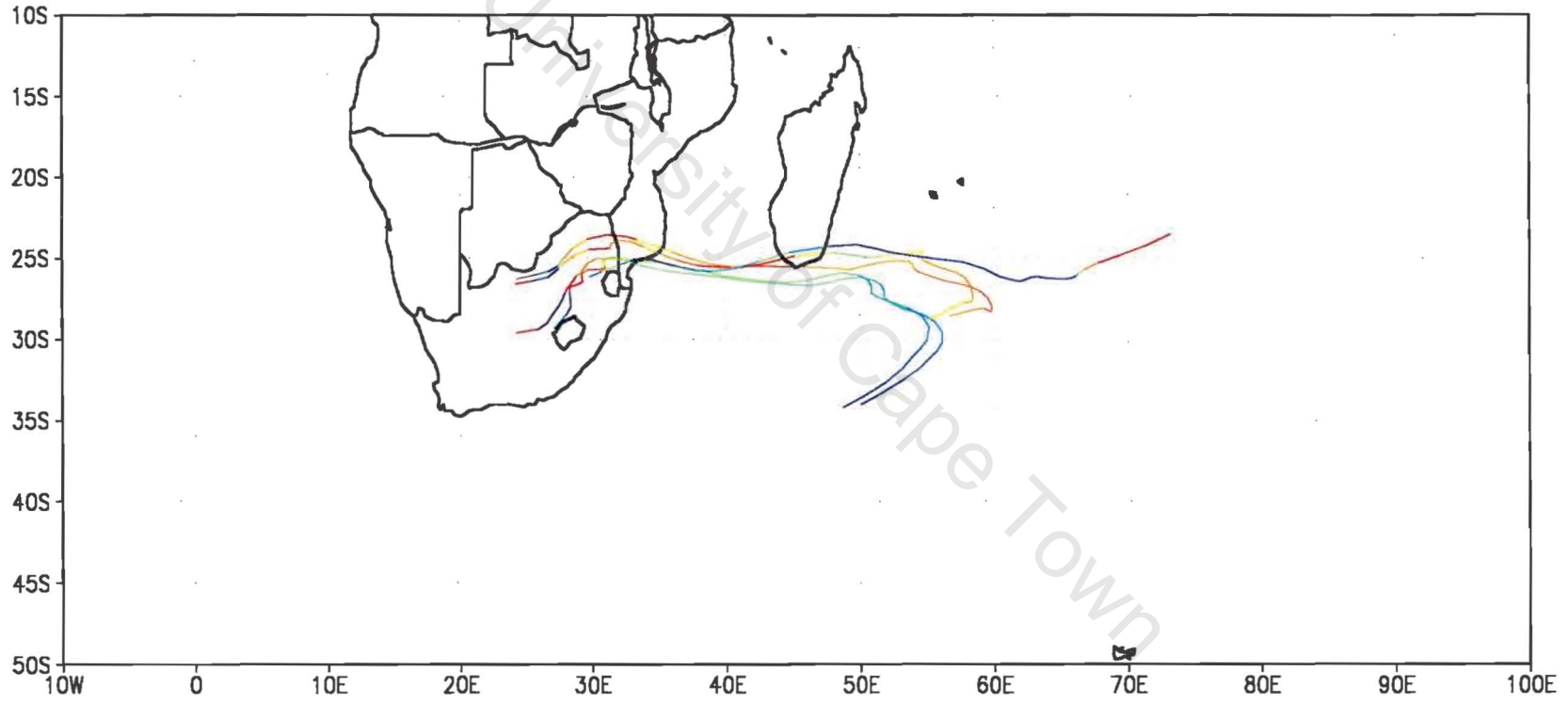
00z23jan81



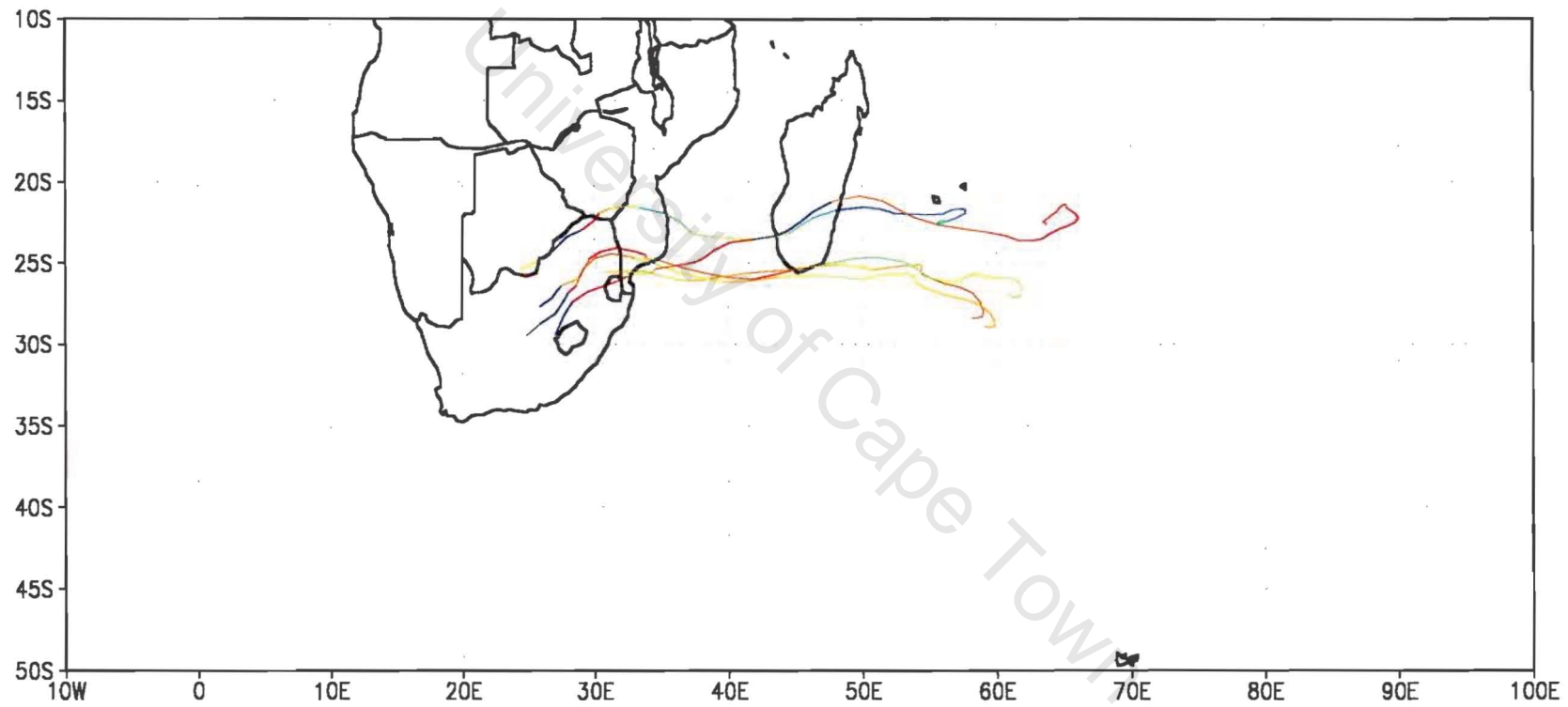
12z23jan81



00z21feb88



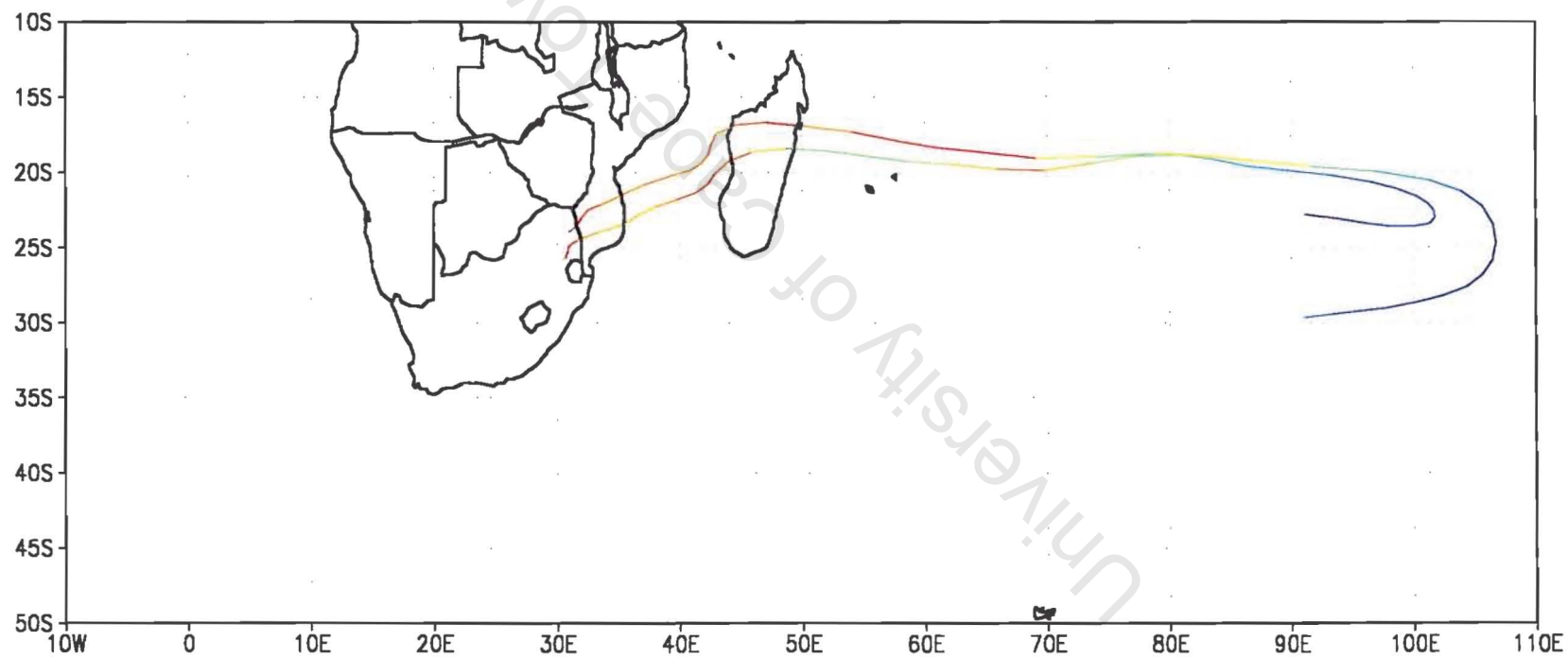
12z21feb88



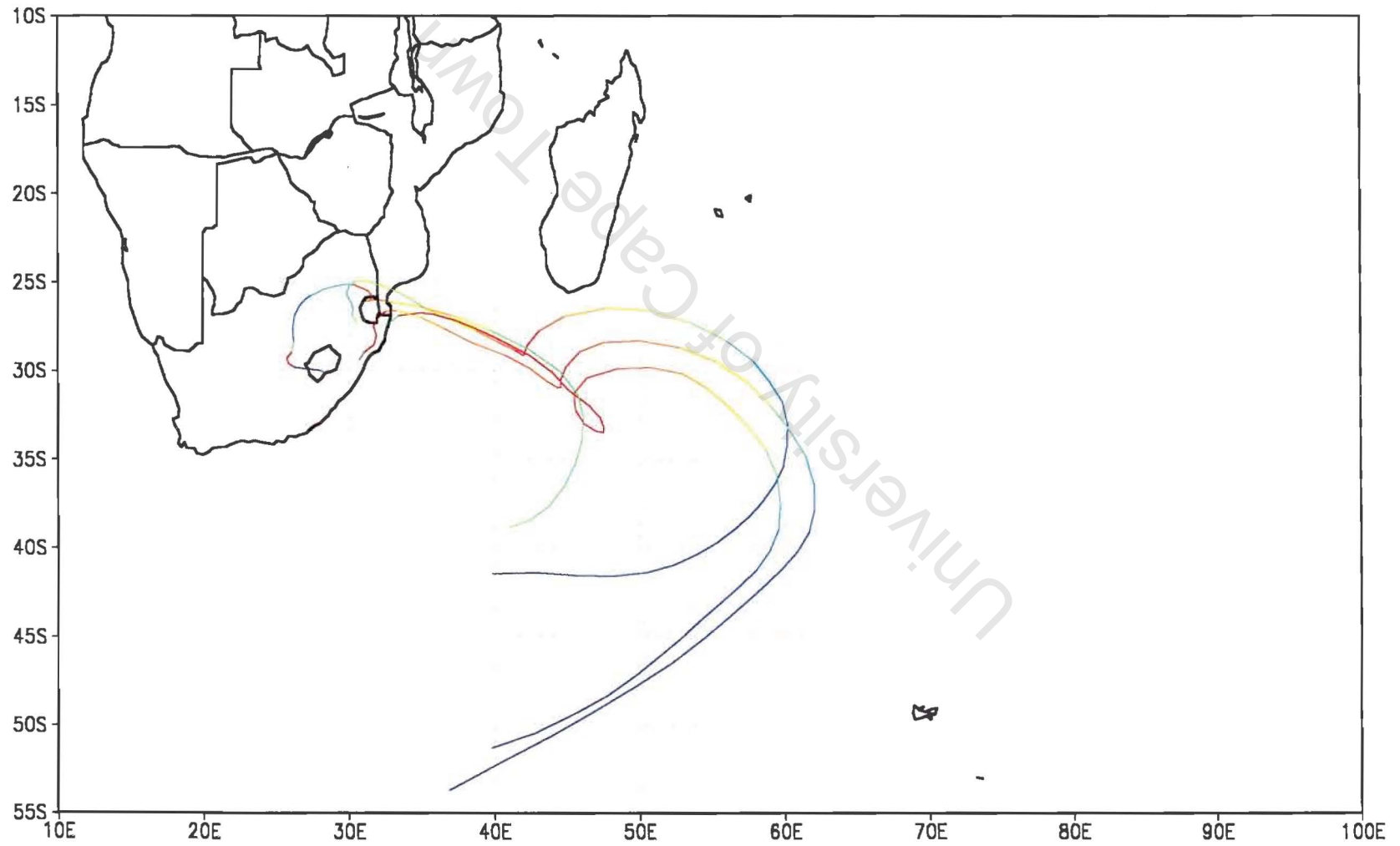
APPENDIX D

University of Cape Town

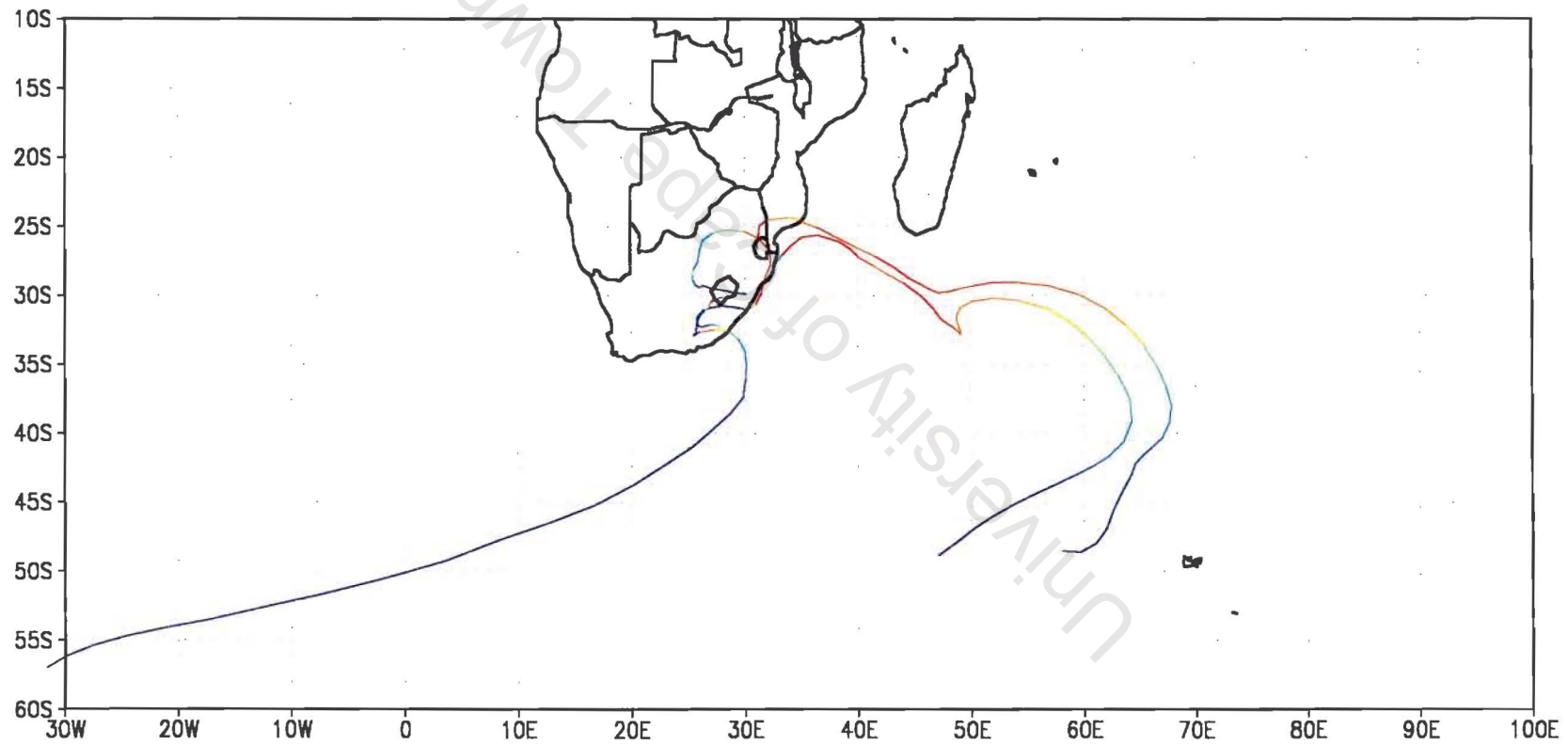
12z23dec92



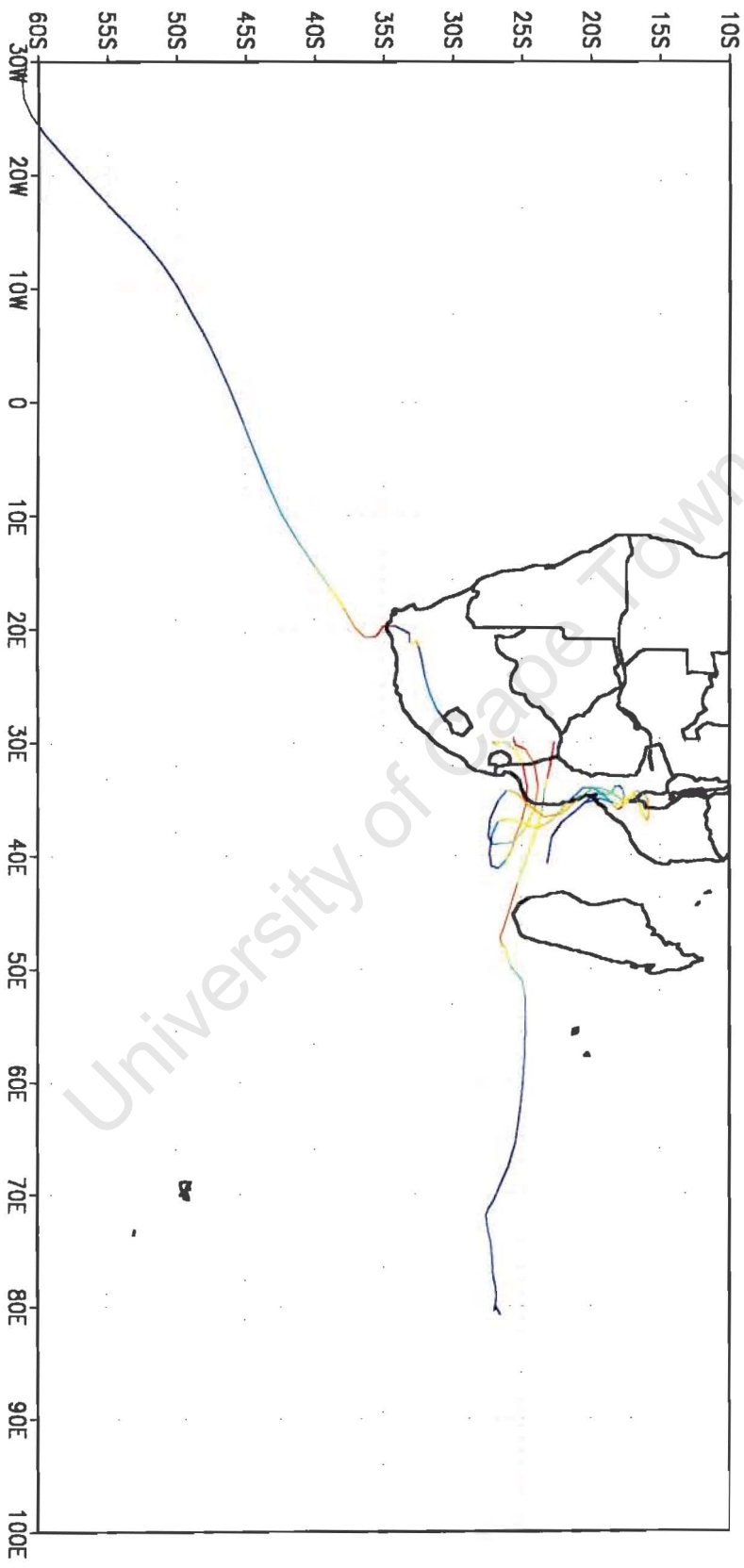
00z13feb89



12z13feb89



00Z5dec90



12z5dec90

